Point-to-Point Responses to Referees' Comments on "Characterization of submicron aerosols influenced by biomass burning at a site in the Sichuan Basin, southwestern China"

Wei Hu, Min Hu*, Wei-Wei Hu#, Hongya Niu, Jing Zheng, Yusheng Wu, Wentai Chen, Chen Chen, Lingyu Li, Min Shao, Shaodong Xie, Yuanhang Zhang

State Key Joint Laboratory of Environmental Simulation and Pollution Control, College of Environmental Sciences and Engineering, Peking University, Beijing 100871, China

#now at: Cooperative Institute for Research in Environmental Sciences, University of Colorado, Boulder, CO 80309, USA

Correspondence to: M. Hu (minhu@pku.edu.cn)

Referee #1

Hu et al. reported the HR-ToF-AMS results at an urban downwind site in Sichuan basin in winter. The chemical composition and size distributions of submicron aerosols were characterized, and the sources of OA were investigated by PMF. The authors also studied the aging of OA using various approaches, e.g., Van Krevelen diagram, f_{44} vs. f_{43}, oxidation states, and OA/CO, etc. This study is helpful to understand aerosol variations and oxidation states in southwestern China. However, the English writing is poor, and I often missed the logic when reading this manuscript. In addition, the data quality needs to be further validated and some data interpretations are not convincing. A major revision is needed.

Response: Thanks very much for Referee' comments. We carefully checked and corrected the English again with the help of a native English speaker, and provided more supplementary materials for further validation of data, and give point-to-point responses to Referee's comments and corrected the manuscript accordingly. Please refer to the responses below and revised manuscript.

Comments:

1. I raised the same comments in my first review of this manuscript. My major concern is the PMF results. Although the author expanded the PMF results, I still didn't see PMF diagnostic plots for other solutions except Table S2 with a simple description of the reasons. In addition, I don't understand why the authors didn't use the VOCs measurements to evaluate the PMF results.

Response: In the last revised manuscript for ACPD, we added PMF **diagnostic plots** and related tables in **Sect. S3** in the supplementary material.

In this revised manuscript, we added the result of 5-factor solution in the supplementary material. As mentioned in **Table S1** (Table S2 in the last version), SV-OOA and HOA in 4-factor solution were split into three factors with similar spectra, however, different time series (**Fig. S4-S6**). These factors can't be identified definitely. So we select 4-factor as the optimum solution.

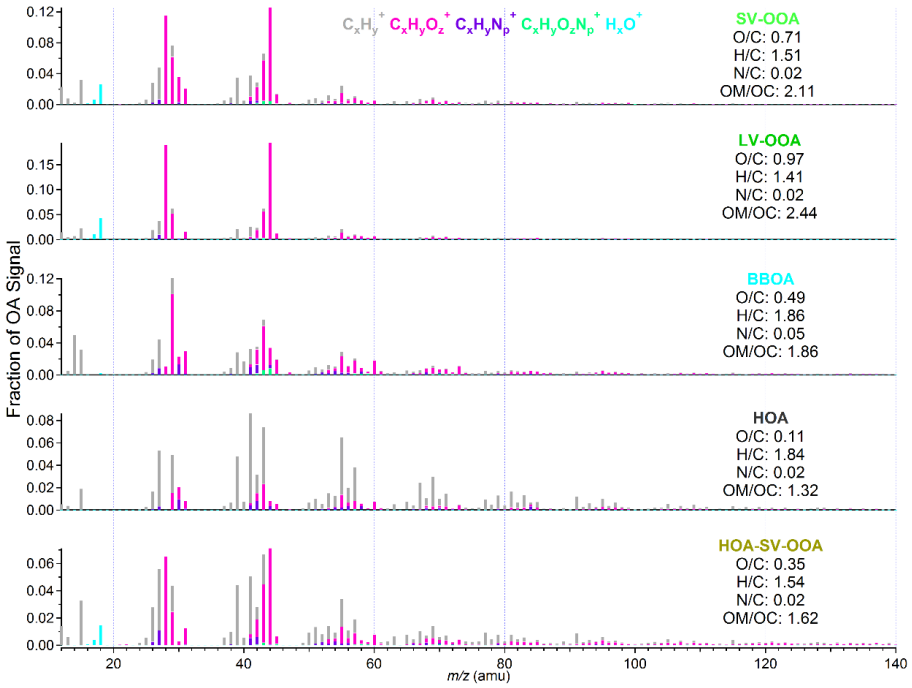

Figure S4. Unit mass spectra of OA factors for 5-factor solution. SV-OOA and HOA for four-factor solution were split into three factors with similar spectra (Fig. S6), marked as SV-OOA, HOA, and HOA-SV-OOA. The other two are marked as LV-OOA and BBOA. The elemental ratios and OA/OC ratios of each component are also added.

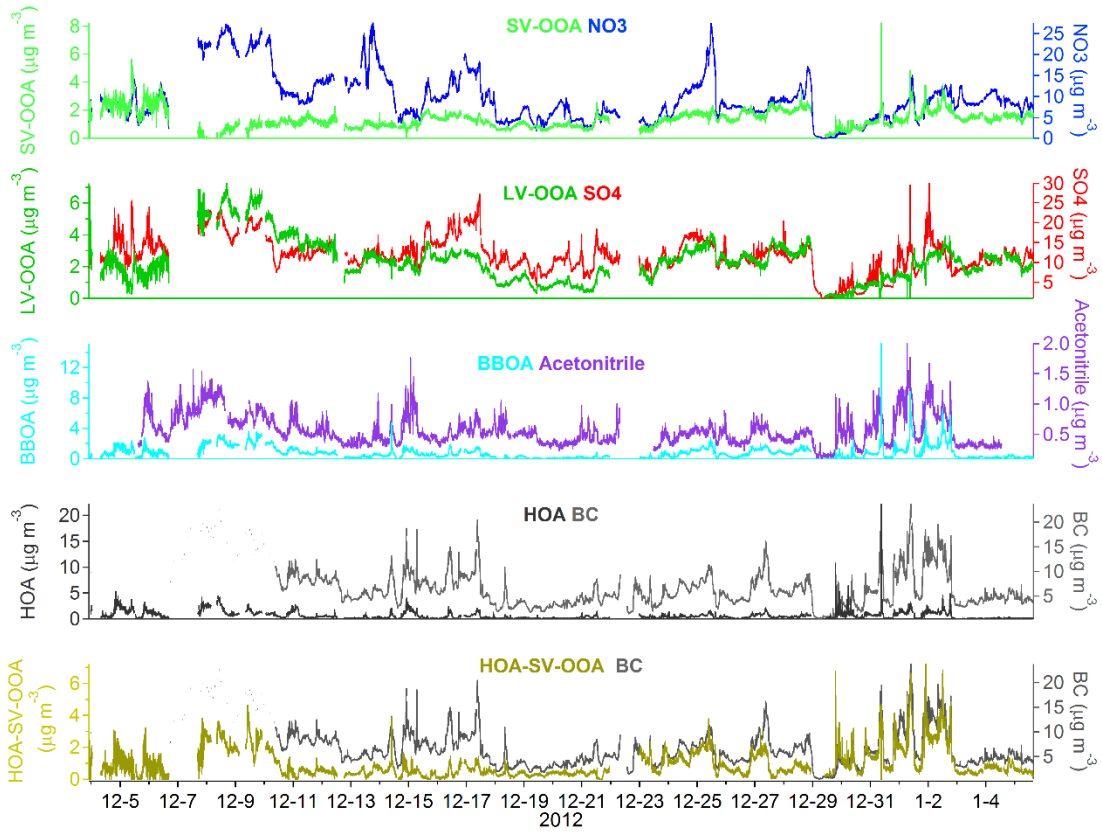

Figure S5. Time series of OA fractions for five-factor solution (marked as SV-OOA, HOA, HOA-SV-OOA, LV-OOA and BBOA) and external tracers (sulfate, nitrate, BC, and acetonitrile).

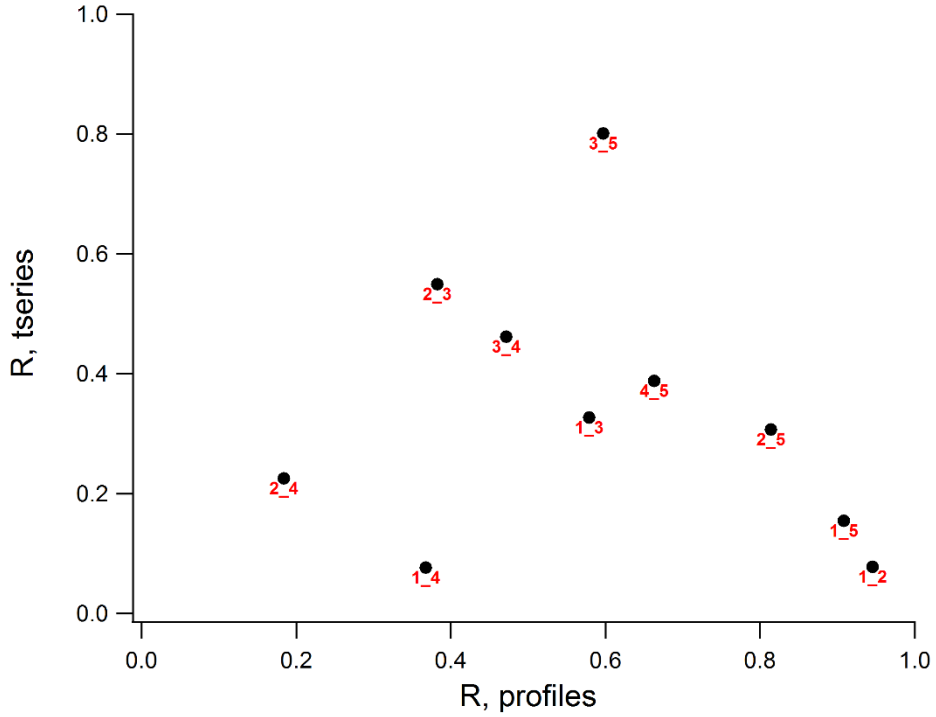

Figure S6. Correlation of time series and unit mass spectra of OA factors for 5-factor solution.

As the uncentered correlations shown in Table S2, the MS of OA factors resolved in this study and the average MS of reported OA factors correlated well. HOA resolved in this study, as a mixed factor of vehicle, cooking and other primary emissions, the MS of which correlated well with the average MS of HOA, BBOA, COA, and Vehicle-OA factors reported in previous studies (Table S2).

In the last revised manuscript, we listed the correlation coefficients of OA factors with acetaldehyde and acetonitrile in Table S3. In this revised manuscript, we added the correlation coefficients of OA factors with another three VOC species, toluene, benzene, and acetone. The primary emitted VOC species show good correlation with POA components (HOA and BBOA). In Page 12, Line 3, "***toluene, and benzene***" was added. More details on the VOC characterization and biomass burning contribution to ambient VOCs can be found in Li et al. (2014).

According to all these evaluation, the PMF results are considered to be reasonable.

Table S3 Correlation coefficients (Pearson's R) of OA factors with gaseous and aerosol species. Correlation coefficients higher than 0.60 are in bold.

	LV-OOA	**SV-OOA**	**HOA**	**BBOA**
SO_4^{2-}	**0.65**	0.36	0.26	0.30
NO_3^-	**0.66**	0.31	0.15	0.21
NH_4^+	**0.68**	0.28	0.36	0.34
Cl^-	0.22	-0.08	0.57	0.49
BC	**0.75**	0.18	**0.73**	**0.77**
$C_2H_4O_2^+$	**0.77**	0.28	**0.80**	**0.85**
SO_2	0.10	0.09	0.39	0.44
NO_x	0.31	-0.13	**0.62**	0.47
NO_y	0.39	-0.09	**0.64**	0.51
O_3	-0.31	0.08	-0.32	-0.21
CO	0.20	-0.09	0.49	0.42
Acetaldehyde	0.34	0.26	**0.65**	**0.77**
Acetonitrile	0.44	-0.02	**0.73**	**0.68**
Toluene	0.57	-0.39	**0.78**	0.52
Benzene	0.55	-0.28	**0.76**	0.58
Acetone	0.48	0.14	0.49	0.54
LV-OOA	**1.00**			
SV-OOA	0.37	**1.00**		
HOA	0.53	0.01	**1.00**	
BBOA	0.55	0.25	**0.78**	**1.00**

2. The authors assumed that aerosol particles were neutralized and then got a RIE = 4.04 for ammonium. How are the authors sure that aerosol particles were neutral? Why didn't the authors use pure ammonium nitrate particles from IE calibration data to get the RIE of ammonium?

Response: As the last response said, in this study we missed the measurenment of ammonium under MS mode. But the RIE of ammonium under BFSP mode was inaccurate, hence there was no data of ammonium nitrate was available for RIE determination based on AMS. According to the ion balance of filter based results, $PM_{2.5}$ was nearly neutral **(Fig. R1**). The predicted NH_4^+ was calculated assuming full neutralization of particulate anions of NO_3^-, SO_4^{2-} and Cl^-. The measured NH_4^+ was less than the predicted NH_4^+ (**Fig. R2**), which was mainly caused by the neutralization of Ca^{2+}, Mg^{2+} and Na^+ in larger sizes (Guo et al., 2010).

Biomass burning can contribute abundant K^+ to ambient fine particles. The average concentration of K^+ in $PM_{2.5}$ was 1.22 μg m^{-3} during the same campaign. Assuming all K^+ existed in submicron size range and PM_1 was neutral, the uncertainty of measured NH_4^+ mass concentration caused by K^+ was 6.7% (**Fig. R3**). Assuming PM_1 was neutral, and K^+ and other crustal ions were ignorable in submicron size range, as RIE=4.04, the predicted and measured NH_4^+ exhibited good consistency with a slope of 0.999 (**Fig. R4**). When the RIE=4.04 was used for ammonium quantification in this study, the uncertainty of measured NH_4^+ mass concentration caused by K^+ was 6.7%.

In the revised manuscript, "***except for ammonium for which RIE=4.04 was used assuming PM_1 was neutral and other metallic species were ignorable in PM_1 (water-soluble K^+, Ca^{2+}, Mg^{2+}, and Na^+ were 1.22, 0.25, 0.04, and 0.21 μg m^{-3} in $PM_{2.5}$).***" was added in **Page 7, Line 16**.

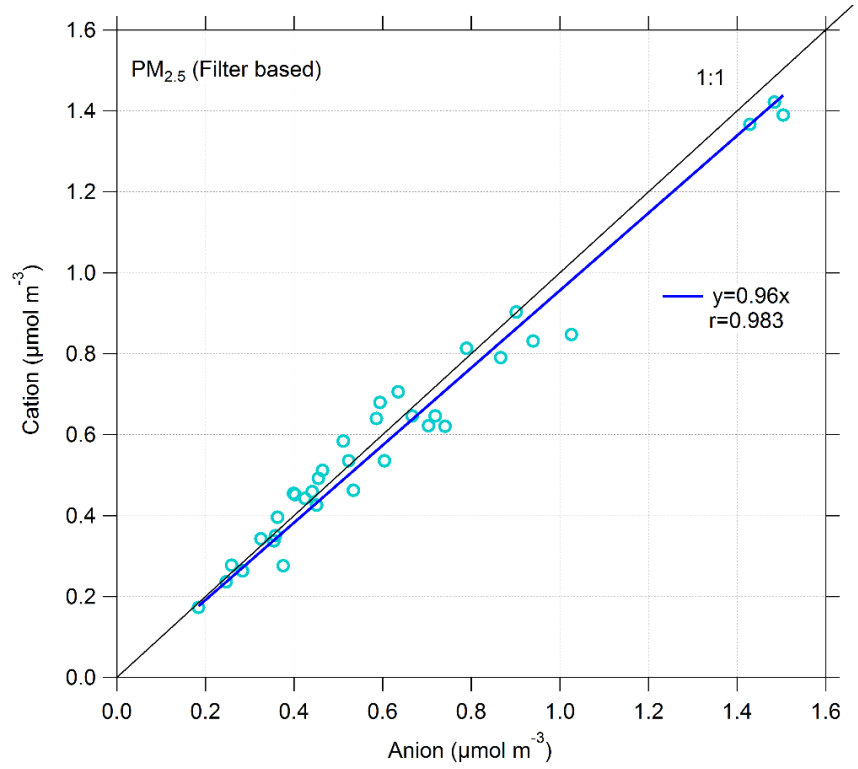

Figure R1. Scatter plots between total cation and anion concentrations in $PM_{2.5}$ filter samples.

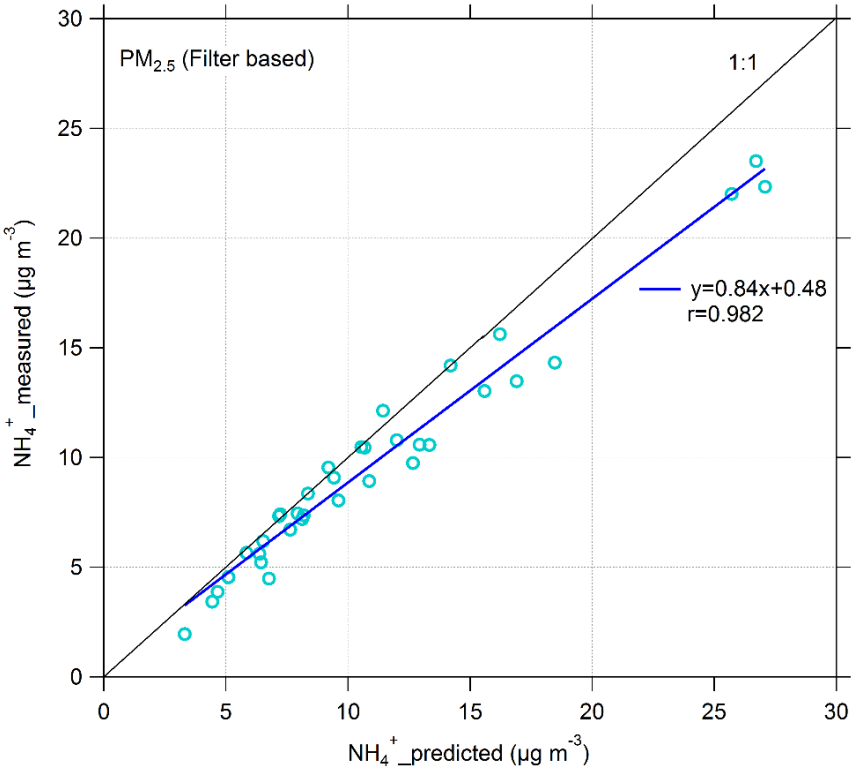

Figure R2. Scatter plots between measured NH_4^+ and predicted NH_4^+ of $PM_{2.5}$ filter samples.

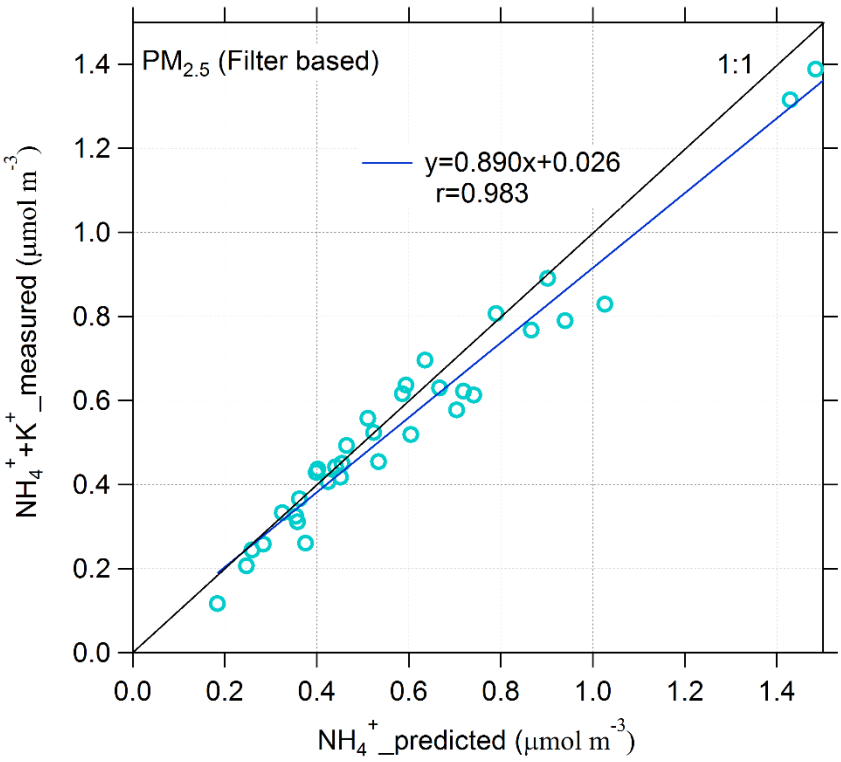

Figure R3. Scatter plots between AMS measured NH_4^+ and K^+, and predicted NH_4^+ mole concentration.

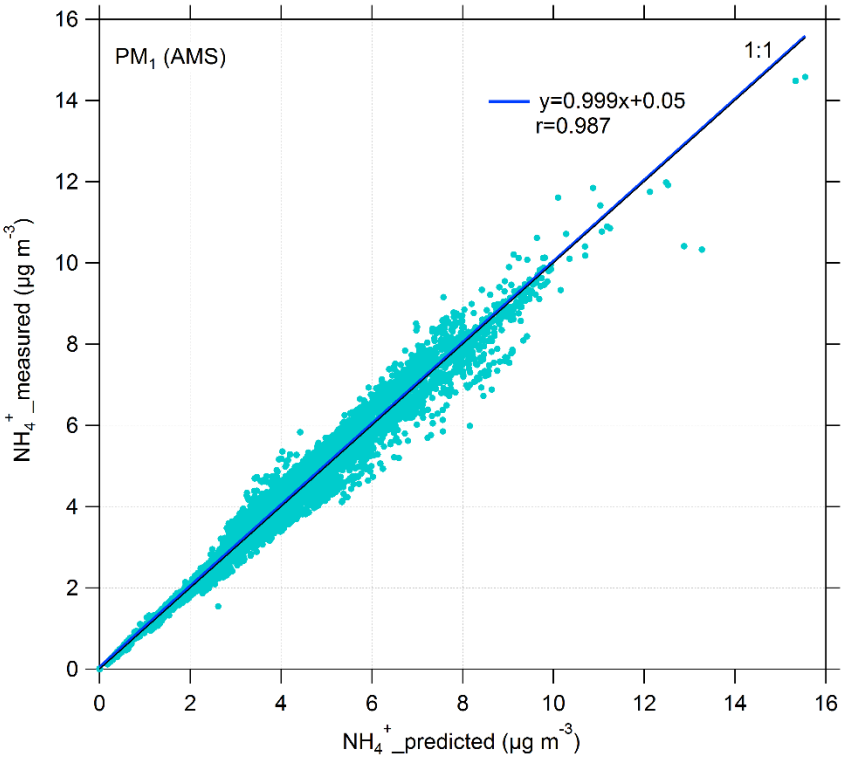

Figure R4. Scatter plots between AMS measured NH_4^+ and predicted NH_4^+.

3. The authors claimed several times the unique of this study "unique geographical and meteorological conditions", particularly in the abstract. But I didn't see the details for this uniqueness (the authors didn't describe it either except high relative humidity).

Response: The "unique geographical and meteorological conditions" in the Sichuan Basin was addressed as "*High emissions of gaseous and particulate pollutants, such as volatile organic compounds (VOCs), SO_2, organic carbon (OC), black carbon (BC) and fine particles ($PM_{2.5}$), are found in the Sichuan Basin over China (He, 2012). Adversely influenced by the particular topographic condition, the Sichuan Basin is within the region of the lowest wind speed and relatively high humidity over China all year round (Chen and Xie, 2013; Yang et al., 2011). The highest annual mean aerosol optical depth (AOD) in the Sichuan Basin from 2000 to 2010 across China reflected the importance of large topography in aerosol accumulation (Luo et al., 2013).*" in Paragraph 1 in the Introduction.

The topography of the Sichuan Basin is shown in Fig. S1 in the supplementary material. The backward trajectory clusters of air masses during the observation periods illustrated in **Fig. 1** showed that "*the atmospheric processes were dominated by the isolated meteorology of the basin*" (**Page 5, Line 21**).

All these gave the details for the "*unique geographical and meteorological conditions*".

4. The authors emphasized "influenced by biomass burning" in the title, however this manuscript appears to miss this point in both abstract and text.

Response: In the abstract, we mentioned that "*During the episode obviously influenced by primary emissions, the contributions of BBOA to OA (26%) and PM_1 (11%) were much higher than those (10-17%, 4-7%) in the clean and other polluted episodes, highlighting the significant influence of biomass burning."*

In the Paragraph 2 in the Introduction, we summarized the contribution of biomass burning to aerosol pollution in the Sichuan Basin, and explained why "*it is necessary to investigate secondary formation in the influence of biomass burning by using high time resolution aerosol mass spectra*".

For the Results and discussion Sect., we resolved the BBOA component of OA, and investigated the secondary formation in the influence of biomass burning (Paragraph 3 in Sect. 3.2.3, Paragraph 3 in Sect.3.3.2, and Sect. 3.3.4).

Thank you very much for your helpful comments. Your any further comments and suggestions are appreciated.

Referee #2

General comments:

The authors present detailed chemical characteristics of atmospheric submicron particles by performing a wintertime field observation at a suburban site in the Sichuan Basin, southwestern China, using multiple advanced instruments such as HR-ToF-AMS, MAAP, GC-MS/FID, PTR-MS, and TEM-EDX. On the basis of AMS high-resolution mass spectra data, four OA factors were identified by PMF source apportionment analysis. Secondary formation and aging process of organic aerosols were also investigated with different approaches; especially, significant influence contributed by biomass burning was discussed.

I would recommend this paper to be accepted after more in depth discussions are included, and after the following specific comments are addressed.

Response: Thanks for Reviewer's comment. We have revised the paper according to Referee's comments to improve the quality of this manuscript. Please see the detailed response below and changes marked in blue in the revised manuscript.

Specific comments:

1. The **Introduction** section is not logically connected well with the Results and Discussion part, which mainly focuses on particle chemical characterization, secondary OA formation, aging processes of OA, and the possible influence of biomass burning on these properties. Relating to the abovementioned topics, previous studies and corresponding results, especially in this studied region, were expected to be summarized in the introduction instead of simply included in results and discussion (e.g. Sect. 3.3.4). The introduction described much previous work on poor visibility/haze issues; however the connections with the discussion part were not clearly illustrated. The authors did not explain well why high time resolution particle chemical characterization in Sichuan Basin is needed, and why it is necessary to investigate secondary formation in the influence of biomass burning by using high time resolution aerosol mass spectra here (**paragraph 2, Page 3**).

Throughout the paper: The authors often use the term **biomass burning** organic aerosol (BBOA) to indicate OA contributed by domestic cooking (COA) and residential heating (e.g. Page 3, line 20). On Page 3, line 22-23, biomass burning is actually included in biogenic sources; thus biomass burning could also originate from other open fires such as rice straw burning and forest fires. On Page 4, line 13-15, the authors have pointed out that BBOA and COA are regarded as two different primary sources of OA in some studies, although complete identification among BBOA, COA, and CCOA with PMF analysis is not easy in practice. To avoid confusion during using these different expressions, it would be better to keep a consistent way, and define biomass burning and BBOA of this study clearly in the very beginning.

I would suggest the authors to reorganize the Introduction to better connect with the topics discussed in this manuscript.

Response: We reorganized the Introduction according to Referee's suggestions.

In the revision, the content in Sect. 3 "*The aging process plays an important role in the life cycle of atmospheric aerosols. The chemical composition, hygroscopicity and solubility of atmospheric aerosols are varied due to the aging process, which not only influences their optical properties and capability to form clouds, but also changes their impacts on environment, climate and human health. The aging process of OA can be characterized by some metrics and tools, including C/H/O atomic ratios, van Krevelen diagram (VK diagram), OA/OC ratio, OA/ΔCO, average carbon oxidation state ($\overline{OS_C}$), and the abundance of characteristic fragment ions (f_{43} and f_{44}), etc., to provide the basis for model simulation of SOA formation (de Gouw and Jimenez, 2009; Kroll et al., 2011; Hu et al., 2013).*" was moved into the Introduction.

The contents of previous work on poor visibility/haze issues in the Introduction "*The Sichuan Basin has suffered from long-term poor visibility since the 1970s (Chen and Xie, 2012, 2013). The visibility degradation primarily results from anthropogenic pollutants and synoptic processes. Anthropogenic aerosols and moisture at the surface are the dominant determinants of the AOD, and the spatial distributions of both AOD and light extinction coefficient (B_{ext}) are strongly influenced by regional*

topography (Wang et al., 2013)." "*Severe visibility deterioration and frequent hazy days have become vital concerns in the Sichuan Basin.*" were deleted.

In the text, we mentioned that "*variability of fine particle concentrations and physiochemical characteristics serves as another crucial factor in explaining the degradation of air quality in the Sichuan Basin*", "*Though several published papers focused on aerosol chemical and physical properties in the Sichuan Basin, highly time-resolved studies are rarely conducted*". In addition, according to previous studies, biomass burning contributes importantly to air pollution in the Sichuan Basin (Wang et al., 2013; Yang et al., 2011), and secondary pollutants from biomass burning significantly influence local and regional air quality, chemical processes, and even climate change (Niu et al., 2016). Therefore, *"high time resolution particle chemical characterization in Sichuan Basin is needed"*, and "*it is also necessary to investigate secondary formation in the influence of biomass burning by using high time resolution aerosol mass spectra*".

In the revision, we added "***Further, biomass burning contributes importantly to air pollution in the Sichuan Basin (Wang et al., 2013; Yang et al., 2011). Secondary formation from biomass burning emissions can significantly influence local and regional air quality, atmospheric processes, and even climate change (Niu et al., 2016).***" in Page 3, Line 11.

We agree with that "*biomass burning could also originate from other open fires such as rice straw burning and forest fires*", but according to the season (winter) of this study and vegetation cover in the Sichuan Basin, house heating with wood and straw is much more common (*Wang et al., 2013; Yang et al., 2011*) than "*rice straw burning and forest fires*". Based on previous studies, COA resolved by AMS-PMF analysis, refers to OA emitted by food during cooking activities, with no relation to fuels for cooking (Allan et al., 2010).

In the revision, "***Noted that COA refers to OA emitted by food during cooking activities, with no relation to fuels for cooking (Allan et al., 2010).***" was added in Page 4, Line 15.

To avoid confusion, Page 3, Line 20, "*biomass burning emissions via residential cooking and heating*" was changed into "***biomass burning as residential fuels***".

Page 12, Line 8, "*cooking emissions*" was changed into "***COA***".

Page 12, Line 10, "*Biomass burning via cooking and house heating*" was changed into "***Residential biomass burning***".

2. **Introduction**, Page 4, line 3-5

How should this sentence be understood? Why is primary organic aerosol excluded from the discussion here (only SOA is included)? Is there any difference between OM and OA?

Response: In the revision, "***Many studies refer to the particulate organic matter (OM)***" was revised into "***Many studies refer to secondary organic aerosols (SOA)***". Particulate organic matter and organic aerosol have the same meaning. To avoid confusing, in the whole manuscript, "OM" (abbreviated form of organic matter or organic mass) was replaced by "OA".

3. **Methodology**, Page 5, line 8

What is the elevation of the sampling site itself? How did you choose the altitude of the starting point of the backward trajectory calculation?

Page 5, line 12, *"Therefore, the atmospheric processes are dominated by the isolated meteorology of the basin."*

Did the backward trajectory analysis really support this idea?

Response: The elevation range of the Sichuan Basin bottom is about 200-800 m (Ziyang, 300-550 m), and the basin was surrounded by plateaus and mountains at the elevation of 2000-3000 m. However, the altitude of the starting point of the backward trajectory calculation **has no relation to the elevation of the sampling site**, and it is the height above ground level (AGL). The altitude of 500 m-AGL was selected as an approximation of the well-mixed boundary layer (Huang et al., 2010; Lu et al., 2012). So the backward trajectory analysis could support that "*the atmospheric processes are dominated by the isolated meteorology of the basin."*

In the revision, "***above ground level***" was added in Page 5, L17.

4. Although the chemical composition analysis is focusing on submicron particles, the actual cut-size of MAAP is $PM_{2.5}$, while that of HR-ToF-AMS is PM_1. How did the authors consider this mismatch

of two different size ranges into the mass fraction calculation, which could vary significantly with different proportions of BC accounted for PM_1? Relevant details should be provided in the measurement and data processing descriptions.

Response: Ambient BC particles are largely found in the Aitken and accumulation modes (i.e., in the submicron range) because of their formation mechanism (Bond et al., 2013; Huang et al., 2012a; Rose et al., 2006). The sum of non-refractory species measured by HR-ToF-AMS and BC measured by instruments such as MAAP or aethalometer with the cut-size of 2.5 μm is often treated as total PM_1 in previous studies (Huang et al., 2010, 2012b, 2013; He et al., 2011; Hu et al., 2013, 2016). In this study, the morphology of individual particles also indicated that the sizes of soot particles were less than 1 μm (Fig. 4). So we thought this match has little influence on PM_1.

In the revision, "***Atmospheric BC particles are mostly in the Aitken and accumulation modes (i.e., in the submicron range) because of their formation mechanisms (Bond et al., 2013).***" was added in Page 6, Line 16.

5. Page 7, line 1-2

Why RIE = 4.04 was applied to ammonium? Can you provide any reference or supporting information?

The recommended value of CE = 0.5 is used. Are there any comparative results or strong supporting evidence to verify its applicability? Middlebrook et al. (2011) have demonstrated the composition-dependence of CE with field measurements, suggesting that CE could be higher when ambient particles are composed of high fraction of ammonium nitrate or strongly acidic sulfate. This phenomenon could be significant especially under high RH conditions. In this sense, these issues may need to be considered, as high RH conditions were frequently observed during the investigation period of this work.

Response: The RIE=4.04 was used for ammonium quantification in this study by assuming PM_1 was neutral, and K^+ and other crustal ions were ignorable in submicron size range. That is, as RIE=4.04, the predicted and measured NH_4^+ exhibited good consistency with a slope of 0.999, and the uncertainty of measured NH_4^+ mass concentration caused by K^+ (assuming all K^+ existed in submicron size range

and PM_1) was neutral was 6.7%. Please refer to the response to Comment 2 of Referee #1 for more details.

In the revised manuscript, "***except for ammonium for which RIE=4.04 was used assuming PM_1 was neutral and other metallic species were ignorable in PM_1 (water-soluble K^+, Ca^{2+}, Mg^{2+}, and Na^+ were 1.22, 0.25, 0.04, and 0.21 $\mu g\ m^{-3}$ in $PM_{2.5}$).***" was added in Page 7, Line 16.

The chemical composition-based estimation of CE was estimated following the method addressed in Middlebrook et al. (2012). Only in the morning and afternoon on 13 December, the calculated CE reached to 0.51 for several hours due to high fraction of ammonium nitrate. The calculated CE showed little variations dependent on aerosol acidity and fraction of ammonium nitrate (mostly 0.45). Therefore, in order to compare with previous studies, here the recommended value of CE = 0.5 was used.

In the revision, "***All algorithm results of AMS collection efficiencies (CE) based on aerosol chemical compositions and sampling line RH (Middlebrook et al., 2012) were approximately 0.5***." was added in Page 7, Line 11.

6. **Results and discussion**, Page 9, line 4

Is this sentence describing inorganic species or organic species?

Response: This sentence "*Since the secondary compositions were dominant in PM_1…*" is describing both inorganic and organic species. As described above, the main chemical compositions, SNA accounted for about 49%, and OA accounted for about 36% of PM_1, to which SOA should contribute a part (we haven't mentioned it until Sect. 3.2). So here we described that "*the secondary compositions were dominant in PM_1*".

7. Page 9, line 7

"However, the humid air caused by the precipitation may favor the aqueous-phase secondary formation and hygroscopic growth of SNA in turn."

How should the reader understand "and hygroscopic growth of SNA in turn" here? Please provide some necessary supporting information and illustrate the connections clearly.

Response: In the revision, "*However, the humid air caused by the precipitation may favor the aqueous-phase secondary formation and hygroscopic growth of SNA in turn*" was changed into "***However, the humid air after the precipitation may favor the aqueous-phase secondary formation and hygroscopic growth of SNA, causing the stable or even slightly increased concentration of SNA (Fig.2)***".

8. **Sect. 3.1.2**, Page 10, line 1

"It was consistent with the morphology and mixing state of single particles, mostly spherical and in internal mixing state (Fig. 4a-d)."

It is not clear to me if Fig.4 really supports the authors' conclusion. At least, some aggregated soot particles can be clearly seen. Besides, the size resolution of TEM images is 2 μm, much larger than submicron or even ultrafine size ranges.

Response: According to **Fig. 4**, the equivalent diameters (Niu et al., 2011, 2012) of most particles were in submicron range. Most particles were spherical and in internal mixing state. Aggregated soot particles only accounted for a very small part because fresh soot particles in chain or aggregate shape could be modified into core-shell structure rapidly in the atmosphere (Niu et al., 2011, 2012). The individual particle analysis is being further conducted and will be prepared to be published.

9. Page 10, line 4

"… indicating that the aerosols at Ziyang site may be ***more aged*** *than in other areas."* How did you arrive at this conclusion? The higher peak sizes only demonstrate that particles are larger.

Response: *"… indicating that the aerosols at Ziyang site may be more aged than in other areas."* was revised into *"****…implying that the aqueous reactions under the high RH condition in Ziyang could cause a faster particle growth rate of secondary species than in other areas (Hu et al., 2016).***"

10. **Sect. 3.2.1**, Page 11, line 10

"The MS of HOA correlated well with the average MS of HOA factor reported in previous studies, as well as that of COA, BBOA and vehicle emitted OA (Vehicle-OA) factors (Table S3). Thus, it was likely that the HOA factor was a mixture of COA and other primary organic aerosols."

In this case, could it be possible to resolve different factors better by increasing the number of factors for the PMF analysis? It is hard to believe that emissions from the three sources (COA, BBOA, and Vehicle-OA) correlate well all the time. The HR-ToF-AMS simply observes fragments. Is there any possibility that there was a specific source of OA during the observation in that area? m/z 60 exists in the HOA factor. Where does it come from: coal combustion or biomass burning?

Response: We tried to resolve more factors for PMF analysis. While according to the dialogistic parameters, correlation between OA factors and external tracers, and uncentered correlations between the MS of OA factors resolved in this study and the average MS of reported OA factors, the result of four factors was the optimal solution as described in Sect. S1.

As described in the text, "*Factor analysis (e.g., PMF analysis) suffers a limitation, as it is incapable of separating independent sources completely, and the resolved factor may be a mixture of various sources.*" HOA is a surrogate for urban, combustion-related POA except the identified factors, such as BBOA, COA, and CCOA (Zhang et al., 2011).

The resolved HOA factor in this study was considered to be a mixture of other primary emitted OA, such as COA and Vehicle-OA according to the results of correlation analysis (Table S2 and Table S3), but we couldn't conclude that the emissions from primary sources, such as COA, BBOA, and Vehicle-OA, correlated well all the time.

Coal combustion emissions can contribute to *m/z 60* ($C_2H_4O_2^+$) (Aiken et al., 2010; Hu et al., 2016). The low abundances of *m/z 60* ($C_2H_4O_2^+$) in both HOA and BBOA factors were also appeared in previous studies (DeCarlo et al., 2010; He et al., 2011; Hu et al., 2016; Huang et al., 2013; Ulbrich et al., 2012). The low abundances of *m/z 60* were also found in the resolved COA factors by Hu et al. (2016) and Huang et al. (2010). So the *m/z 60* in HOA factor in this study could be from coal combustion or other combustion emission sources.

11. **Sect. 3.2.2**, Page 12, line 13

"… presented good correlations with BC and acetaldehyde (Table S4), which were mainly emitted from ***primary sources****."*

Can you tell that it is only emitted from biomass burning, or is it also contributed by other types of primary sources?

Response: We cannot assure that BC and acetaldehyde were only emitted from biomass burning. BC and acetaldehyde can also be contributed by other types of primary sources. So we described that they "*were mainly emitted from primary sources"*.

In the revision, "*which were mainly emitted from primary sources*" was revised into "***which could be partly emitted from biomass burning***".

12. **Sect. 3.2.3**, Page 12, line 18

"… as the influence of biomass burning is ***negligible****."*

Applicability of this assumption depends on characteristics of specific observation site, even though some studies have suggested insignificant influences of biomass burning on OA. The authors have also highlighted that BBOA contributes significantly to their data. Accordingly, this concept may not be justified in this study.

Response: Jimenez et al. (2009) reviewed that there is strong evidence that most atmospheric OOA is secondary, and OOA levels are consistent with SOA estimates using other methods. Ng et al. (2011) also concluded that OOA are good surrogates for SOA under most conditions. Herndon et al. (2008) and Lanz et al. (2007) resolved both BBOA and OOA factors in their studies, and also found that increases in OOA are strongly correlated with photochemical activity and other secondary species.

In the revision, "*… as the influence of biomass burning is negligible*" was changed into "***…under most conditions (Jimenez et al., 2009; Ng et al., 2011)***".

13. Page 13, line 4

"In this study, LV-OOA ***correlated well*** *with SNA (r=0.66-0.68)".*

Is the reported ***r* value** considered as an indication of good correlation?

Response: The significance of Pearson correlation coefficient "***p<0.01***" was added in Page, Line, and also added after other Pearson correlation coefficients in the whole manuscript.

14. Page 13, line 8

"LV-OOA also showed a similar trend to BC (r=0.75), ***maybe because*** *BC was difficult to diffuse and mixed well in the static air."*

The statement is confusing and ambiguous. How should readers understand it?

Response: In the revision, *"LV-OOA also showed a similar trend to BC (r=0.75),* ***maybe because*** *BC was difficult to diffuse and mixed well in the static air"* was changed into *"****LV-OOA also showed a similar trend to BC (r=0.75), because the aged OA can mix well with BC due to the static air in the basin.****"*

15. **Sect. 3.3.4**, Page 19, line 2

"The increase of OA …, ***which*** *was approximate to that reported at Changdao Island …"*

Does the "which" mean the slope of increased OA or contribution of SOA?

Response: Herein "which" means the slope of increased OA. In the revision, "*The increase of OA (1.2 μg* m^{-3} *ppmv*$^{-1}$ h^{-1}*) was almost completely attributed to the contribution of SOA, which was approximate to that reported at Changdao Island (1.3 μg* m^{-3} *ppmv*$^{-1}$ h^{-1}*) and lower than the ratios (2-5 ppmv*$^{-1}$ h^{-1}*) reported in Mexico City and the US (Hu et al., 2013).*" was changed into "***The increasing slope of OA (1.2 μg*** m^{-3} ***ppmv***$^{-1}$ h^{-1}***), which was approximate to that at Changdao Island (1.3 μg*** m^{-3} ***ppmv***$^{-1}$ h^{-1}***) and lower than those (~2-5 ppmv***$^{-1}$ h^{-1}***) in Mexico City and the US (Hu et al., 2013), was almost completely attributed to the contribution of SOA.***"

16. Page 19, line 5

"… the average OA/ΔCO ratio decreased with photochemical age, caused by the decrease of LV-OOA/ΔCO ratio." Is it still valid if the *SV-OOA/ΔCO ratio* increased at the same time?

The following descriptions of the subsequent sentence are unclear. Please clarify them so that the readers can understand it clearly. Namely, how should the readers understand the "**relatively stable** SV-OOA concentrations" resulted from "inhibited evolution from POA to SV-OOA", while "inhibited evolution from POA to LV-OOA resulting in **lower** LV-OOA"?

Response: *"… the average OA/ΔCO ratio decreased with photochemical age, caused by the decrease of LV-OOA/ΔCO ratio"* is a description of the data in Fig. 11a. It was still valid in this study as the SV-OOA/ΔCO ratio slightly increased at the same time. In the revision, "***(Fig. 11a)***"was added in Page 19, Line 16.

According to atmospheric observations and laboratory experiments, as photochemistry proceeds, the signature of OA is transformed and the OA spectra become more similar first to that of ambient SV-OOA and then increasingly to that of LV-OOA. Atmospheric oxidation of OA converges toward highly aged LV-OOA regardless of the original OA sources, with the original source signature being replaced by that of atmospheric oxidation (Jimenez et al., 2009). In this study, the intermediate product, SV-OOA, was already dominant in OA with the increase of the photochemical age, consistent with previous observations in the urban, suburban and even rural areas (Jimenez et al., 2009). So the "lower LV-OOA concentrations" can result from "inhibited evolution from POA to LV-OOA", while the SV-OOA concentration maintained relatively stable.

In the revision, "***Atmospheric oxidation of OA converges toward greatly aged LV-OOA despite of the original OA sources (Jimenez et al., 2009).***" was added in Page 19, Line 16.

In Page 19, Line 20, "***because SV-OOA was already dominant in OA (Jimenez et al., 2009)***" was added.

17. Page 19, line 10

"SOA dominated OA (56-84%) in both ***fresh*** *and aged plumes…"*

Do you need to define the "fresh" plume in this work to distinguish it from "aged" ones, or provide a certain threshold value in terms of different photochemical ages?

Response: According to Fig. 11b, OOA dominated OA at different photochemical ages, so here we didn't define the "fresh" plumes to distinguish it from "aged" ones. In the revision, *"SOA dominated OA (56-84%) in both fresh and aged plumes…"* was changed into "***OOA dominated OA (56-84%) in both fresh and aged plumes…****"*.

18. Page 19, line 15

"… implying that the photochemical formation of SV-OOA was more efficiently than that of LV-OOA in this campaign."

Is this conclusion applicable only to cases for longer photochemical age? We can find from Fig.11 that the fractions of SV-OOA are not always higher than that for LV-OOA, especially when the photochemical age is less than about 6h.

Response: **Page 20, Line 1**, "*In aged plumes*" was revised into "***as the photochemical age longer than 6 h (Fig. 11)***".

19. Figure 1

In addition to wind speed, wind direction is also an important indicator of air mass origin or possible influence by transportation. Perhaps you can try to display both wind speed and direction parameters in Fig.1 (a) and discuss accordingly.

Response: As mentioned in the manuscript, "*the stagnant air prevailed in the one-month campaign due to the basin terrain"* (Page 5, Line 19) and "*during the whole campaign, calm occurred frequently (Fig. 2a)*" (Page 9, Line 3), so we didn't display the wind direction.

20. The whole passage is generally well organized; however some important statistics of chemical information are expected to be presented in the manuscript, instead of the supplementary materials. For example, **Table S1** actually contains many new and interesting primary results obtained from this study. The mass concentrations of BC under different meteorological conditions could also be a good case. The contribution of BC to PM_1 has been included in abstract and conclusion sections, indicating the importance of BC in chemical characteristics of submicron particles. The corresponding results would be more straightforward to readers if shown in the manuscript.

Response: Thanks for Referee's Comment. Table S1 was moved into the manuscript as Table 1, and the contents related to Table 1 were revised accordingly.

Technical corrections:

1. **Introduction**, Page 2, line 9

"… has become one of the most polluted regions in China."

Corresponding references are needed, as well as for the specific values that are not obtained from this study (e.g., Page 3, line 17 and 19).

Response: "*(Chen and Xie, 2012)*" was added after "*… has become one of the most polluted regions in China."*

"*The concentration of OA in molecular level using GC/MS analysis was extremely high (9.7 μg m^{-3} in winter) in Chongqing because of its active industrialization and urbanization. Anthropogenic sources, such as coal combustion, cooking and vehicle emissions, contributed to OA primarily. Levoglucosan occupied around 90% of total identified sugars in winter (700 ng m^{-3}) and summer (123 ng m^{-3}). The high levels of levoglucosan were most likely caused by biomass burning emissions via residential cooking and heating, especially in winter (Wang et al., 2006).*" was revised into "***Wang et al. (2006) reported that the concentration of OA identified in molecular level was extremely high (9.7 μg m^{-3}) in winter in Chongqing because of its active industrialization and urbanization. Anthropogenic sources, such as coal combustion, cooking and vehicle emissions, contributed to OA primarily. High levels of levoglucosan, most likely emitted from biomass burning as residential fuels, occupied around 90% of total identified sugars (700 ng m^{-3}) (Wang et al., 2006).***"

2. **Methodology**, Page 7, line 13

"… the diurnal patterns of different factors, etc. (Zhang et al., 2011)".

Please specify the "etc" clearly.

Response: *As described in Zhang et al. (2011), "the interpretability of the OA factors should be evaluated on the basis of their mass spectral features and temporal variation patterns." "The interpretations of the OA factors are usually based on the following considerations:*

1. the temporal correlations of factors with tracer species representative of specific emissions and processes;

2. the mass spectral features of each factor, for example peak distribution patterns, signature fragments, and oxidation state;

3. the repetitive temporal or diurnal variation patterns that are indicative of specific human activities or meteorological patterns (for example traffic rush hours, dilution because of the increase of the planetary boundary layer, cooking emissions during mealtimes, photochemical production of secondary species, etc.);

4. the estimated size distributions of OA factors (or tracer ions) and their evolution patterns;

5. information regarding airmass trajectories and locations of upwind source regions; and

6. other collocated observations that enable the isolation of special cases (e.g., new particle formation and growth events identified according to scanning mobility particle sizer measurements and well-defined SOA growth events)."

In the revision, *"…be defined via comparing … the diurnal patterns of different factors, etc. (Zhang et al., 2011)" was revised into "**…be evaluated via comparing … the diurnal patterns of different factors (Zhang et al., 2011).**"*

3. **Sect. 3.2**, Page 10

*"**SOA** (OOA) dominated in OA as much as 71% …"*

*"… secondary formation (**SOA**+SNA) …"*

Please be careful when using SOA and OOA, as OOA is not completely the same as SOA.

Response: As mentioned in the response to Comment 12, OOA are good surrogates for SOA under most conditions.

In the revision, *"**SOA** (OOA) dominated in OA as much as 71% …" was revised into "**OOA dominated in OA as much as 71% …**", "secondary formation (**SOA**+SNA) contributed to PM_1 as high as 76%" was revised into "**secondary formation (OOA+SNA) contributed to PM_1 as high as 76%**".*

4. **Sect. 3.3.4**, Page 19, line 21

"… and reached saturation frequently (Table S1)."

Does it mean average RH or RH?

Response: It means the measured RH, and the measurement time-resolution for meteorological parameters was one minute. In the revision, "*The average RH in Ziyang during the campaign was 80±19% (12-100%), and reached saturation frequently (Table S1)*" was changed into "***The RH in Ziyang during the campaign was 80±19% (12-100%) on average (Table 1), and reached saturation frequently***".

Thank you very much for your helpful comments. Your any further comments and suggestions are appreciated.

Reference:

Aiken, A. C., de Foy, B., Wiedinmyer, C., DeCarlo, P. F., Ulbrich, I. M., Wehrli, M. N., Szidat, S., Prevot, A. S. H., Noda, J., Wacker, L., Volkamer, R., Fortner, E., Wang, J., Laskin, A., Shutthanandan, V., Zheng, J., Zhang, R., Paredes-Miranda, G., Arnott, W. P., Molina, L. T., Sosa, G., Querol, X., and Jimenez, J. L.: Mexico city aerosol analysis during MILAGRO using high resolution aerosol mass spectrometry at the urban supersite (T0) - Part 2: Analysis of the biomass burning contribution and the non-fossil carbon fraction, Atmos. Chem. Phys., 10, 5315-5341, 2010.

Allan, J. D., Williams, P. I., Morgan, W. T., Martin, C. L., Flynn, M. J., Lee, J., Nemitz, E., Phillips, G. J., Gallagher, M. W., and Coe, H.: Contributions from transport, solid fuel burning and cooking to primary organic aerosols in two UK cities, Atmos. Chem. Phys., 10, 647-668, 2010.

Bond, T. C., Doherty, S. J., Fahey, D. W., Forster, P. M., Berntsen, T., DeAngelo, B. J., Flanner, M. G., Ghan, S., Kärcher, B., Koch, D., Kinne, S., Kondo, Y., Quinn, P. K., Sarofim, M. C., Schultz, M. G., Schulz, M., Venkataraman, C., Zhang, H., Zhang, S., Bellouin, N., Guttikunda, S. K., Hopke, P. K., Jacobson, M. Z., Kaiser, J. W., Klimont, Z., Lohmann, U., Schwarz, J. P., Shindell, D., Storelvmo, T., Warren, S. G., and Zender, C. S.: Bounding the role of black carbon in the climate system: A scientific assessment, J. Geophys. Res. Atmos., 118, 5380-5552, 10.1002/jgrd.50171, 2013.

Chen, Y., and Xie, S.: Long-term trends and characteristics of visibility in two megacities in southwest China: Chengdu and Chongqing. J. Air Waste Man. Ass., 63, 1058-1069, 2013.

Chen, Y., and Xie, S.: Temporal and spatial visibility trends in the Sichuan Basin, China, 1973 to 2010. Atmos. Res., 112, 25-34, 2012.

DeCarlo, P. F., Ulbrich, I. M., Crounse, J., de Foy, B., Dunlea, E. J., Aiken, A. C., Knapp, D., Weinheimer, A. J., Campos, T., Wennberg, P. O., and Jimenez, J. L.: Investigation of the sources and processing of organic aerosol over the Central Mexican Plateau from aircraft measurements during MILAGRO, Atmos. Chem. Phys., 10, 5257-5280, 2010.

Guo, S., Hu, M., Wang, Z., Slanina, J., and Zhao, Y.: Size-resolved aerosol water-soluble ionic compositions in the summer of Beijing: implication of regional secondary formation, Atmos. Chem. Phys., 10, 947-959, 2010.

He, L. Y., Huang, X. F., Xue, L., Hu, M., Lin, Y., Zheng, J., Zhang, R., and Zhang, Y. H.: Submicron aerosol analysis and organic source apportionment in an urban atmosphere in Pearl River Delta of China using high−resolution aerosol mass spectrometry, J. Geophys. Res. Atmos., 116, 2011.

He, L. Y., Lin, Y., Huang, X. F., Guo, S., Xue, L., Su, Q., Hu, M., Luan, S. J., and Zhang, Y. H.: Characterization of high-resolution aerosol mass spectra of primary organic aerosol emissions from Chinese cooking and biomass burning, Atmos. Chem. Phys., 10, 11535-11543, 2010.

Herndon, S. C., Onasch, T. B., Wood, E. C., Kroll, J. H., Canagaratna, M. R., Jayne, J. T., Zavala, M. A., Knighton, W. B., Mazzoleni, C., Dubey, M. K., Ulbrich, I. M., Jimenez, J. L., Seila, R., de Gouw, J. A., de Foy, B., Fast, J., Molina, L. T., Kolb, C. E., and Worsnop, D. R.: Correlation of secondary organic aerosol with odd oxygen in Mexico City, Geophys. Res. Lett., 35, 2008.

Hu, W. W., Hu, M., Yuan, B., Jimenez, J. L., Tang, Q., Peng, J. F., Hu, W., Shao, M., Wang, M., Zeng, L. M., Wu, Y. S., Gong, Z. H., Huang, X. F., and He, L. Y.: Insights on organic aerosol aging and the influence of coal combustion at a regional receptor site of central eastern China, Atmos. Chem. Phys., 13, 10095-10112, 2013.

Hu, W., Hu, M., Hu, W., Jimenez, J. L., Yuan, B., Chen, W., Wang, M., Wu, Y., Chen, C., Wang, Z., Peng, J., Zeng, L., and Shao, M.: Chemical composition, sources and aging process of sub-micron aerosols in Beijing: contrast between summer and winter, J. Geophys. Res. Atmos., 10.1002/2015JD024020, 2016.

Huang, X.-F., He, L.-Y., Hu, M., Canagaratna, M., Sun, Y., Zhang, Q., Zhu, T., Xue, L., Zeng, L.-W., and Liu, X.-G.: Highly time-resolved chemical characterization of atmospheric submicron particles during 2008 Beijing Olympic Games using an Aerodyne High-Resolution Aerosol Mass Spectrometer, Atmos. Chem. Phys., 10, 8933-8945, 2010.

Huang, X.-F., Sun, T.-L., Zeng, L.-W., Yu, G.-H., and Luan, S.-J.: Black carbon aerosol characterization in a coastal city in South China using a single particle soot photometer, Atmos. Environ., 51, 21-28, 2012.

Huang, X.-F., He, L.-Y., Xue, L., Sun, T.-L., Zeng, L.-W., Gong, Z.-H., Hu, M., and Zhu, T.: Highly time-resolved chemical characterization of atmospheric fine particles during 2010 Shanghai World Expo, Atmos. Chem. Phys., 12, 4897-4907, 2012.

Huang, X.-F., Xue, L., Tian, X.-D., Shao, W.-W., Sun, T.-L., Gong, Z.-H., Ju, W.-W., Jiang, B., Hu, M., and He, L.-Y.: Highly time-resolved carbonaceous aerosol characterization in Yangtze River Delta of China: Composition, mixing state and secondary formation, Atmos. Environ., 64, 200-207, 2013.

Huang, X., Yun, H., Gong, Z., Li, X., He, L., Zhang, Y., and Hu, M.: Source apportionment and secondary organic aerosol estimation of $PM_{2.5}$ in an urban atmosphere in China, Sci. China Earth Sci., 57, 1352-1362, 2013.

Jimenez, J. L., Canagaratna, M. R., Donahue, N. M., Prevot, A. S. H., Zhang, Q., Kroll, J. H., DeCarlo, P. F., Allan, J. D., Coe, H., Ng, N. L., Aiken, A. C., Docherty, K. S., Ulbrich, I. M., Grieshop, A. P., Robinson, A. L., Duplissy, J., Smith, J. D., Wilson, K. R., Lanz, V. A., Hueglin, C., Sun, Y. L., Tian, J., Laaksonen, A., Raatikainen, T., Rautiainen, J., Vaattovaara, P., Ehn, M., Kulmala, M., Tomlinson, J. M., Collins, D. R., Cubison, M. J., Dunlea, J., Huffman, J. A., Onasch, T. B., Alfarra, M. R., Williams, P. I., Bower, K., Kondo, Y., Schneider, J., Drewnick, F., Borrmann, S., Weimer, S., Demerjian, K., Salcedo, D., Cottrell, L., Griffin, R., Takami, A., Miyoshi, T., Hatakeyama, S., Shimono, A., Sun, J. Y., Zhang, Y. M., Dzepina, K., Kimmel, J. R., Sueper, D., Jayne, J. T., Herndon, S. C., Trimborn, A. M., Williams, L. R., Wood, E. C., Middlebrook, A. M., Kolb, C. E., Baltensperger, U., and Worsnop, D. R.: Evolution of Organic Aerosols in the Atmosphere, Science, 326, 1525-1529, 10.1126/science.1180353, 2009.

Lanz, V. A., Alfarra, M. R., B., B., Buchmann, U., Hueglin, C. a., and H., P. e. o. A. S.: Source apportionment of submicron organic aerosols at an urban site by factor analytical modelling of aerosol mass spectra, Atmos. Chem. Phys., 7, 1503–1522, 2007.

Li, L., Chen, Y., Zeng, L., Shao, M., Xie, S., Chen, W., Lu, S., Wu, Y., and Cao, W.: Biomass burning contribution to ambient volatile organic compounds (VOCs) in the Chengdu–Chongqing Region (CCR), China, Atmos. Environ. 99, 403-410, 2014.

Lu, Z., Streets, D. G., Zhang, Q., and Wang, S.: A novel back-trajectory analysis of the origin of black carbon transported to the Himalayas and Tibetan Plateau during 1996-2010, Geophys. Res. Lett., 39, 10.1029/2011gl049903, 2012.

Middlebrook, A. M., Bahreini, R., Jimenez, J. L., and Canagaratna, M. R.: Evaluation of composition-dependent collection efficiencies for the Aerodyne aerosol mass spectrometer using field data, Aerosol. Sci. Tech., 46, 258–271, 2011.

Ng, N. L., Canagaratna, M. R., Jimenez, J. L., Chhabra, P. S., Seinfeld, J. H., and Worsnop, D. R.: Changes in organic aerosol composition with aging inferred from aerosol mass spectra, Atmos. Chem. Phys., 11, 6465-6474, 2011.

Niu, H., Cheng, W., Hu, W., and Pian, W.: Characteristics of individual particles in a severe short-period haze episode induced by biomass burning in Beijing, Atmos. Pollut. Res., 10.1016/j.apr.2016.05.011, 2016.

Niu, H., Shao, L., and Zhang, D.: Aged status of soot particles during the passage of a weak cyclone in Beijing, Atmos. Environ., 45, 2699-2703, 2011.

Niu, H., Shao, L., and Zhang, D.: Soot particles at an elevated site in eastern China during the passage of a strong cyclone, Sci. Total Environ., 430, 217-222, 2012.

Ulbrich, I. M., Canagaratna, M. R., Cubison, M. J., Zhang, Q., Ng, N. L., Aiken, A. C., and Jimenez, J. L.: Three-dimensional factorization of size-resolved organic aerosol mass spectra from Mexico City, Atmos. Meas. Tech., 5, 195-224, 2012.

Wang, G. H., Kawamura, K., Lee, S., Ho, K. F., and Cao, J. J.: Molecular, seasonal, and spatial distributions of organic aerosols from fourteen Chinese cities, Environ. Sci. Tech., 40, 4619-4625, 2006.

Wang, Q. Y., Cao, J. J., Tao, J., Li, N., Su, X. O., Chen, L. W. A., Wang, P., Shen, Z. X., Liu, S. X., and Dai, W. T.: Long-Term Trends in Visibility and at Chengdu, China, Plos One, 8, doi: 10.1371/journal.pone.0068894, 2013.

Yang, F., Tan, J., Zhao, Q., Du, Z., He, K., Ma, Y., Duan, F., Chen, G., and Zhao, Q.: Characteristics of $PM_{2.5}$ speciation in representative megacities and across China, Atmos. Chem. Phys., 11, 5207-5219, 2011.

Zhang, Q., Jimenez, J. L., Canagaratna, M. R., Ulbrich, I. M., Ng, N. L., Worsnop, D. R., and Sun, Y.: Understanding atmospheric organic aerosols via factor analysis of aerosol mass spectrometry: a review, Anal. Bioanal. Chem., 401, 3045-3067, 2011.

Characterization of submicron aerosols influenced by biomass burning at a site in the Sichuan Basin, southwestern China

Wei Hu, Min Hu*, Wei-Wei Hu#, Hongya Niu, Jing Zheng, Yusheng Wu, Wentai Chen, Chen Chen, Lingyu Li, Min Shao, Shaodong Xie, Yuanhang Zhang

State Key Joint Laboratory of Environmental Simulation and Pollution Control, College of Environmental Sciences and Engineering, Peking University, Beijing 100871, China

#now at: Cooperative Institute for Research in Environmental Sciences, University of Colorado, Boulder, CO 80309, USA

Correspondence to: M. Hu (minhu@pku.edu.cn)

Abstract. Severe air pollution, which is caused by large amount of pollutants and adverse synoptic processes, appears often in Asia. However, limited studies on aerosols have been conducted under high emission intensity and under unique geographical and meteorological conditions. In this study, an Aerodyne high resolution time-of-flight aerosol mass spectrometry (HR-ToF-AMS) and other state-of-the-art instruments were utilized at a suburban site, Ziyang, in the Sichuan Basin during December 2012 to January 2013. The chemical compositions of atmospheric submicron aerosols (PM_1) were determined, the sources of organic aerosols (OA) were apportioned, and the aerosol secondary formation and aging process were explored as well. Due to high humidity and static air, PM_1 maintained a relatively stable level during the whole campaign, with the mean concentration of 59.7±24.1 μg m^{-3}. OA was the most abundant component (36%) in PM_1, characterized by a relatively high oxidation state. Positive matrix factorization analysis was applied to the high resolution organic mass spectral matrix, which deconvolved OA mass spectra into four factors: low volatility (LV-OOA) and semi-volatile oxygenated OA (SV-OOA), biomass burning (BBOA) and hydrocarbon-like OA (HOA). OOA (sum of LV-OOA and SV-OOA) dominated OA as high as 71%. In total, secondary inorganic and organic formation contributed 76% of PM_1. Secondary inorganic species correlated well with relative humidity (RH), indicating the humid air can favor the formation of secondary inorganic aerosols.

With the increase of photochemical age, OA became more aged with a higher oxidation state, and secondary organic aerosol formation contributed more significantly to OA. The slope of OOA against O_x (=O_3+NO_2) steepened with the increase of RH, implying that besides the photochemical transformation, the aqueous-phase oxidation was also an important pathway of the OOA formation. Primary emissions, especially biomass burning, resulted in high concentration and proportion of black carbon (BC) in PM_1. During the episode obviously influenced by primary emissions, the contributions of BBOA to OA (26%) and PM_1 (11%) were much higher than those (10-17%, 4-7%) in the clean and other polluted episodes, highlighting the significant influence of biomass burning.

1 Introduction

With its dense population and rapid economic development in the past decades, the Sichuan Basin suffers from serious fine particle pollution and has become one of the most polluted regions in China (Chen and Xie, 2012). The basin, located in the southwest of China, is one of the most populous regions in China and the world, with a population density of approximate 400 people per square kilometer. The two megalopolises, Chongqing and Chengdu, in the basin with the largest populations of about 30 and 14 million, respectively, have been seeing increases in industrial added values by an annual rate of over 10%. High emissions of gaseous and particulate pollutants, such as volatile organic compounds (VOCs), SO_2, organic carbon (OC), black carbon (BC), and fine particles ($PM_{2.5}$), are found in the Sichuan Basin over China (He, 2012). Adversely influenced by the particular topographic condition, the Sichuan Basin is within the region of the lowest wind speed and relatively high humidity over China all year round (Chen and Xie, 2013; Yang et al., 2011). The highest annual mean aerosol optical depth (AOD) in the Sichuan Basin from 2000 to 2010 across China reflected the importance of large topography in aerosol accumulation (Luo et al., 2013). Under the stable weather system, high relative humidity (RH) in Chengdu, and high RH, high pressure and low wind speed in Chongqing resulted in the low visibility. Since the 2000s, the air quality has been aggravated in the Sichuan Basin for more intense anthropogenic emissions (Chen and Xie, 2013). The unique geographical and meteorological conditions in the region favor the accumulation of local and regional atmospheric pollutants (Yang et al., 2011), making environmental threats in Sichuan more severe.

In addition to the adverse topographical and meteorological conditions, variability of fine particle concentrations and physiochemical characteristics serves as another crucial factor in explaining the degradation of air quality in the Sichuan Basin. Yang et al. (2011) reported that during cold periods, high $PM_{2.5}$ levels at 129 and 156 μg m^{-3}, of which organics and sulfate accounted for over 50%, were observed in Chengdu and Chongqing, respectively. High SO_4^{2-}/NO_3^- ratio indicated that local and stationary sources were predominant in the region where high-sulfur coal fuels are regularly consumed in large quantity; high K^+ concentration (more than 6 μg m^{-3}) in Chongqing during the winter suggested that biomass burning from residential heating also accounted for an important source of pollution (Yang et al., 2011; Cao et al., 2012). Wang et al. (2013) concluded that organics, ammonium bisulfate, ammonium nitrate, and moisture in fine particles contributed more than 86% to the B_{ext} in Chengdu; biomass burning, coal combustion, vehicular and industrial emissions were the main contributors to both $PM_{2.5}$ and the light-scattering coefficient. Though several published papers focused on aerosol chemical and physical properties in the Sichuan Basin, highly time-resolved studies are rarely conducted. Further, biomass burning contributes importantly to air pollution in the Sichuan Basin (Wang et al., 2013; Yang et al., 2011). Secondary formation from biomass burning emissions can significantly influence local and regional air quality, atmospheric processes, and even climate change (Niu et al., 2016). Therefore, it is necessary to explore secondary formation in the influence of biomass burning by using high time resolution aerosol mass spectrum.

Organic aerosols (OA) are very significant components in fine particulate matter (Zhang et al., 2007). Several results on the compositions and sources of OA in the Sichuan Basin have also been reported. Wang et al. (2006) found that the concentration of OA in molecular level was extremely high (9.7 μg m^{-3}) in winter in Chongqing because of its active industrialization and urbanization. Anthropogenic sources, such as coal combustion, cooking and vehicle emissions, contributed to OA primarily. High levels of levoglucosan that were most likely emitted from residential biomass burning, occupied around 90% of total identified sugars (700 ng m^{-3}) (Wang et al., 2006). Li et al. (2013a) drew that about 15-21% of the OC could be apportioned to biogenic sources and processes, e.g., biomass burning, isoprene oxidation products and fungal spores, at a forest site and an urban site in Ya'an in the Sichuan Basin, during the summer of 2010. High organic and elemental carbon (OC and EC) concentrations and OC/EC ratio were observed in urban Chengdu, which revealed that the formation of secondary organic

carbon (SOC) contributed to OC as 55% based on the EC tracer method (Zhang et al., 2008). These results suggested the important contributions of biomass burning and other primary emissions, as well as secondary formation to OA in the Sichuan Basin.

Many studies refer to secondary organic aerosols (SOA), as a product of atmospheric processes including the oxidation of VOCs, shifting of chemical equilibrium, re-partitioning of semi-volatile species, adsorption/absorption through heterogeneous physical and chemical processes, and cloud physiochemical processes (Kroll et al., 2005; Hallquist, et al., 2009). SOA makes up about 20-80% of OA in the atmosphere (Carlton et al., 2009), yet the formation mechanisms of SOA remain essentially speculative, causing discrepancies between observed SOA and model simulations. What precursors and chemical mechanisms are important therefore remains unclear (Hallquist, et al., 2009).

The employment of aerosol mass spectrometry (AMS, Aerodyne Research Inc., USA) not only can obtain high-resolution chemical composition of submicron aerosols, but also can allow source apportionment of primary organic aerosols (POA) and SOA (Ng et al., 2010). OA mass spectral matrix from Aerodyne AMS analyzed with a positive matrix factorization (PMF) technique (Paatero, 1997) resolved OA into several factors: oxygenated organic aerosol (OOA) factors described as low volatility and semi-volatile OOA (LV-OOA and SV-OOA), hydrocarbon-like (HOA), biomass burning (BBOA), cooking (COA) and coal combustion OA (CCOA), etc. (Jimenez et al., 2009; Ng et al., 2011; Hu et al., 2013, 2016). Noted that COA refers to OA emitted by food during cooking activities, with no relation to fuels for cooking (Allan et al., 2010). HOA, BBOA, COA and CCOA could be considered as POA; the OOA component has been shown to be a good surrogate SOA in many studies (Ng et al., 2010). Discrimination of different OA components can favor quantifying the primary and secondary contributions, and probing into secondary formation mechanisms and aging processes of OA (Ulbrich et al., 2009).

The aging process plays an important role in the life cycle of atmospheric aerosols. The chemical composition, hygroscopicity and solubility of atmospheric aerosols are varied due to the aging process, which not only influences their optical properties and capability to form clouds, but also changes their impacts on environment, climate and human health. The aging process of OA can be characterized by some metrics and tools, including C/H/O atomic ratios, van Krevelen diagram (VK diagram), OA/OC ratio, OA/ΔCO, average carbon oxidation state ($\overline{OS_C}$), and the abundance of characteristic fragment ions (f_{43} and f_{44}),

etc., to provide the basis for model simulation of SOA formation (de Gouw and Jimenez, 2009; Kroll et al., 2011; Hu et al., 2013).

In this study, an Aerodyne high resolution time-of-flight AMS (HR-ToF-AMS) was deployed at a suburban site in Ziyang, downwind of Chengdu City in the Sichuan Basin, in the heavily polluted winter. We obtained highly time-resolved chemical compositions and size distributions of non-refractory submicron aerosols (NR-PM_1), then apportioned the sources of OA, as well as investigated the secondary formation and aging process of OA under unique geographical and meteorological conditions. The results will give hints to the mechanism of haze formation and help control the serious air pollution in the Sichuan Basin.

2 Methodology

2.1 Sampling site

An intensive field campaign was carried out on the campus of a primary school in Ziyang (30.15° N, 104.64° E) during the wintertime from 3 December 2012 to 5 January 2013. The location of the observation site is shown in Fig. 1, and the topography of the Sichuan Basin is shown in Fig. S1 in the supplementary material. There were no obvious industrial sources around this site. Ziyang is a county-level city located in central Sichuan Basin, downwind of Chengdu Plain, and in between two megalopolises (90 km south of Chengdu and 260 km to the west of Chongqing). The observation site was selected and considered to be a fine representative to characterize the air pollution in the Sichuan Basin. The 72-h backward trajectories of air parcels at Ziyang site at an altitude of 500 m above ground level during the campaign were calculated by NOAA's HYSPLIT4.9 model (www.arl.noaa.gov/hysplit.html), starting a new trajectory every 6 hours, and the result of clustering is shown in Fig. 1. The stagnant air prevailed in the one-month campaign due to the basin terrain. The only interruption of the atmospheric isolation was an invasion of long-distance transported air mass from northwest China accompanied with strong wind on 29 December. Therefore, the atmospheric processes were dominated by the isolated meteorology of the basin.

The HR-ToF-AMS was deployed along with other relevant measurement instruments to characterize chemical compositions of atmospheric submicron aerosols and evaluate the aerosol secondary formation and aging process. This is the first application

of the HR-ToF-AMS in the Sichuan Basin. The collocated measurement instruments included a multi-angle absorption photometer (MAAP, Thermo Fisher Scientific Inc.) for BC, online gas chromatography-mass spectrometry/flame ionization detector (GC-MS/FID, TH-017, Wuhan-Tianhong Instrument Co.; Li et al., 2014) and proton transfer reaction-mass spectrometer (PTR-MS, Ionicon Analytik GmbH) for VOCs and an ambient air quality monitoring system for meteorological parameters and gaseous pollutant concentrations, etc. All instruments were placed in two containers placed on the open playground on the campus. The instrument setting, operation, and data processing were carried out as described in Hu et al. (2013). Ambient particles were also collected on the copper mesh at the site in some days during the campaign. Particles were photographed and investigated using the transmission electron microscope coupled with an energy dispersive X-ray spectrometer (TEM-EDX, Tecnai G2 T20, FEI Corp.) in the Electron Microscopy Laboratory of Peking University.

2.2 HR-ToF-AMS operation and data processing

The HR-ToF-AMS measures the mass concentrations and size distributions of non-refractory species in submicron aerosols, including organics, sulfate, nitrate, ammonium and chloride (DeCarlo et al., 2006; Hu et al., 2013).

A $PM_{2.5}$ impactor inlet was set on the roof of the container to remove coarse particles. Airstream was introduced in through a copper tube at a flow rate of 8 L min^{-1} and subsequently sampled into the HR-ToF-AMS at a flow rate of 0.09 L min^{-1}, isokinetically from the center of the copper tube. Before entering the instrument, the airstream was dried with a Nafion drier (Perma pure, Inc.), and kept RH below 30%. Atmospheric BC particles are mostly in the Aitken and accumulation modes (i.e., in the submicron range) because of their formation mechanisms (Bond et al., 2013). In order to make a better mass closure of refractory species, BC was measured simultaneously at a 5-min time resolution with the MAAP coupled with a $PM_{2.5}$ cutoff cyclone.

The HR-ToF-AMS operated in a cycle of 5 minutes during the campaign. Under the V-mode, it functioned on mass spectrum (MS) mode for 1 min to obtain the mass concentrations of the non-refractory species, and on separate PToF (particle time-of-flight) mode for 1.5 min to determine size distributions of species. Under the W-mode, only high resolution mass spectral data (HR-MS) was obtained for 2.5 min. The ionization efficiency (IE), sampling flow, and particle sizing of HR-ToF-AMS were

calibrated following the standard protocols (Drewnick et al., 2005). The calibrations of IE and the particle sizing used size-selected pure ammonium nitrate particles with nominal diameters of 400 nm and 60-650 nm, respectively. According to the definition of detection limits (DLs) of different species determined by AMS (Huang et al., 2011), the DLs (V-mode) of organics, sulfate, nitrate, ammonium, and chloride during the campaign were calculated to be 0.24, 0.07, 0.04, 0.05, and 0.01 μg m^{-3}, respectively.

V-Mode provides data with lower resolution while W-Mode produces data with higher one. V-mode data are used to generate unit mass resolution (UMR) spectra, from which mass concentrations and size distributions of species are determined (DeCarlo et al., 2006); W-mode data serve to separate ion fragments with the same nominal *m/z* but different elemental compositions (Aiken et al., 2007). The standard AMS data analysis software packages (SQUIRREL version 1.57I and PIKA version 1.16H), downloaded from the ToF-AMS-Resources webpage (http://cires.colorado.edu/jimenez-group/ToFAMSResources) compiled and executed on Igor Pro 6.22A, were used to generate UMR- and HR-MS from the V- and W-mode data, respectively. All algorithm results of AMS collection efficiencies (CE) based on aerosol chemical compositions and sampling line RH (Middlebrook et al., 2012) were approximately 0.5. Here a CE factor of 0.5, which performed well in many previous field studies (Aiken et al., 2009), was used to calculate mass concentrations. The default relative ionization efficiency (RIE) values (Jimenez et al., 2003) were applied in this study, except for ammonium for which RIE=4.04 was used assuming PM_1 was neutral and other metallic species were ignorable in PM_1 (water-soluble K^+, Ca^{2+}, Mg^{2+}, and Na^+ were 1.22, 0.25, 0.04, and 0.21 μg m^{-3} in $PM_{2.5}$). The reported O/C and H/C ratios of OA in previous studies were mostly biased low. In this study, the "Improved-Ambient" correction (Canagaratna et al., 2015) was applied to calculate the O/C and H/C ratios of OA. The "Improved-Ambient" corrected results of elemental ratios reported in previous studies are taken from Canagaratna et al. (2015) and Chen et al. (2015).

The technical details on Aerodyne HR-ToF-AMS data process, as well as the implementation and validation of the PMF results, could be seen in previous papers (e.g., Huang et al., 2010; Hu et al., 2013). The HR-MS (*m/z* 12-255) was analyzed by the PMF model to identify major OA components, which can much better separate different OA components than UMR spectra (Aiken et al., 2009; DeCarlo et al., 2010). Elemental analysis of the OA components identified by PMF was carried out with

the methods based on HR-MS as described previously (Aiken et al., 2007; Canagaratna et al., 2015). Besides evaluating the reliability and stability of the outcome of PMF model through several parameters (Sect. S3 in the supplementary material), the optimum solution can also be evaluated via comparing the output mass spectra with those of the known sources, comparing the time series of factors with external tracers, and analyzing the diurnal patterns of different factors (Zhang et al., 2011). The uncentered correlation (UC) coefficient of MS, i.e., the cosine of the angle between a pair of MS as vectors, was also used as a qualitative metric to support factor identification (Ulbrich et al., 2009). The UC coefficients between the MS of OA factors resolved in this study and the single or average MS of OA factors reported in previous studies are listed in Table S2. Based on all the tests, the four factors, f_{Peak}=0 and seed=0 solution was chosen as the optimal solution for this analysis.

3 Results and discussion

3.1 Chemical compositions and size distribution of PM_1

3.1.1 Variations of chemical species

The time series of main chemical compositions of submicron aerosols and meteorological parameters during the observation period are shown in Fig. 2. Throughout the observation period, the average PM_1 mass concentration (sum of NR-PM_1 measured by AMS and BC by MAAP) was 59.7±24.1 μg m^{-3}. The lowest and highest PM_1 concentrations were 3.0 μg m^{-3} in 29 December 2012 and 172.5 μg m^{-3} in 1 January 2013, respectively. Organics, accounting for about 36.0±6.1% of PM_1, were identified as the most abundant components, followed by sulfate (20.5±4.7%), nitrate (15.0±5.2%), ammonium (13.8±2.3%), BC (11.1±3.1%) and chloride (3.5±3.5%). Compared with the reported results in China (Table 1), the submicron aerosol pollution during this campaign was at a higher level. PM_1 mass concentration at Ziyang site was comparable to that of Beijing, but higher than at other urban (Shanghai and Shenzhen), coastal/background (Backgarden and Changdao Island), and suburban/rural sites (Jiaxing, Kaiping and Heshan). At almost all of these sites, OM dominated submicron aerosols (about 30-40%); while at Ziyang site, the concentration of BC (6.5 μg m^{-3}) was significantly higher among these sites, indicating strong local primary emissions.

To illustrate the factors influencing air pollution, four episodes were selected according to different pollution levels (as Fig. 2c shown), including three pollution periods (Episode P1, P2 and P3) and a clean day (Episode C). The average PM_1 mass concentrations during Episode P1 and P2 were as high as 91.6 and 71.8 μg m^{-3}, respectively. During the whole campaign, calm occurred frequently (Fig. 2a). Only Episode C (29 December) is a perfectly sunny and clean day, due to the diffusion effect of strong wind (Fig. 2a). The PM_1 concentration plummeted to the lowest level, 7.6 μg m^{-3} on average. Yet PM_1 concentration boosted rapidly in the following Episode P3 (30 December 2012 to 3 January 2013) due to apparent primary emissions. The concentrations of organics, sulfate, BC and chloride rose to different extents (Table 1), and the average PM_1 mass concentration was 56.9 μg m^{-3}. The local emissions may result from smoking bacon with biomass burning, a traditional and common method of preserving pork and sausages in the Sichuan Basin in winter.

The concentrations of secondary inorganic species (SNA, an acronym for sulfate, nitrate and ammonium) step-wisely increased during Episode P1 and P2, especially for nitrate, with much higher average concentrations (Table 1). The concentrations of SNA correlated well with RH (Pearson correlation coefficient r=0.536, 0.415 and 0.555, $p<0.01$), suggesting this was probably induced by the more effective secondary transformation in the humid air. In Episode C, as the strong wind from northwestern China caused atmospheric pollutant diffusion, the RH decreased to a minimum (Fig. 2b). Each chemical species in submicron aerosols was at the lowest level, which can be considered as the background concentration. The components of organics, sulfate, nitrate, ammonium, BC and chloride accounted for 38.1%, 27.5%, 6.2%, 13.8%, 10.9% and 3.4% of PM_1, respectively. In Episode P3, the proportions of organics, BC and chloride accounted for PM_1 increased due to the strong primary emissions; hence those of SNA decreased. These results reflected the significant impact of meteorology conditions and emission sources on air pollution level.

Since the secondary compositions were dominant in PM_1, variation of PM_1 depended on secondary formation processes and removal processes, i.e., strong wind and wet deposition. During the campaign, six short-term precipitation events, the main removal approach in Ziyang, were observed, which could eliminate the heavy PM pollution partly (Fig. 2c). However, the humid air after the precipitation may favor the aqueous-phase secondary formation and hygroscopic growth of SNA, causing the stable or even slightly increased concentrations of SNA (Fig.2). The probability density of PM_1 mass concentration during

the campaign followed normal distribution approximately (as the white curve shown in Fig. 3a), and concentrated in a mono-mode between 30 μg m^{-3} and 80 μg m^{-3}, which was mainly caused by the adverse geological and meteorological conditions. The probability distribution of PM_1 mass concentration in Ziyang was similar to that in summer in Beijing, where the stagnant air mass prevented diffusion of pollutants, and high humidity and temperature favored secondary formation (Huang et al., 2010). It contrasted the distribution patterns observed at Changdao Island (Hu et al., 2013) and in Beijing (23 January to 2 March 2013; Fig. 3d) in cold period, with broader ranges of PM_1 mass concentration. During these two campaigns, clean days appeared more frequently due to the intruding clean air mass carried by strong wind. The probabilities of PM_1 mass concentration lower than 35 μg m^{-3} were over 40%, while it was only about 10% in Ziyang. These results suggested the relatively stable state of submicron aerosol pollution at Ziyang site.

The proportion variations of different chemical species with the increase of PM_1 mass concentration are shown in Fig. 3a. The relative contributions of inorganic and organic varied insignificantly, with PM_1 mass concentration ranging from 35 μg m^{-3} to 120 μg m^{-3}. When PM_1 mass concentration was below 35 μg m^{-3}, the fraction of organics increased slightly to 40% or above. High fractions of organics, chloride, and BC caused by strong primary emissions were found as PM_1 was above 140 μg m^{-3}.

3.1.2 Size distribution of chemical species

The average vacuum aerodynamic (d_{va}) size distributions of the non-refractory species in submicron aerosols are shown in Fig. 3b. Organics and secondary inorganics featured similar size distribution patterns and existed primarily in accumulation mode with peaks around 600-800 nm, implying that the particles were internally mixed. This was consistent with the morphology and mixing state of single particles, mostly spherical and in internal mixing state (Fig. 4a-d). The peak sizes of all species were larger than those in winter in Beijing (Fig. 3e), Mexico City and Changdao Island (Aiken et al., 2009; Hu et al., 2013), implying that the aqueous reactions under the high RH condition in Ziyang could cause a faster particle growth rate of secondary species than in other areas (Hu et al., 2016). Organics and chloride exhibited broader size distributions than SNA, with obvious mass enhancement at small sizes (100-500 nm), indicating contributions of primary emissions like biomass burning and coal combustion (Huang et al., 2010; Hu et al., 2013). With the increasing of particle size (d_{va}>200 nm), the proportion of organics in submicron aerosols decreased slightly, while those of sulfate, nitrate and ammonium increased gradually (Fig. 3c),

suggesting that SNA were the main contributors as the particles grew up in Ziyang. In contrast, sulfate made a more significant contribution to particle growth in Beijing winter (Fig. 3f).

3.2 Investigating OA sources with PMF

By conducting PMF analysis on the high mass resolution OA spectral matrix, four factors of OA were resolved, i.e., LV-OOA, SV-OOA, HOA and BBOA, with distinct mass spectral profiles (Fig. 5) and temporal variations (Fig. 6). They accounted for 34.7%, 36.5%, 14.9% and 13.9% of total OA mass, respectively, as shown in Fig. 8a. The former two factors are good surrogates of aged and fresh SOA, while the latter two are classified into POA, respectively (Jimenez et al., 2009). OOA dominated in OA as much as 71%, approximate to or higher than the reported results in China (Table 1), implying the high oxidation state of OA in Ziyang. In total, secondary formation (OOA+SNA) contributed to PM_1 as high as 76%, in accordance with the results of single particle analysis (See Sect. S5). Further strengthening of gaseous precursor's control, therefore, should be pursued.

3.2.1 Hydrocarbon-like OA (HOA)

The average mass spectrum of HOA (Fig. 5) is similar to previously reported reference spectra of HOA (Aiken et al., 2009; Huang et al., 2010, 2011). In this spectrum, alkyl fragments are dominant, especially the saturated alkyl fragments ($C_nH_{2n+1}^+$) and the alkenyl fragments ($C_nH_{2n-1}^+$). The OA/OC and O/C ratios of HOA factor were about 1.31 and 0.10, respectively, which were approximate to those previous results (OA/OC: 1.34-1.43, O/C: 0.11-0.20) in other areas in China (Canagaratna et al., 2015; He et al., 2011; Huang et al., 2012, 2013; Gong et al., 2012). Factor analysis (e.g., PMF analysis) suffers a limitation, as it is incapable of separating independent sources completely, and the resolved factor may be a mixture of various sources. The abundant characteristic fragments for COA (*m/z* 55, 57, etc.) and CCOA (*m/z* 67, 69, 91, etc.) can be seen in the mass spectrum of HOA factor (He et al., 2010; Hu et al., 2013). The scatter plot between f_{55} vs. f_{57} in Ziyang is shown in Fig. 7. HOA resolved in this study had high m/z 55 vs. m/z 57 ratio of 1.71, which was between the ratios (2.2-2.8) in COA and those (0.9-1.1) in other non-cooking POA components (Mohr et al., 2012). The ratios of $C_3H_3O^+/C_3H_5O^+$ and $C_4H_7^+/C_4H_9^+$ in HOA resolved in this study were 1.5 and 1.7, respectively, which were also in the ranges (1-2 and 1-2.5) between HOA and COA summarized

by Mohr et al. (2012). The MS of HOA correlated well with the average MS of HOA factor reported in previous studies, as well as that of COA, BBOA and vehicle emitted OA (Vehicle-OA) factors (Table S2). HOA tracked well (r=0.6-0.7, p<0.01) with primary source tracers (e.g., chloride, NO_x, BC, acetonitrile, acetaldehyde, toluene, and benzene), as shown in Table S3. Among them, chloride and acetonitrile are the tracers of coal combustion and biomass burning emissions, respectively. Thus, it was likely that the HOA factor was a mixture of COA and other primary organic aerosols. The diurnal cycle of HOA presented a peak at around 10:00, which may be related to the living habits of local residents. In rural and suburban areas in southwestern China, residents usually have two meals a day, especially in winter due to short daytime and less labor, so the influence of COA was weaker at noon.

3.2.2 Biomass burning OA (BBOA)

Residential biomass burning plays an important role in aerosol pollution in the winter in southwestern China (Wang et al., 2006; Cao et al., 2012). Levoglucosan is an important tracer of biomass burning aerosols, the fragment of which, $C_2H_4O_2^+$, contributed to *m/z* 60 is regarded as a tracer ion of BBOA. The highest abundance of *m/z* 60 (~1.3%) is a prominent characteristic in the MS of BBOA factor (Fig. 5), which is much higher than that (0.3%) in plumes with negligible biomass burning influence (Cubison et al., 2011). The MS of BBOA resolved in this study showed good correlation with the average MS of BBOA in previous studies (Table S2). In addition, BBOA tracked well with $C_2H_4O_2^+$ (r=0.85, p<0.01), further verifying the rationality of the resolved BBOA factor (Table S3). Compared with the O/C ratio of HOA (0.10), that (0.32) of BBOA was higher and in the range of 0.25-0.55 reported previously (Canagaratna et al., 2015). There was a phenomenon of burning straw and wood randomly, especially which is an effective energy for cooking and heating in winter in Southern China (Song et al., 2009). High BBOA contribution (14±7%) to OA was consistent with significant biomass burning contribution (9-37%) to atmospheric VOC species during the same campaign (Li et al., 2014). Soot aggregates and sulfur-, chlorine- and potassium-containing particles were observed using TEM-EDX (Fig. 4e), also implying that biomass burning was a major contributor to aerosol pollution (See Sect. S5). BBOA was probably emitted from residential houses, makeshift stoves built by migrant workers nearby, and waste incineration observationally.

BBOA displayed a very similar diurnal pattern with HOA and BC, with lower concentrations during the daytime and higher ones in the morning and nighttime (Fig. 8b and Fig. S7), indicating that they may be emitted by similar processes, such as residential emissions via cooking, heating, and smoking bacon. The previous emission inventory (Guo et al., 2015) showed that residential sources of OA were significant in the Sichuan Basin during the winter 2010 (Fig. 1). All the patterns were likely corresponding to the living habits of local residents as well as the diurnal variation of atmospheric boundary layer. The time series of BBOA tracked well ($r=0.67$, $p<0.01$) with another tracer of biomass burning events, acetonitrile (Fig. 6 and Table S3). BBOA also presented good correlations with BC and acetaldehyde (Table S3), which could be partly emitted from biomass burning. In Episode P3, the contributions of BBOA to total OA (26%) and PM_1 (11%) were much higher than those (10-17%, 4-7%) in other episodes defined above (Table 1), indicating far stronger biomass burning during Episode P3.

3.2.3 Semi-volatile and low-volatility oxygenated OA (SV-OOA and LV-OOA)

In a large number of studies, OOA has been widely investigated (Zhang et al., 2005; Aiken et al., 2009; Ng et al., 2011; Hu et al., 2016), which is considered a good alternative to SOA under most conditions (Jimenez et al., 2009; Ng et al., 2011). As Fig. 5 shown, the identified mass spectra of LV-OOA and SV-OOA are both characterized by the oxygenated fragments ($C_xH_yO_z^+$), mainly from carboxylic acid and aldehyde, especially CO_2^+ (*m/z* 44) and $C_2H_3O^+$ (*m/z* 43). The abundance of $C_xH_yO_z^+$ in LV-OOA was higher than that of SV-OOA. In this study, the abundances of CO_2^+ in LV-OOA and SV-OOA were 18% and 14%, respectively. LV-OOA with higher OA/OC and O/C ratios (2.52 and 1.02) was more oxygenated and aged than SV-OOA with lower ratios (2.12 and 0.73). The O/C ratios of LV-OOA and SV-OOA at Ziyang site were quite higher than the average O/C ratios for LV-OOA (0.84) and SV-OOA (0.53) summarized by Canagaratna et al. (2015), indicating OA was highly oxygenated in Ziyang. Besides, the effect of biomass burning cannot be completely ruled out, which may also result in higher O/C ratio of SV-OOA.

Generally, OOA tracks well with SNA. LV-OOA correlates better with sulfate, and SV-OOA correlates better with nitrate, for their common volatility. In this study, LV-OOA correlated well with SNA ($r=0.66$-0.68, $p<0.01$), while the correlation between SV-OOA and SNA were slightly weaker (Table S3). The time series of SV-OOA roughly trended well towards that of nitrate except in two intervals, 7-10 and 24-26 December. The total OOA (LV-OOA and SV-OOA) and secondary inorganic species

(sulfate and nitrate) displayed good correlation (r=0.88, p<0.01), in accordance with the dominant secondary origin of OOA. LV-OOA also showed a similar trend to BC (r=0.75, p<0.01), because the aged OA can mix well with BC due to the static air in the basin.

The diurnal variation of LV-OOA showed a valley in the early morning (Fig. 8b, c), and increased from 9:00 to 14:00, indicating a significant secondary formation in the daytime. It displayed another peak in the evening, which may be influenced by the low-volatility particle-phase compounds from biomass burning (Murphy et al., 2014). The SV-OOA concentrations showed a small peak in the afternoon for more efficient photochemical reactions. The fractions of LV-OOA in OA exhibited a relatively stable diurnal pattern, implying LV-OOA was of regional characteristics. The fractions of SV-OOA in total OA varied a little diurnally and only increased slightly to 30% in the afternoon (13:00-18:00). Conversely, the fractions of HOA and BBOA decreased in the corresponding interval.

Depending on the pollution severity, the contributions of OOA components were distinct. In Episode P1 and P2, OOA was prominent (66% and 76%) in OA, and especially LV-OOA dominated in total OOA as 78% and 53%, respectively. In Episode C, SV-OOA predominated in total OA and OOA as high as 61% and 98%, respectively. While, in Episode P3, POA (sum of HOA and BBOA) and OOA almost contributed equivalently on average, and the contribution (56%) of SV-OOA to OOA was higher than that of LV-OOA (Table 1).

The proportion of each OA component in total OA as a function of OA concentration and the probability density distribution of OA concentrations are shown in Fig. 8d. OA concentrations were approximately skewed-normally distributed, and mainly in the range of 10-40 μg m^{-3}. In this range, OOA especially LV-OOA dominated the increase of OA concentration, contributed up to over 80% of OA. As the OA concentration was below 10 μg m^{-3}, SV-OOA transformed from gaseous precursors contributed to OA predominantly. When the OA concentration was greater than 50 μg m^{-3}, OA was mainly from strong primary emissions, such as biomass burning. The proportion of LV-OOA and SV-OOA in OA decreased, while the fraction of POA increased dramatically. Specifically, corresponding to strong primary emissions during Episode P3, OA was mainly composed of POA and SV-OOA (as the spikes shown in Fig. 8d) due to the clean background atmosphere. Due to the highly oxidized and aged state of SV-OOA in Ziyang, the MS of SV-OOA was quite similar to that of LV-OOA (Table S2). However, they

contributed discriminatively at different OA concentrations (Fig. 8d), which should be consistent with the trend of OOA oxidation.

3.3 Secondary formation and aging process of OA

3.3.1 Elemental compositions of OA and VK diagram

The HR-MS was used to calculate the elemental compositions of OA and OA/OC ratio. During the overall observation period, on average, C, H, O and N contributed 49.5%, 6.4%, 42.9% and 1.2% to the total organic mass, respectively. As for atomic number ratios, the average elemental ratios of O/C, H/C, and N/C were 0.65±0.11, 1.56±0.06, and 0.02±0.00, respectively. The average O/C and H/C ratios were close to O/C ratios (0.6) for downwind locations, and H/C ratios (1.5) for remote/rural locations (Chen et al., 2015). The average OA/OC (2.02±0.14, in the range of 1.37-2.35) and O/C ratios were higher than those in urban and suburban/rural areas in China (Table 1), indicating that OA was highly oxidized in Ziyang. Due to primary emissions from 29 December 2012 to 2 January 2013 (Episode P3), the O/C ratio apparently declined; while the H/C ratio varied oppositely. In Episode C and P3, the O/C ratios (0.46, 0.52) were much lower than those (0.65, 0.69) during Episode P1 and P2 (Table 1). As local primary emissions contributing to OA substantially (the uppermost data points in the plot), the O/C ratio decreased to the lowest level, and the H/C ratio reached up to about 1.9.

The VK diagram, displaying the variation of O/C versus H/C, can be used as a tool to probe bulk oxidation reaction mechanisms for organic aerosols (Hu et al., 2013). The slope and intercept of VK diagram for OA at Ziyang site was −0.44 (r^2=0.70) and 1.84, respectively (Fig. 9a). The slope was shallower than those (−1.0 to −0.7, −0.58±0.04 for mean fit) observed across the world, which may be more consistent with chemical aging, and the intercept fell into the range (1.8-2.2) for remote/rural sites (Chen et al., 2015). The slope was close to −0.5, which suggests net changes equivalent to the addition of acid groups with fragmentation and/or both acid and alcohol/peroxide functional groups without fragmentation (Ng et al., 2011). During the Episode P1, P2, C and P3, the slopes of VK diagram were −0.46, −0.57, −0.84 and −0.52, respectively. The intercepts of the fitting lines were about 1.87-1.95. This result indicated that carboxylic acid functionalization with fragmentation was

dominated during the pollution episodes, while carboxylic acid functionalization without fragmentation or addition of an alcohol and carbonyl group on different carbons was more active during the clean episode.

The photochemical age metric, −log (NO_x/NO_y), was used to investigate the relationship between OA oxidation and the photochemical aging. The ratio is higher in the more aged plume (Decarlo et al., 2008, 2010). When the metric −log (NO_x/NO_y) <0.1, it is considered to be fresh plume (Liang et al., 1998). Coloring the scattering data points in VK diagram (Fig. 9a) with −log (NO_x/NO_y), there was a clear trend (from the upper left to the lower right) that the aged plumes agreed with higher OA oxidation levels (higher O/C ratios), except for the data in the clean day (7:00-18:00 29 December; lower middle). The plume was probably well aged photochemically due to strong solar radiation, and the OOA was predominated by freshly formed SV-OOA (Fig. 8d). The OA factors resolved by AMS-PMF analysis are also marked in Fig. 9a. In the order from POA (HOA and BBOA) to SOA (SV-OOA and LV-OOA), the OA factors evolved along with the direction to a higher oxidation state, which was consistent with the oxidation characteristics of the factors (Ng et al., 2011), although SV-OOA evolved along a line with a smooth slope to LV-OOA.

3.3.2 Triangle plot (f_{44} vs. f_{43} and f_{44} vs. f_{60})

OA evolution can also be characterized in terms of the varying abundances of the two most dominant oxygen-containing ions in the OOA spectra, *m/z* 43 and *m/z* 44 (mostly CO_2^+ in ambient data). Since *m/z* 44 is found to be proportional to the acid species, it seems that acid group formation plays a significant role in OOA aging process (Ng et al., 2011). The *m/z* 43 fragments are mainly $C_2H_3O^+$, predominantly due to non-acid oxygenates, for the OOA fraction, and $C_3H_7^+$ for the HOA fraction. To avert the effects of atmospheric dispersion and dilution capability, *m/z* 43 and *m/z* 44 fractions in organic mass spectra (f_{43} and f_{44}) were used to characterize the oxidation of OA.

The scatterplot of f_{44} against f_{43} is shown in Fig. 9b, and colored with −log (NO_x/NO_y). The f_{44} ranged from 0.03 to 0.17, and the f_{43} was in a narrow range of 0.05 to 0.09, which fitted the triangle space for OA components (Ng et al., 2011). With increasing photochemical age (−log (NO_x/NO_y)), f_{44} increased and f_{43} decreased, reflecting the photochemical aging of OA (Ng et al., 2010). The locations of OA factors are also marked in the plot. OA showed the evolution trends moving from the

bottom (HOA and BBOA, f_{44}<0.05), to an intermediate location (SV-OOA), and to the top (LV-OOA) in the triangle. Data points gradually moved upward from the lower half of the triangle with enhancement of OA oxidation in smoke chamber experiments and field observations (Ng et al., 2010). The location of SV-OOA on the upper half of the triangle is close to that of LV-OOA (Fig. 9b), highlighting the high oxidation level of SV-OOA.

The scatterplot of f_{44} against f_{60} (Fig. 9c), colored with −log (NO_x/NO_y), was also applied here to facilitate understanding the secondary formation and transformation of primary BBOA in Ziyang. Cubison et al. (2011) reported that in the f_{44} against f_{60} space, data with negligible biomass burning influence were concentrated on the left side as a band shape (f_{60}=0.2-0.4%), while data from biomass burning appeared in the lower right part. Almost all data points fell into the left side of the conceptual space for BBOA (Cubison et al., 2011), indicating the important contribution of biomass burning to OA during the whole observation period. HOA and SV-OOA resolved in this study were located out of the conceptual space for BBOA, while BBOA and LV-OOA were located in it. In addition, *m/z* 60 accounted for 0.8%, 0.5%, 0.7%, and 1.3% of LV-OOA, SV-OOA, HOA, and BBOA, respectively. Higher abundance of *m/z* 60 indicated that LV-OOA and HOA were probably associated with biomass burning processes and had been referred to as LV-bbSOA and bbPOA (bb, biomass burning) by Murphy et al. (2014). There was no trend for the variation of f_{60} of OA upon the increase of −log (NO_x/NO_y), suggesting that there was no dependence of the contribution of biomass burning to OA on photochemical aging.

3.3.3 Average carbon oxidation state of OA

The average oxidation state of the carbon ($\overline{OS_C} \approx 2 \times O/C - H/C$) is an ideal metric for the degree of oxidation of organic species in the atmosphere, and serves as a key quantity to describe organic mixtures that are as chemically complex as organic aerosols (Kroll et al., 2011). The $\overline{OS_C}$ in Ziyang was calculated as -0.26 ± 0.27 on average, ranging from −1.59 to 0.36. It was within the $\overline{OS_C}$ ranges in downwind and remote/rural environment (Chen et al., 2015), lower than those of ambient OA in the aged (Whistler Mountain) and coastal/background (Changdao Island) atmosphere, much higher than or comparable to those of other urban and suburban sites in China and laboratory-generated POA and SOA (Fig. 10 and Table 1), also implying OA was highly oxygenated.

A strong correlation between $\overline{OS_C}$ and f_{44} (Fig. 9d) indicated that carboxylic groups can fragment into a large amount of CO_2^+ ions, and explain for the high $\overline{OS_C}$ observed. The fitted line for the overall data has a slope of 11.5 and an intercept of −1.64, suggesting that the $\overline{OS_C}$ of non-acid moieties in OA was −1.64. The −log (NO_x/NO_y) increased with increasing $\overline{OS_C}$ and f_{44} (Fig. 9d), indicating that it is a good qualitative clock for photochemical age (Decarlo et al., 2008), except for the data of 29 December as mentioned above. The average $\overline{OS_C}$ of HOA, BBOA, SV-OOA and LV-OOA were −1.61, −1.04, −0.19 and 0.59, respectively. The results were in the ranges of previously reported ones (Fig. 10), and in accordance with that $\overline{OS_C}$ must increase upon oxidation of OA and those non-acid oxygenated groups may undergo further oxidation during their atmospheric lifetime if conditions permit (Kroll et al., 2011). The $\overline{OS_C}$ in Episode C and P3 were decreased due to the freshly emitted organic aerosols; while in Episode P1 and P2, the $\overline{OS_C}$ increased to −0.65 and −0.69 (Fig. 10 and Table 1), indicating the OA during the hazy periods may contain relatively more abundant oxygenated groups other than the carboxylic group, such as carbonyl and hydroxyl groups (Li et al., 2013b).

3.3.4 Evolution of OA/ΔCO ratio with chemical conversions

In order to understand the effects of chemical conversions on the properties of organic aerosols in the atmosphere, it is necessary to avoid the influences of emissions and transport of OA by normalizing OA to a relatively inert combustion tracer over the time scales of interest, e.g., CO (de Gouw and Jimenez, 2009). The OA/ΔCO ratios are used to evaluate the secondary formation of OA, where ΔCO indicates that the regional background concentration of CO (0.2 ppmv, the average concentration in Episode C) has been subtracted. OA/ΔCO ratio is lower for the primary emission plume from source region, and becomes higher after substantial SOA formation (DeCarlo et al., 2010). The average OA/ΔCO ratio in Ziyang during the campaign was 41.7±23.0 μg m^{-3} $ppmv^{-1}$, which was lower than the average level (70±20 μg m^{-3} $ppmv^{-1}$) around the world (de Gouw and Jimenez, 2009). In more polluted periods, SOA/ΔCO accounted for 70-80% of OA/ΔCO, implying higher contribution of secondary formation. The influence of biomass burning emission can also cause high OA/ΔCO ratio, often similar to or even higher than SOA/ΔCO ratio from aged plumes (Cubison et al., 2011). In Episode P3, the OA/ΔCO reached the highest value as 209.2 μg m^{-3} $ppmv^{-1}$. It was similar to the ever reported highest results 210 μg m^{-3} $ppmv^{-1}$ in Mexico City when influenced by strong biomass burning emissions (Decarlo et al., 2010), indicating the important contribution of biomass burning to OA.

Furthermore, SV-OOA/ΔCO increased from 7.7 (P1) and 16.1 (P2) to 19.8 μg m^{-3} $ppmv^{-1}$ for SV-OOA can be quickly formed in the plumes.

Photochemical age was calculated using ratios of m+p-xylene to ethylbenzene concentrations with an initial emission ratio of 2.2 ppbv $ppbv^{-1}$ (Fig. S8, Yuan et al., 2013). The average OH radical concentration applied here is 1.6×10^{6} molecule cm^{-3} in order to compare with other studies (DeCarlo et al., 2010; Hu et al., 2013). A detailed description of the determination of photochemical age can be found in Yuan et al. (2013). The variations of PMF resolved OA factors to ΔCO as a function of photochemical age are shown in Fig. 11a. With the increase of photochemical age, POA components (BBOA and HOA) maintained a stable level, implying the stable background concentration of POA in the daytime. However, roughly, SOA surrogate components (LV-OOA and SV-OOA) enhanced with the increase of photochemical age, which was consistent with the photochemical processing of OA. Specifically, the regression slopes of average LV-OOA/ΔCO and SV-OOA/ΔCO versus photochemical age in the range of 2.6-7.1 hours were 0.48 μg m^{-3} $ppmv^{-1}$ h^{-1} and 0.60 μg m^{-3} $ppmv^{-1}$ h^{-1} (Fig. S9), respectively, which may result from the efficient secondary formations from plenty of emitted POA, especially BBOA (Robinson et al., 2007). The increasing slope of OA (1.2 μg m^{-3} $ppmv^{-1}$ h^{-1}), which was approximate to that at Changdao Island (1.3 μg m^{-3} $ppmv^{-1}$ h^{-1}) and lower than those (~2-5 $ppmv^{-1}$ h^{-1}) in Mexico City and the US (Hu et al., 2013), was almost completely attributed to the contribution of SOA. As the photochemical age was longer than 7 hours, the average OA/ΔCO ratio decreased with the photochemical age, caused by the decrease of LV-OOA/ΔCO ratio (Fig. 11a). Atmospheric oxidation of OA converges toward greatly aged LV-OOA despite of the original OA sources (Jimenez et al., 2009). Given the concentrations of OA components in aged air during this campaign, the evolution from POA, to SV-OOA, and to LV-OOA may be inhibited by lower concentration of POA (about one third of those in fresh air), resulting in lower LV-OOA concentrations, but relatively stable SV-OOA concentrations because SV-OOA was already dominant in OA (Jimenez et al., 2009).

The average fractions of OA components in total OA at each bin versus the photochemical age are shown in Fig. 11b. OOA dominated OA (56-84%) in both fresh and aged plumes, suggesting a high oxidation state of OA. When the photochemical age was nominally very short, POA (HOA+BBOA) accounted for 44% of total OA. While, due to the unique geographical and meteorological conditions in the basin terrain, it is reasonable that the aged OA mixed with freshly emitted gaseous

pollutants in the air, resulting in the substantial fraction of OOA at low apparent ages (Hu et al., 2013). The POA fraction in total OA decreased rapidly with the increasing of photochemical age. As the photochemical age longer than 6 h, the percentage of SV-OOA (54%) was much higher than that of LV-OOA (27%) in total OA (Fig. 11), implying that the photochemical formation of SV-OOA was more efficiently than that of LV-OOA.

The good correlations between OOA and O_x (O_x=O_3+NO_2, surrogate of total oxidant) were considered to be useful for empirical predictions of SOA productions in previous studies in Mexico City and Houston (Herndon et al., 2008; Wood et al., 2010). However, OOA didn't correlate well with O_x in Ziyang (Fig. S10), indicating the SOA formation mechanisms in Ziyang differed greatly from those in Mexico City and Houston. The RH in Ziyang during the campaign was 80±19% (12-100%) on average (Table 1), and reached saturation frequently. Colored the scatter plot with RH, it can be found that the slope of OOA against O_x steepened with the increasing RH (Fig. S10), indicating that both photochemical and aqueous-phase oxidation can dominate the secondary formation of OA in the atmosphere in Ziyang (Hu et al., 2016). In drier air (RH<40%), OOA formation was dominated by photochemical processes, while the aqueous-phase oxidation probably became a more significant and efficient approach to OOA production in humid atmosphere (RH>40%) in Ziyang.

4 Conclusions

We investigated the chemical compositions of atmospheric submicron aerosols with a HR-ToF-AMS at a suburban site, Ziyang, located in the Sichuan Basin, China during the wintertime from December 2012 to January 2013. This study provided a special case of studying the characteristics and sources of aerosol pollution under the specific geographical and meteorological conditions in the basin terrain.

The mass concentrations of PM_1 maintained a moderate level (59.7±24.1 μg m^{-3}) during the whole campaign. OA was the most abundant PM_1 component (36%). High OA/OC, O/C ratios and average carbon oxidation state indicated that organic aerosols were in a high oxidation state. Using AMS-PMF analysis, four OA fractions defined as LV-OOA (34.7%), SV-OOA (36.5%), HOA (14.9%) and BBOA (13.9%) were identified. Secondary formation contributed predominantly to OA (71%) and PM_1 (76%). Secondary inorganic species (SNA) contributed significantly to the heavy aerosol pollution, due to the more effective secondary formation and hygroscopic growth in the humid air. The OA factors evolved along with the direction to a

higher oxidation state, from POA (HOA and BBOA) to SOA (SV-OOA and LV-OOA). With the increase of photochemical age, OA became more aged with higher oxidation state (higher O/C ratio, f_{44}, and $\overline{OS_C}$), and LV-OOA/ΔCO and SV-OOA/ΔCO also increased, implying photochemical processing contributed significantly to OA. The photochemical formation of SV-OOA was more efficient than that of LV-OOA during this campaign. The aqueous-phase oxidation can also contribute significantly to SOA production in humid atmosphere, with the OOA/O_x ratio and RH increased simultaneously to some extent.

The concentration and proportion of BC in PM_1 at Ziyang site were at a much higher level among those reported results in China, indicating the severe primary emissions. During the episode obviously affected by primary emissions, the contributions of BBOA to OA and PM_1 were much higher than those in other polluted episodes, highlighting the critical influence of biomass burning.

These results provide a better understanding of the role of primary emissions and secondary formation in submicron aerosol pollution in the Sichuan Basin. In the future, further work should be done to elucidate more details of the haze formation mechanisms, and to assess the effects of aerosol pollution in the Sichuan Basin.

Acknowledgements

This work was supported by the National Basic Research Program of China (2013CB228503), the Strategic Priority Research Program of the Chinese Academy of Sciences (XDB05010500) and the China Ministry of Environmental Protection's Special Funds for Scientific Research on Public Welfare (20130916). We would like to thank the observation team in Ziyang for their kind help, in particular for Sichuan Provincial Monitoring Center. We appreciate Dr. D. R. Worsnop, Dr. S. Guo and Dr. J. Peng for their helpful comments, Mr. Z. Gong for his guidance of data processing, Prof. Q. Zhang for sharing the database of Multi-resolution Emission Inventory for China (MEIC), and Miss Y. Tian and Prof. J. Morrow for their English polishing.

References

Aiken, A. C., DeCarlo, P. F., and Jimenez, J. L.: Elemental Analysis of Organic Species with Electron Ionization High-Resolution Mass Spectrometry. Anal. Chem., 79, 8350-8358, 2007.

Aiken, A. C., Salcedo, D., Cubison, M. J., Huffman, J. A., DeCarlo, P. F., Ulbrich, I. M., Docherty, K. S., Sueper, D., Kimmel, J. R., Worsnop, D. R., Trimborn, A., Northway, M., Stone, E.A., Schauer, J. J., Volkamer, R. M., Fortner, E., de Foy, B., Wang, J., Laskin, A., Shutthanandan, V., Zheng, J., Zhang, R., Gaffney, J., Marley, N. A., Paredes-Miranda, G., Arnott, W.P., Molina, L.T., Sosa, G., and Jimenez, J.L.: Mexico City aerosol analysis during MILAGRO using high resolution aerosol mass spectrometry at the urban supersite (T0) - Part 1: Fine particle composition and organic source apportionment. Atmos. Chem. Phys., 9, 6633-6653, 2009.

Allan, J. D., Williams, P. I., Morgan, W. T., Martin, C. L., Flynn, M. J., Lee, J., Nemitz, E., Phillips, G. J., Gallagher, M. W., and Coe, H.: Contributions from transport, solid fuel burning and cooking to primary organic aerosols in two UK cities, Atmos. Chem. Phys., 10, 647-668, 2010.

Bond, T. C., Doherty, S. J., Fahey, D. W., Forster, P. M., Berntsen, T., DeAngelo, B. J., Flanner, M. G., Ghan, S., Kärcher, B., Koch, D., Kinne, S., Kondo, Y., Quinn, P. K., Sarofim, M. C., Schultz, M. G., Schulz, M., Venkataraman, C., Zhang, H., Zhang, S., Bellouin, N., Guttikunda, S. K., Hopke, P. K., Jacobson, M. Z., Kaiser, J. W., Klimont, Z., Lohmann, U., Schwarz, J. P., Shindell, D., Storelvmo, T., Warren, S. G., and Zender, C. S.: Bounding the role of black carbon in the climate system: A scientific assessment, J. Geophys. Res. Atmos., 118, 5380-5552, 2013.

Canagaratna, M. R., Jimenez, J. L., Kroll, J. H., Chen, Q., Kessler, S. H., Massoli, P., Hildebrandt Ruiz, L., Fortner, E., Williams, L. R., Wilson, K. R., Surratt, J. D., Donahue, N. M., Jayne, J. T., and Worsnop, D. R.: Elemental ratio measurements of organic compounds using aerosol mass spectrometry: characterization, improved calibration, and implications, Atmos. Chem. Phys., 15, 253-272, 2015.

Cao, J. J., Shen, Z. X., Chow, J. C., Watson, J. G., Lee, S.-C., Tie, X.-X., Ho, K.-F., Wang, G.-H., and Han, Y.-M.: Winter and Summer $PM_{2.5}$ Chemical Compositions in Fourteen Chinese Cities. J. Air Waste Man. Ass., 62, 1214-1226, 2012.

Carlton, A. G., Wiedinmyer, C., and Kroll, J. H.: A review of Secondary Organic Aerosol (SOA) formation from isoprene. Atmos. Chem. Phys., 9, 4987-5005, 2009.

Chen, Q., Heald, C. L., Jimenez, J. L., Canagaratna, M. R., Zhang, Q., He, L. Y., Huang, X. F., Campuzano‐Jost, P., Palm, B. B., and Poulain, L.: Elemental Composition of Organic Aerosol: The Gap Between Ambient and Laboratory Measurements, Geophys. Res. Lett., 42, doi:10.1002/2015GL063693, 2015.

Chen, Y., and Xie, S.: Long-term trends and characteristics of visibility in two megacities in southwest China: Chengdu and Chongqing. J. Air Waste Man. Ass., 63, 1058-1069, 2013.

Chen, Y., and Xie, S.: Temporal and spatial visibility trends in the Sichuan Basin, China, 1973 to 2010. Atmos. Res., 112, 25-34, 2012.

Cheung, H. C., Wang, T., Baumann, K., and Guo, H.: Influence of regional pollution outflow on the concentrations of fine particulate matter and visibility in the coastal area of southern China, Atmos. Environ., 39, 6463-6474, 2005.

Cubison, M. J., Ortega, A. M., Hayes, P. L., Farmer, D. K., Day, D., Lechner, M. J., Brune, W. H., Apel, E., Diskin, G. S., Fisher, J. A., Fuelberg, H. E., Hecobian, A., Knapp, D. J., Mikoviny, T., Riemer, D., Sachse, G. W., Sessions, W., Weber, R. J., Weinheimer, A. J., Wisthaler, A., and Jimenez, J. L.: Effects of aging on organic aerosol from open biomass burning smoke in aircraft and laboratory studies. Atmos. Chem. Phys., 11, 12049-12064, 2011.

de Gouw, J., and Jimenez, J.L.: Organic Aerosols in the Earth's Atmosphere. Environ. Sci. Tech., 43, 7614-7618, 2009.

DeCarlo, P. F., Dunlea, E. J., Kimmel, J. R., Aiken, A. C., Sueper, D., Crounse, J., Wennberg, P. O., Emmons, L., Shinozuka, Y., Clarke, A., Zhou, J., Tomlinson, J., Collins, D. R., Knapp, D., Weinheimer, A. J., Montzka, D. D., Campos, T., and Jimenez, J. L.: Fast airborne aerosol size and chemistry measurements above Mexico City and Central Mexico during the MILAGRO campaign, Atmos. Chem. Phys., 8, 4027-4048, 2008.

DeCarlo, P. F., Kimmel, J. R., Trimborn, A., Northway, M. J., Jayne, J. T., Aiken, A. C., Gonin, M., Fuhrer, K., Horvath, T., and Docherty, K. S.: Field-deployable, high-resolution, time-of-flight aerosol mass spectrometer, Anal. Chem., 78, 8281-8289, 2006.

DeCarlo, P. F., Ulbrich, I. M., Crounse, J., de Foy, B., Dunlea, E. J., Aiken, A. C., Knapp, D., Weinheimer, A. J., Campos, T., Wennberg, P. O., and Jimenez, J. L.: Investigation of the sources and processing of organic aerosol over the Central Mexican Plateau from aircraft measurements during MILAGRO. Atmos. Chem. Phys., 10, 5257-5280, 2010.

Drewnick, F., Hings, S., DeCarlo, P., Jayne, J., Gonin, M., Fuhrer, K., Weimer, S., Jimenez, J., Demerjian, K., Borrmann, S., and Worsnop, D.: A New Time-of-Flight Aerosol Mass Spectrometer (TOF-AMS)-Instrument Description and First Field Deployment. Aerosol Sci. Tech., 39, 637-658, 2005.

Gong, Z., Lan, Z., Xue, L., Zeng, L., He, L., and Huang, X.: Characterization of submicron aerosols in the urban outflow of the central Pearl River Delta region of China, Front. Environ. Sci. Eng., 6, 725-733, 2012.

Guo, Q., Hu, M., Guo, S., Wu, Z., Hu, W., Peng, J., Hu, W., Wu, Y., Yuan, B., Zhang, Q., and Song, Y.: The identification of source regions of black carbon at a receptor site off the eastern coast of China, Atmos. Environ., 100, 78-84, 2015.

Hallquist, M., Wenger, J., Baltensperger, U., Rudich, Y., Simpson, D., Claeys, M., Dommen, J., Donahue, N., George, C., and Goldstein, A.: The formation, properties and impact of secondary organic aerosol: current and emerging issues. Atmos. Chem. Phys., 9, 5155-5236, 2009.

He, K., 2012. Multi-resolution Emission Inventory for China (MEIC): model framework and 1990-2010 anthropogenic emissions, AGU Fall Meeting Abstracts, Vol.1, p. 05.

He, L. Y., Huang, X .F., Xue, L., Hu, M., Lin, Y., Zheng, J., Zhang, R., and Zhang, Y. H.: Submicron aerosol analysis and organic source apportionment in an urban atmosphere in Pearl River Delta of China using high-resolution aerosol mass spectrometry. J. Geophys. Res. Atmos., 116, doi: 10.1029/2010JD014566, 2011.

He, L. Y., Lin, Y., Huang, X. F., Guo, S., Xue, L., Su, Q., Hu, M., Luan, S. J., and Zhang, Y. H.: Characterization of high-resolution aerosol mass spectra of primary organic aerosol emissions from Chinese cooking and biomass burning, Atmos. Chem. Phys., 10, 11535-11543, 2010.

Herndon, S. C., Onasch, T. B., Wood, E. C., Kroll, J. H., Canagaratna, M. R., Jayne, J. T., Zavala, M. A., Knighton, W. B., Mazzoleni, C., Dubey, M. K., Ulbrich, I. M., Jimenez, J. L., Seila, R., de Gouw, J. A., de Foy, B., Fast, J., Molina, L. T., Kolb, C. E., and Worsnop, D. R.: Correlation of secondary organic aerosol with odd oxygen in Mexico City, Geophys. Res. Lett., 35, doi: 10.1029/2008GL034058, 2008.

Hu, W. W., Hu, M., Hu, W., Jimenez, J. L., Yuan, B., Chen, W., Wang, M., Wu, Y., Chen, C., Wang, Z., Peng, J., Yang, K., Zeng, L., and Shao, M.: Chemical composition, sources and aging process of sub-micron aerosols in Beijing: contrast between summer and winter. J. Geophys. Res. Atmos., doi: 10.1002/2015JD024020, 2016.

Hu, W. W., Hu, M., Yuan, B., Jimenez, J. L., Tang, Q., Peng, J. F., Hu, W., Shao, M., Wang, M., Zeng, L. M., Wu, Y. S., Gong, Z. H., Huang, X. F., and He, L. Y.: Insights on organic aerosol aging and the influence of coal combustion at a regional receptor site of central eastern China, Atmos. Chem. Phys., 13, 10095-10112, 2013.

Huang, X. F., He, L. Y., Hu, M., Canagaratna, M. R., Kroll, J. H., Ng, N. L., Zhang, Y. H., Lin, Y., Xue, L., Sun, T. L., Liu, X. G., Shao, M., Jayne, J. T., and Worsnop, D. R.: Characterization of submicron aerosols at a rural site in Pearl River Delta of China using an Aerodyne High-Resolution Aerosol Mass Spectrometer, Atmos. Chem. Phys., 11, 1865-1877, 2011.

Huang, X. F., He, L. Y., Hu, M., Canagaratna, M. R., Sun, Y., Zhang, Q., Zhu, T., Xue, L., Zeng, L. W., Liu, X. G., Zhang, Y. H., Jayne, J. T., Ng, N. L., and Worsnop, D. R.: Highly time-resolved chemical characterization of atmospheric submicron particles during 2008 Beijing Olympic Games using an Aerodyne High-Resolution Aerosol Mass Spectrometer, Atmos. Chem. Phys., 10, 8933-8945, 2010.

Huang, X. F., He, L. Y., Xue, L., Sun, T. L., Zeng, L. W., Gong, Z. H., Hu, M., and Zhu, T.: Highly time-resolved chemical characterization of atmospheric fine particles during 2010 Shanghai World Expo, Atmos. Chem. Phys., 12, 4897-4907, 2012.

Huang, X. F., Xue, L., Tian, X. D., Shao, W. W., Sun, T. L., Gong, Z. H., Ju, W. W., Jiang, B., Hu, M., and He, L. Y.: Highly time-resolved carbonaceous aerosol characterization in Yangtze River Delta of China: Composition, mixing state and secondary formation, Atmos. Environ., 64, 200-207, 2013.

Jimenez, J. L., Canagaratna, M. R., Donahue, N. M., Prevot, A. S. H., Zhang, Q., Kroll, J. H., DeCarlo, P. F., Allan, J. D., Coe, H., Ng, N. L., Aiken, A. C., Docherty, K. S., Ulbrich, I. M., Grieshop, A. P., Robinson, A. L., Duplissy, J., Smith, J. D., Wilson, K. R., Lanz, V. A., Hueglin, C., Sun, Y. L., Tian, J., Laaksonen, A., Raatikainen, T., Rautiainen, J., Vaattovaara, P., Ehn, M., Kulmala, M., Tomlinson, J. M., Collins, D. R., Cubison, M. J., Dunlea, J., Huffman, J. A., Onasch, T. B., Alfarra, M. R., Williams, P. I., Bower, K., Kondo, Y., Schneider, J., Drewnick, F., Borrmann, S., Weimer, S., Demerjian, K., Salcedo, D., Cottrell, L., Griffin, R., Takami, A., Miyoshi, T., Hatakeyama, S., Shimono, A., Sun, J. Y., Zhang, Y. M., Dzepina, K., Kimmel,

J. R., Sueper, D., Jayne, J. T., Herndon, S. C., Trimborn, A. M., Williams, L. R., Wood, E. C., Middlebrook, A. M., Kolb, C. E., Baltensperger, U., and Worsnop, D. R.: Evolution of Organic Aerosols in the Atmosphere, Science, 326, 1525-1529, 2009.

Jimenez, J. L., Jayne, J. T., Shi, Q., Kolb, C. E., Worsnop, D. R., Yourshaw, I., Seinfeld, J. H., Flagan, R. C., Zhang, X. F., Smith, K. A., Morris, J. W., and Davidovits, P.: Ambient aerosol sampling using the Aerodyne Aerosol Mass Spectrometer, J. Geophys. Res. Atmos., 108, doi: 10.1029/2001JD001213, 2003.

Kroll, J. H., Donahue, N. M., Jimenez, J. L., Kessler, S. H., Canagaratna, M. R., Wilson, K. R., Altieri, K. E., Mazzoleni, L. R., Wozniak, A. S., Bluhm, H., Mysak, E. R., Smith, J. D., Kolb, C. E., and Worsnop, D. R.: Carbon oxidation state as a metric for describing the chemistry of atmospheric organic aerosol, Nat. Chem., 3, 133-139, 2011.

Kroll, J. H., Ng, N. L., Murphy, S. M., Varutbangkul, V., Flagan, R. C., and Seinfeld, J. H.: Chamber studies of secondary organic aerosol growth by reactive uptake of simple carbonyl compounds, J. Geophys. Res. Atmos., 110, doi: 10.1029/2005JD006004, 2005.

Li, L., Dai, D., Deng, S., Feng, J., Zhao, M., Wu, J., Liu, L., Yang, X., Wu, S., Qi, H., Yang, G., Zhang, X., Wang, Y., and Zhang, Y.: Concentration, distribution and variation of polar organic aerosol tracers in Ya'an, a middle-sized city in western China, Atmos. Res., 120-121, 29-42, 2013a.

Li, L., Chen, Y., Zeng, L., Shao, M., Xie, S., Chen, W., Lu, S., Wu, Y., and Cao, W.: Biomass burning contribution to ambient volatile organic compounds (VOCs) in the Chengdu–Chongqing Region (CCR), China, Atmos. Environ., 99, 403-410, 2014.

Li, Y. J., Lee, B. Y. L., Yu, J. Z., Ng, N. L., and Chan, C. K.: Evaluating the degree of oxygenation of organic aerosol during foggy and hazy days in Hong Kong using high-resolution time-of-flight aerosol mass spectrometry (HR-ToF-AMS), Atmos. Chem. Phys., 13, 8739-8753, 2013b.

Liang, J., Horowitz, L. W., Jacob, D. J., Wang, Y., Fiore, A. M., Logan, J. A., Gardner, G. M., and Munger, J. W.: Seasonal budgets of reactive nitrogen species and ozone over the United States, and export fluxes to the global atmosphere, J. Geophys. Res. Atmos., 103, 13435-13450, 1998.

Luo, Y., Zheng, X., Zhao, T., Chen, J., 2014. A climatology of aerosol optical depth over China from recent 10 years of MODIS remote sensing data. International Journal of Climatology 34, 863-870.

Malm, W. C., and Day, D. E.: Estimates of aerosol species scattering characteristics as a function of relative humidity, Atmos. Environ., 35, 2845-2860, 2001.

Middlebrook, A. M., Bahreini, R., Jimenez, J. L., and Canagaratna, M. R.: Evaluation of composition-dependent collection efficiencies for the Aerodyne aerosol mass spectrometer using field data, Aerosol. Sci. Tech., 46, 258–271, 2011.

Mohr, C., DeCarlo, P. F., Heringa, M. F., Chirico, R., Slowik, J. G., Richter, R., Reche, C., Alastuey, A., Querol, X., Seco, R., Penuelas, J., Jimenez, J. L., Crippa, M., Zimmermann, R., Baltensperger, U., and Prevot, A. S. H.: Identification and quantification of organic aerosol from cooking and other sources in Barcelona using aerosol mass spectrometer data, Atmos. Chem. Phys., 12, 1649-1665, 2012.

Murphy, B. N., Donahue, N. M., Robinson, A. L., and Pandis, S. N.: A naming convention for atmospheric organic aerosol, Atmos. Chem. Phys., 14, 5825-5839, 2014.

Ng, N. L., Canagaratna, M. R., Jimenez, J. L., Chhabra, P. S., Seinfeld, J. H., and Worsnop, D. R.: Changes in organic aerosol composition with aging inferred from aerosol mass spectra, Atmos. Chem. Phys., 11, 6465-6474, 2011.

Ng, N. L., Canagaratna, M. R., Zhang, Q., Jimenez, J. L., Tian, J., Ulbrich, I. M., Kroll, J. H., Docherty, K. S., Chhabra, P. S., Bahreini, R., Murphy, S. M., Seinfeld, J. H., Hildebrandt, L., Donahue, N. M., DeCarlo, P. F., Lanz, V. A., Prévôt, A. S. H., Dinar, E., Rudich, Y., and Worsnop, D. R.: Organic aerosol components observed in Northern Hemispheric datasets from Aerosol Mass Spectrometry, Atmos. Chem. Phys., 10, 4625-4641, 2010.

Niu, H., Cheng, W., Hu, W., and Pian, W.: Characteristics of individual particles in a severe short-period haze episode induced by biomass burning in Beijing, Atmos. Pollut. Res., 10.1016/j.apr.2016.05.011, 2016.

Paatero, P.: Least squares formulation of robust non-negative factor analysis, Chemom. Intell. Lab. Syst., 37, 23-35, 1997.

Robinson, A. L., Donahue, N. M., Shrivastava, M. K., Weitkamp, E. A., Sage, A. M., Grieshop, A. P., Lane, T. E., Pierce, J. R., and Pandis, S. N.: Rethinking organic aerosols: Semivolatile emissions and photochemical aging, Science, 315, 1259-1262, 2007.

Sisler, J. F., and Malm, W. C.: Interpretation of Trends of $PM_{2.5}$ and Reconstructed Visibility from the IMPROVE Network, J. Air Waste Man. Ass., 50, 775-789, 2000.

Song, Y., Liu, B., Miao, W., Chang, D., and Zhang, Y.: Spatiotemporal variation in nonagricultural open fire emissions in China from 2000 to 2007, Glob. Biogeochem. Cy., 23, doi: 10.1029/2008GB003344, 2009.

Ulbrich, I. M., Canagaratna, M. R., Zhang, Q., Worsnop, D. R., and Jimenez, J. L.: Interpretation of organic components from Positive Matrix Factorization of aerosol mass spectrometric data, Atmos. Chem. Phys., 9, 2891–2918, 2009.

Wang, G. H., Kawamura, K., Lee, S., Ho, K. F., and Cao, J. J.: Molecular, seasonal, and spatial distributions of organic aerosols from fourteen Chinese cities, Environ. Sci. Tech., 40, 4619-4625, 2006.

Wang, Q. Y., Cao, J. J., Tao, J., Li, N., Su, X. O., Chen, L. W. A., Wang, P., Shen, Z. X., Liu, S. X., and Dai, W. T.: Long-Term Trends in Visibility and at Chengdu, China, Plos One, 8, doi: 10.1371/journal.pone.0068894, 2013.

Wood, E. C., Canagaratna, M. R., Herndon, S. C., Onasch, T. B., Kolb, C. E., Worsnop, D. R., Kroll, J. H., Knighton, W. B., Seila, R., Zavala, M., Molina, L. T., DeCarlo, P. F., Jimenez, J. L., Weinheimer, A. J., Knapp, D. J., Jobson, B. T., Stutz, J., Kuster, W. C., and Williams, E. J.: Investigation of the correlation between odd oxygen and secondary organic aerosol in Mexico City and Houston, Atmos. Chem. Phys., 10, 8947-8968, 2010.

Yang, F., Tan, J., Zhao, Q., Du, Z., He, K., Ma, Y., Duan, F., Chen, G., and Zhao, Q.: Characteristics of $PM_{2.5}$ speciation in representative megacities and across China, Atmos. Chem. Phys., 11, 5207-5219, 2011.

Yuan, B., Hu, W. W., Shao, M., Wang, M., Chen, W. T., Lu, S. H., Zeng, L. M., and Hu, M.: VOC emissions, evolutions and contributions to SOA formation at a receptor site in eastern China, Atmos. Chem. Phys., 13, 8815-8832, 2013.

Zhang, Q., Alfarra, M. R., Worsnop, D. R., Allan, J. D., Coe, H., Canagaratna, M. R., and Jimenez, J. L.: Deconvolution and quantification of hydrocarbon-like and oxygenated organic aerosols based on aerosol mass spectrometry, Environ. Sci. Tech., 39, 4938-4952, 2005.

Zhang, Q., Jimenez, J. L., Canagaratna, M. R., Allan, J. D., Coe, H., Ulbrich, I., Alfarra, M. R., Takami, A., Middlebrook, A. M., Sun, Y. L., Dzepina, K., Dunlea, E., Docherty, K., DeCarlo, P. F., Salcedo, D., Onasch, T., Jayne, J. T., Miyoshi, T., Shimono, A., Hatakeyama, S., Takegawa, N., Kondo, Y., Schneider, J., Drewnick, F., Borrmann, S., Weimer, S., Demerjian, K., Williams, P., Bower, K., Bahreini, R., Cottrell, L., Griffin, R. J., Rautiainen, J., Sun, J. Y., Zhang, Y. M., and Worsnop, D. R.: Ubiquity and dominance of oxygenated species in organic aerosols in anthropogenically-influenced Northern Hemisphere midlatitudes, Geophys. Res. Lett., 34, doi:10.1029/2007GL029979, 2007.

Zhang, Q., Jimenez, J. L., Canagaratna, M. R., Ulbrich, I. M., Ng, N. L., Worsnop, D. R., and Sun, Y.: Understanding atmospheric organic aerosols via factor analysis of aerosol mass spectrometry: a review, Anal. Bioanal. Chem., 401, 3045-3067, 2011.

Zhang, X. Y., Wang, Y. Q., Zhang, X. C., Guo, W., and Gong, S. L.: Carbonaceous aerosol composition over various regions of China during 2006, J. Geophys. Res. Atmos., 113, doi:10.1029/2007JD009525, 2008.

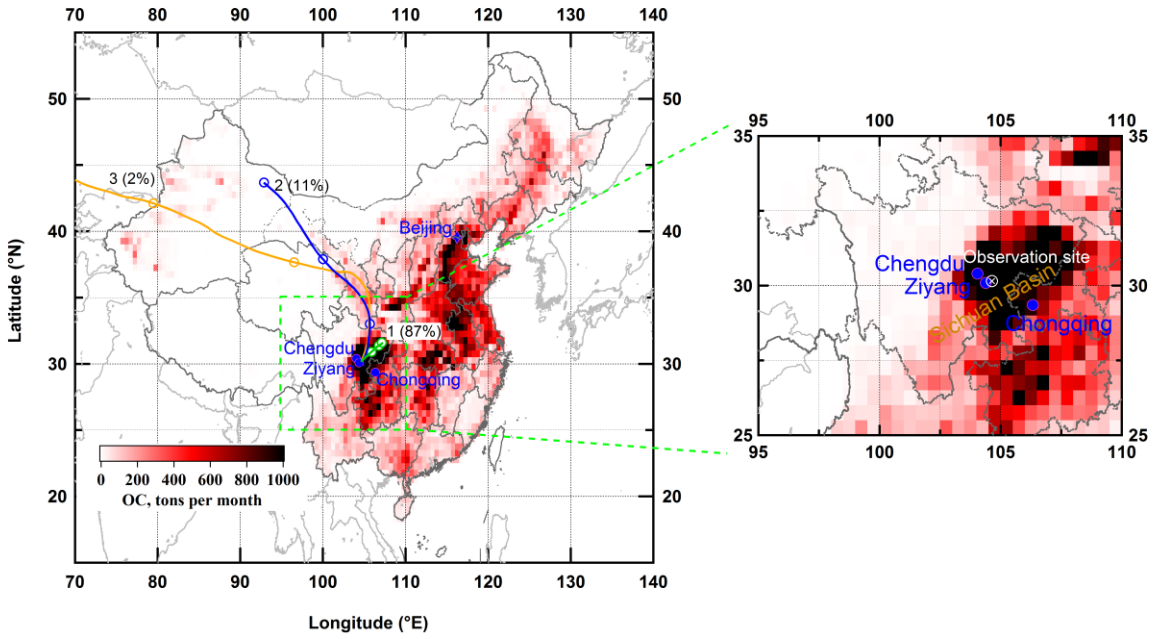

Figure 1. Location of the observation site in Ziyang in the Sichuan Basin. Back-trajectories of air masses at the site calculated by HYSPLIT model are illustrated as lines (circles marking 24-h intervals). The map of China is color-coded according to residential OC emissions in January 2010 modeled by Multi-resolution Emission Inventory for China (MEIC, http://www.meicmodel.org).

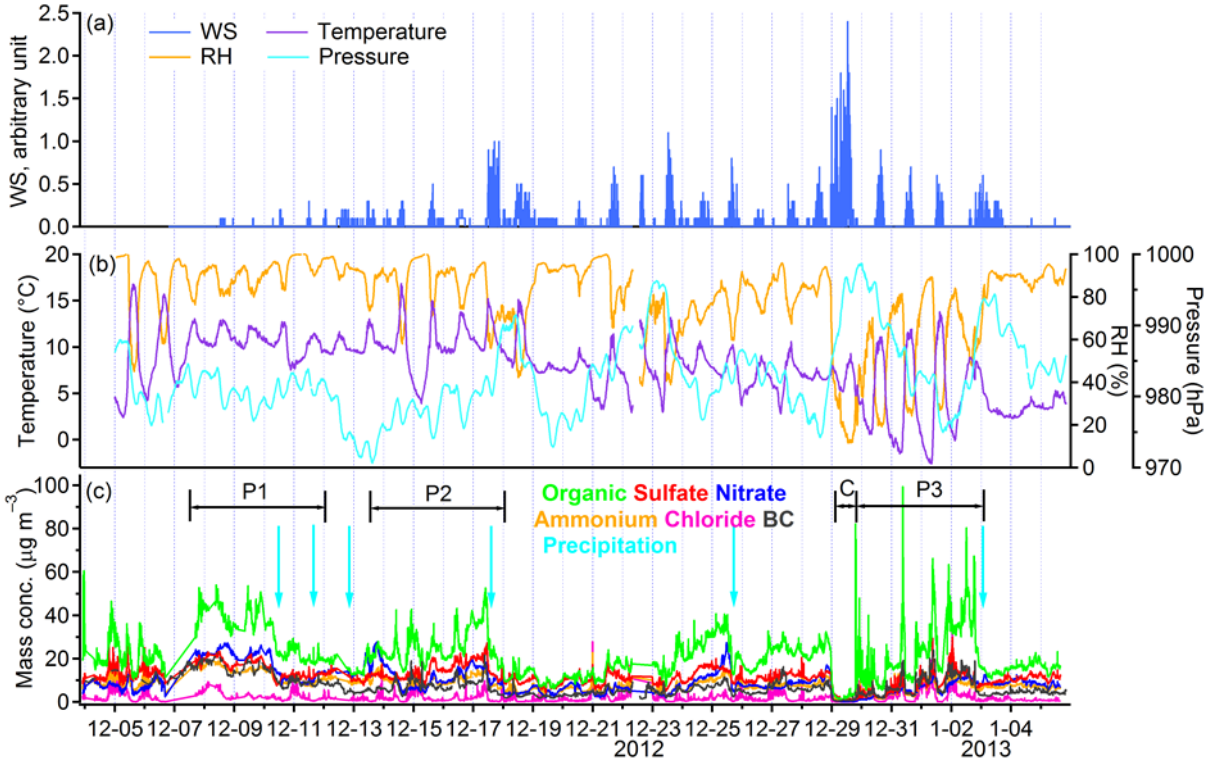

Figure 2. Time series of meteorological parameters and concentrations of chemical compositions in submicron aerosols during the campaign. (a) Wind speed (WS), relative values; (b) relative humidity (RH), temperature and atmospheric pressure; (c) concentrations of chemical compositions in submicron aerosols. Short-term precipitation events are marked by the light blue arrows.

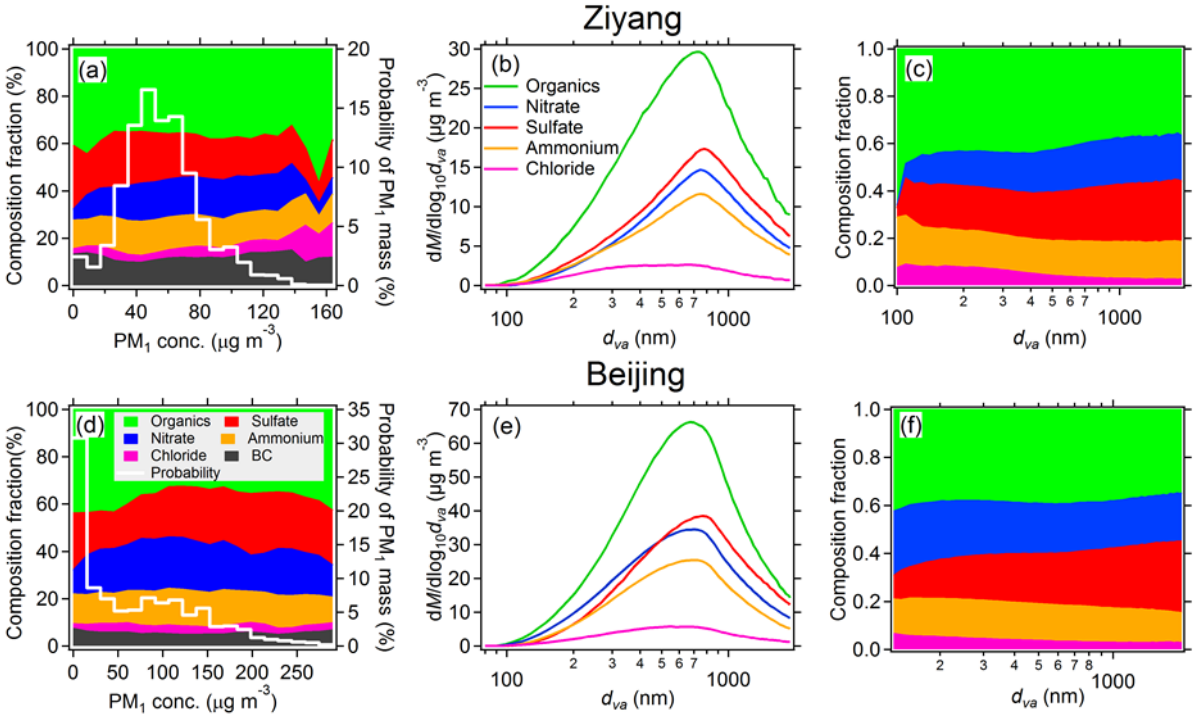

Figure 3. Comparison of the results between Ziyang site (upper) and an urban site in Beijing (lower) during the near wintertime. (a, d) Fractions of main chemical components in PM_1 as a function of PM_1 mass concentrations (left) and the probability density of PM_1 mass concentrations (right); (b, e) Average size-resolved mass concentration distributions of chemical species in submicron aerosols; (c, f) Fractions of chemical species in total NR-PM_1 as a function of vacuum aerodynamic size (d_{va}).

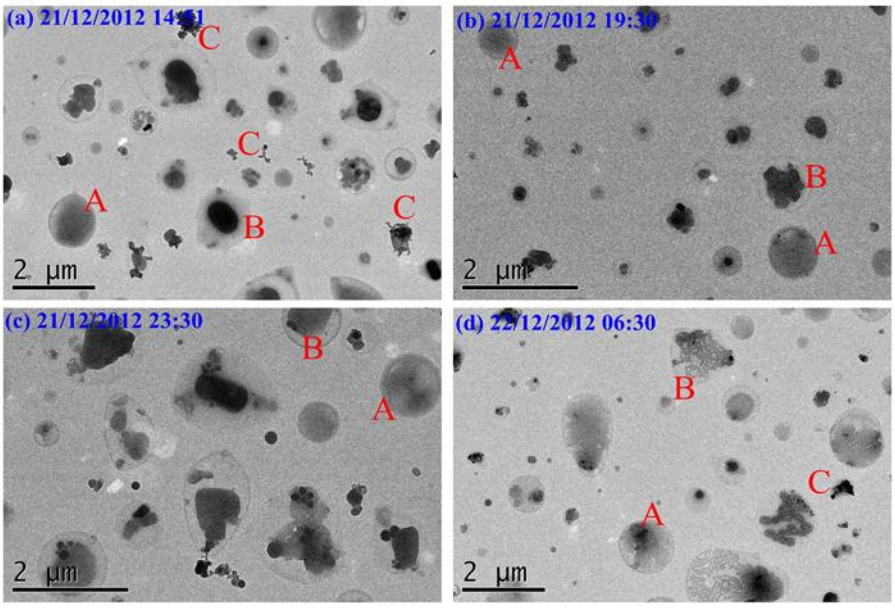

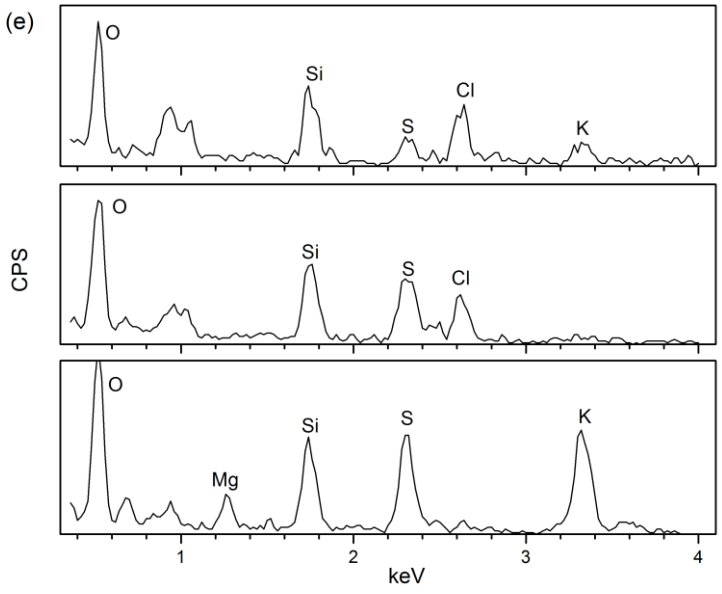

Figure 4. (a-d) Morphology and the mixing state of single particles in hazy days at Ziyang site. The predominant particles are spherical ones without or with coating (Type A and B), and in internal mixing state; some fresh and aged soot aggregates (Type C) were also observed. (e) Examples of elemental compositions in single particles collected at Ziyang site. CPS, counts per second.

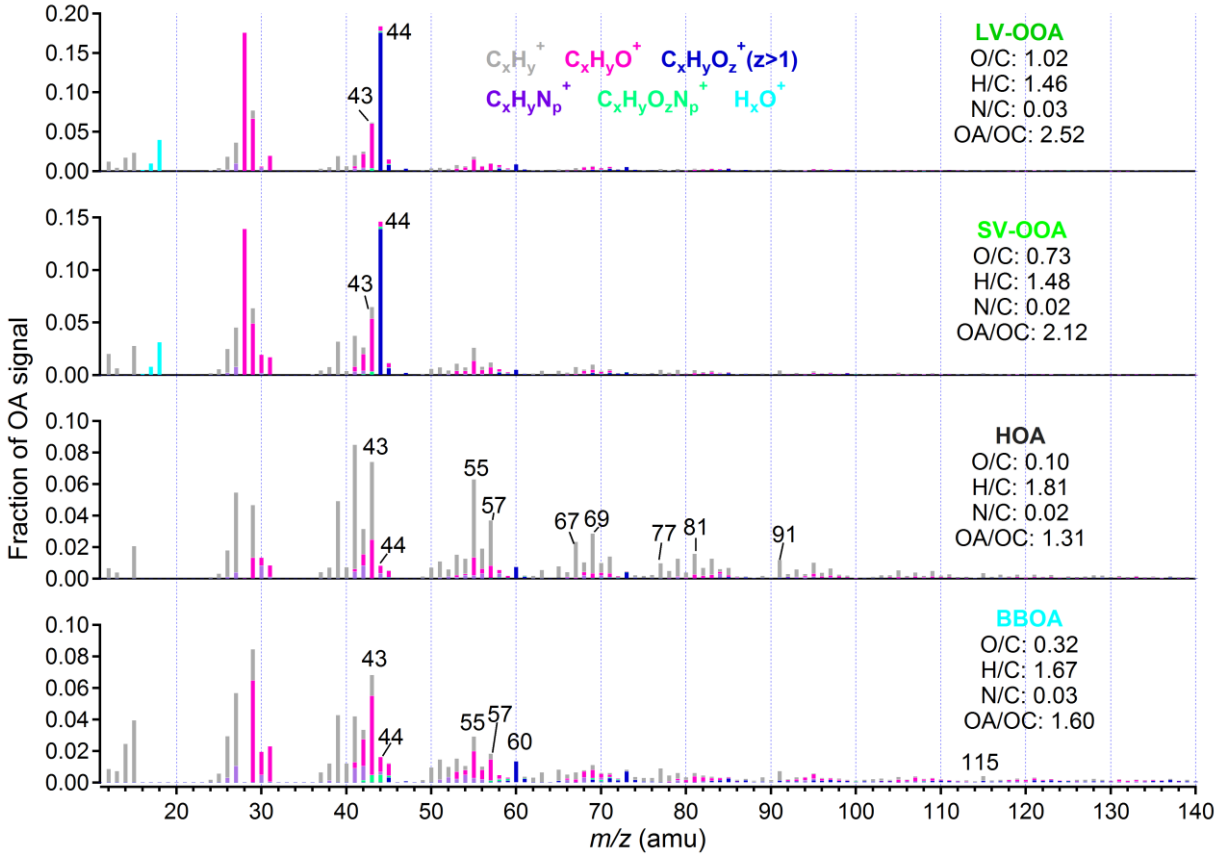

Figure 5. Unit mass spectra of OA factors: LV-OOA, SV-OOA, HOA and BBOA. The elemental ratios and OA/OC ratios of each component are also added.

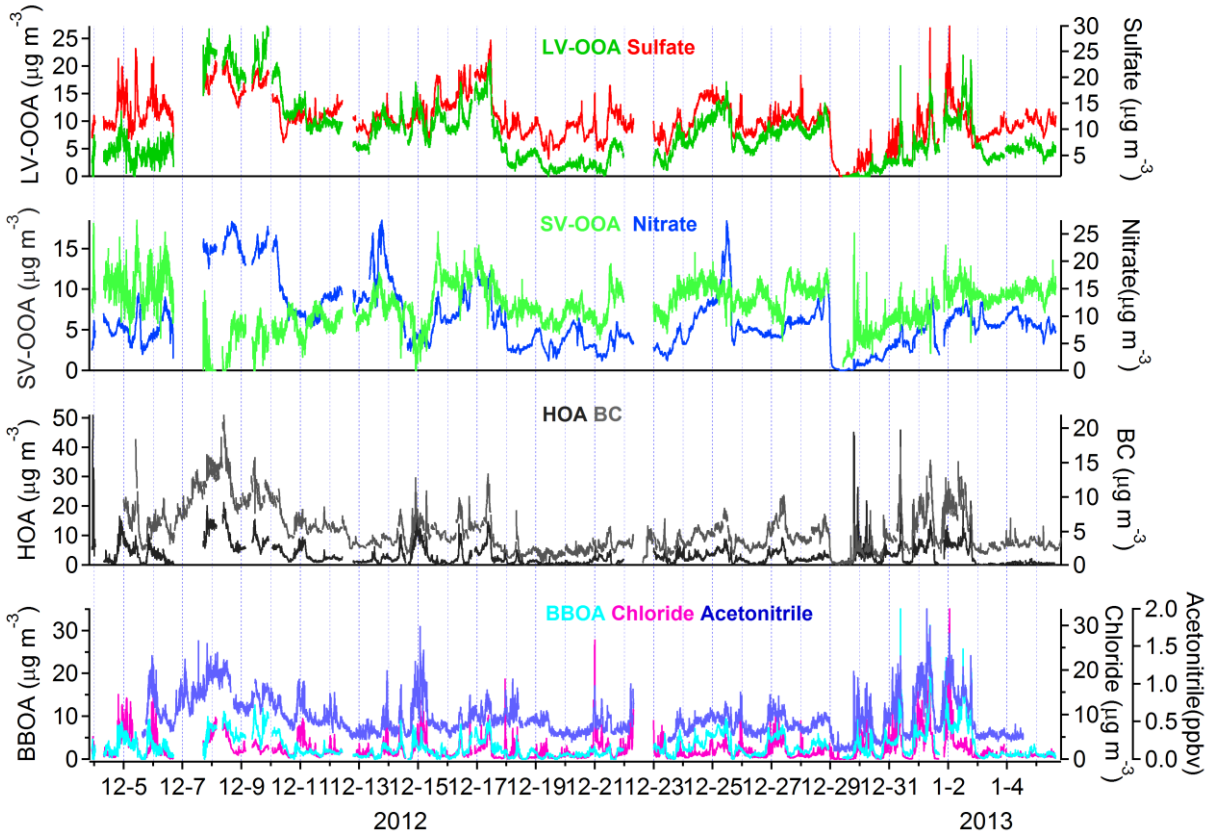

Figure 6. Time series of OA fractions and external tracers (sulfate, nitrate, BC, chloride and acetonitrile).

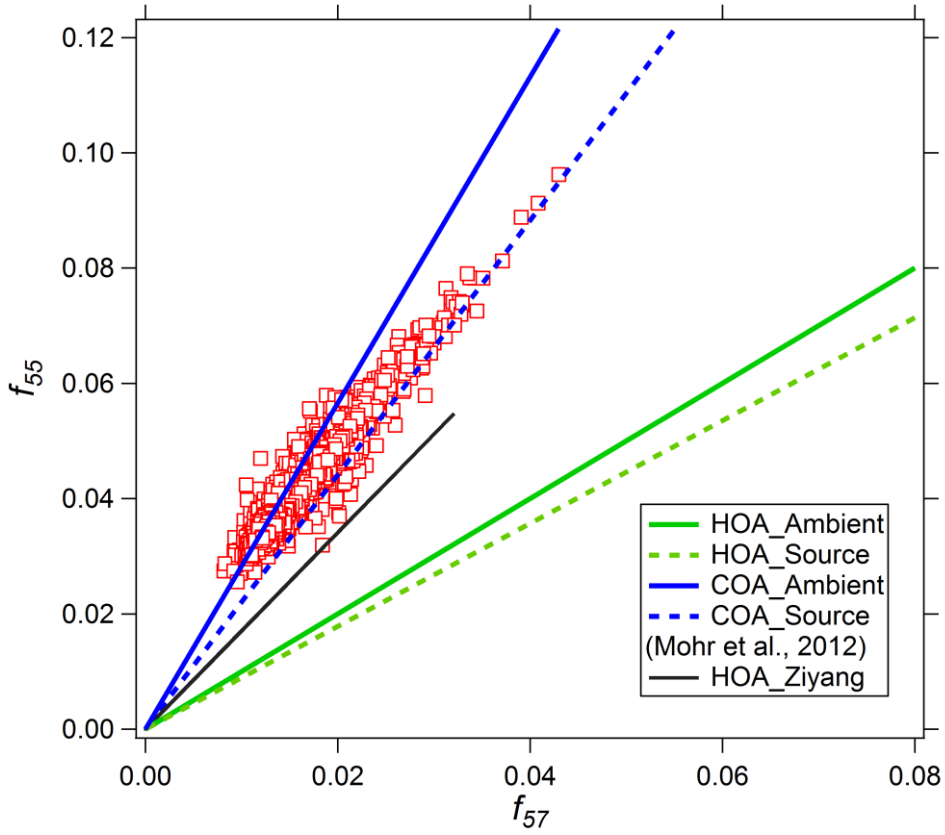

Figure 7. Scatter plot between f_{55} vs. f_{57}. The f_{55} vs. f_{57} ratios of "HOA_Ambient" and "COA_Ambient" represent average f_{55} vs. f_{57} values from various PMF HOA and COA factors, and those of "HOA_Source" and "COA_Source" represent f_{55} vs. f_{57} values averaged from several source emission studies reported in Mohr et al. (2012).

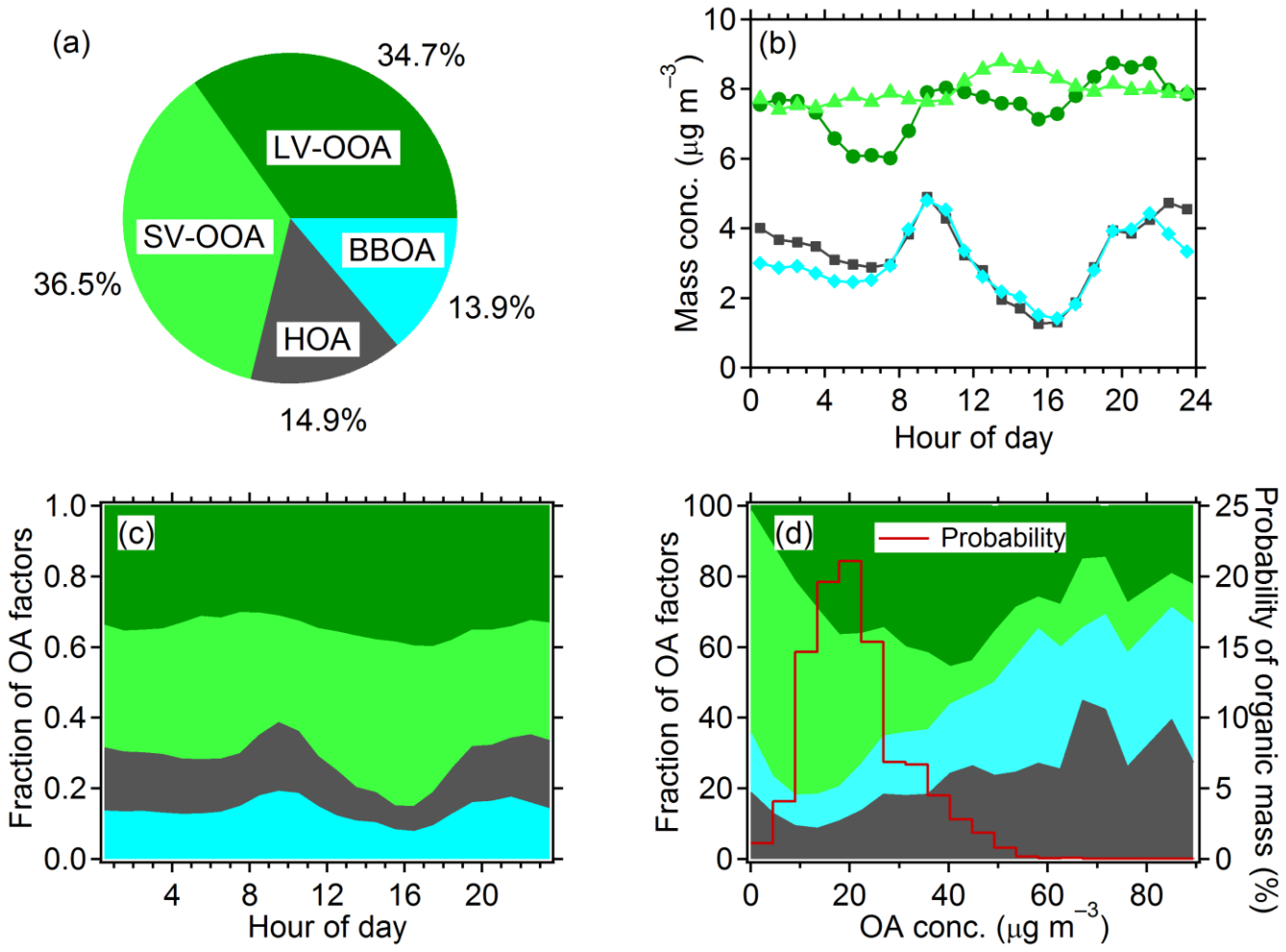

Figure 8. (a) Average mass fraction of each OA component. Diurnal variations of concentrations (b) and fractions in OA (c) for different OA components. (d) Fractions of different OA components in total OA (left) depending on OA concentrations and the probability density of OA concentrations (right).

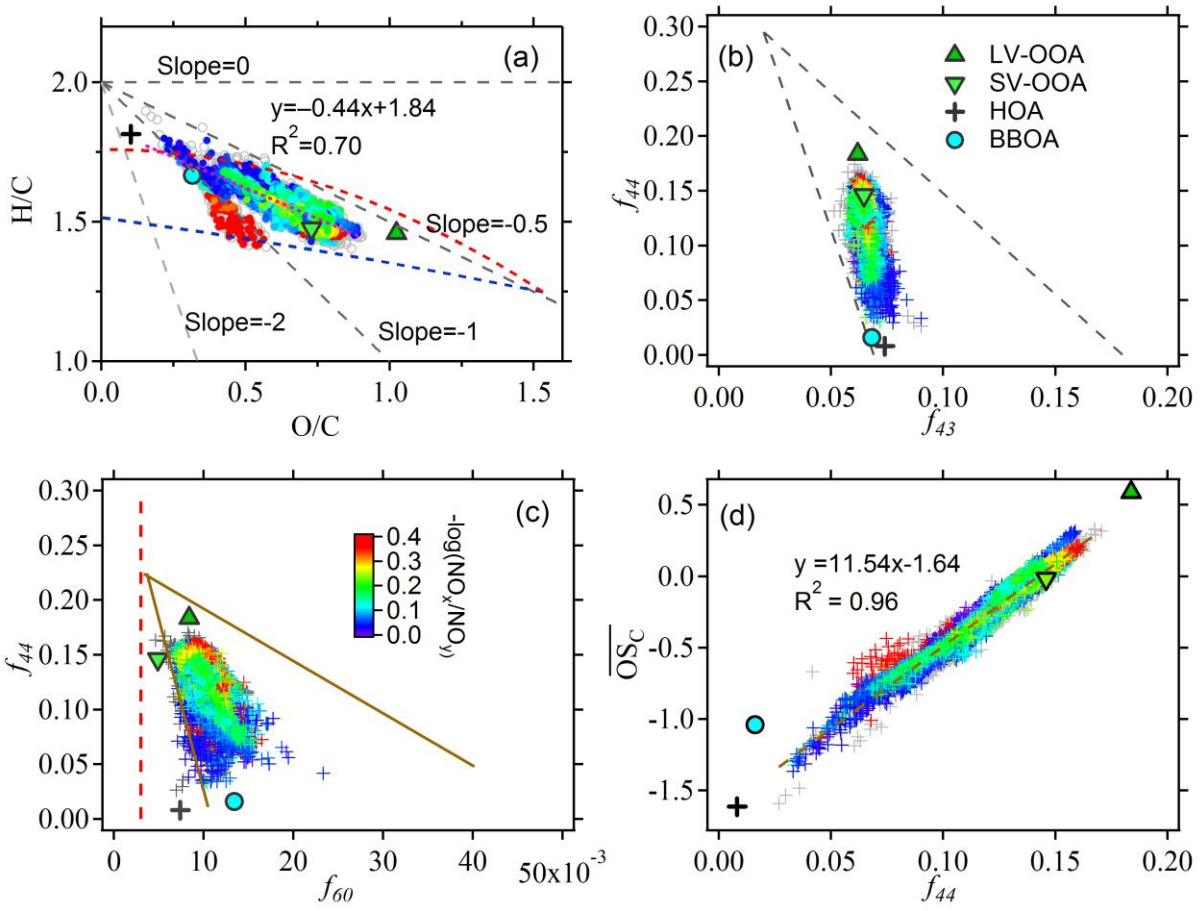

Figure 9. (a) Van Krevelen diagram of organic aerosols. The majority of the data fall into colored triangle lines (Ng et al., 2011). (b) Scattering plot of f_{44} (m/z 44 fraction in organic mass spectra) vs. f_{43}. The triangular space defined by dash lines (Ng et al., 2011) indicates the region where the data of OA components fall into. (c) Scattering plot of f_{44} vs. f_{60}. The conceptual space for BBOA and the nominal background value at 0.3% (Cubison et al., 2011) are marked by solid and vertical dash lines, respectively. (d) Average carbon oxidation state ($\overline{OS_C}$) vs. f_{44} at Ziyang site. The scattering data points are colored by the photochemical age metric –log (NO_x/NO_y). The locations of OA factors are also marked in all diagrams.

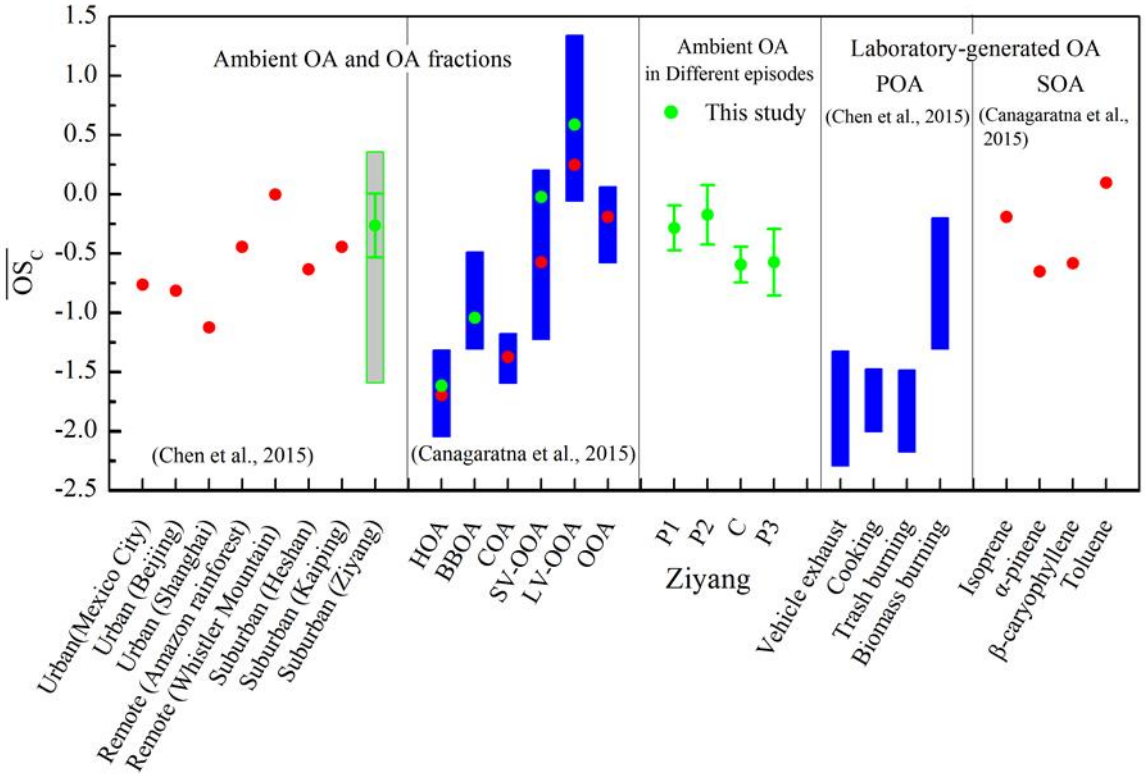

Figure 10. Improved-Ambient results of $\overline{OS_C}$ for OA. The previously reported results are from the summary by Chen et al. (2015) and Canagaratna et al. (2015). The floating bar, dot and error bar mean the range, average and standard deviation of $\overline{OS_C}$.

5

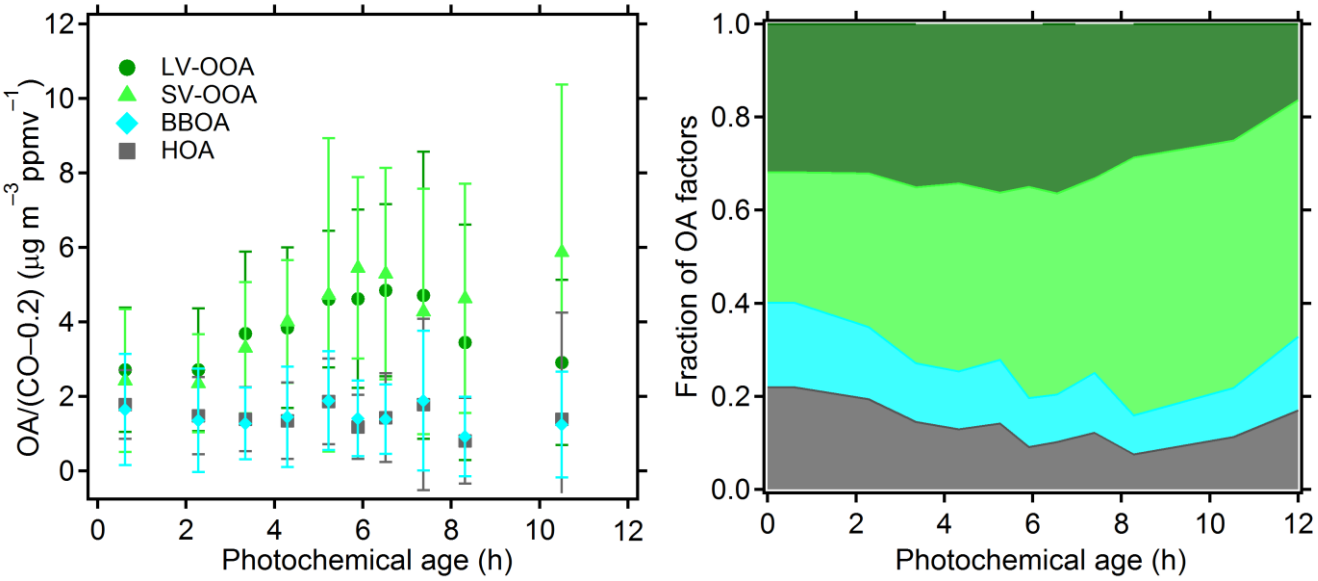

Figure 11. (a) The variations of LV-OOA/ΔCO, SV-OOA/ΔCO, BBOA/ΔCO and HOA/ΔCO with the photochemical age. The dot point and bar in each photochemical age bin are the average value and standard deviation. (b) Mass fraction of each OA component as a function of photochemical age. The photochemical age is classified into 10 bins by decile.

Table 1 Average concentrations and fractions of chemical species in submicron aerosols in different sites in China. The numbers in parenthesis are the proportions of chemical components in PM_1. The O/C and H/C ratios of OA are corrected herein by the "Improved-Ambient" method (Canagaratna et al., 2015). Unit of mass concentrations: μg m^{-3}. *The two factors are defined as OOA-1 and OOA-2; #, + and ≠ are factors defined as OOA, COA and CCOA, respectively. [a] data are not corrected by the "Improved-Ambient" method.

	Ziyang (This study)					Beijing[1]	Shanghai[2]	Shenzhen[3, 4]		Jiaxing[5]		Heshan[6]	Kaiping[7]	Backgarden [8]	Changdao Island[9]
Site type	Suburban					Urban				Suburban/Rural				Coastal/ Background	
Sampling time	Overall	P1	P2	C	P3	Summer	Summer	Summer	Autumn	Summer	Winter	Autumn	Autumn	Summer	Spring
RH (%)	80	91	86	24	57	67	66	73	63	73	65	67	69	78	56
T (℃)	8	11	10	7	4	28	21	29	20	29	9	20	24	29	8
PM_1	59.7	91.6	71.8	7.6	56.9	63.1	29.2	51.1	44.5	32.9	41.9	47.9	33.1	35.4	46.6
Organics	21.5(36)	31.7(35)	25.6(36)	2.9(38)	23.8(42)	23.9(38)	8.4(29)	19.4(38)	17.7(40)	10.6(32)	12.7(30)	17.4(36)	11.2(34)	13.4(38)	13.4(30)
LV-OOA	7.5(13)	16.3(18)	10.4(15)	0.04(0.5)	5.5(10)	8.1(13)*	2.4(8)	5.6(11)	4.9(11)	7.2(22)#	3.8(9)#	6.8(14)	4.0(12)	5.1(14)	6.1(13)
SV-OOA	7.9(13)	4.6(5)	9.1(13)	1.8(23)	7.1(12)	5.7(9)*	3.9(14)	7.7(15)	3.3(8)			5.0(10)	4.4(13)	3.8(11)	3.3(7)
HOA	3.2(5)	6.3(7)	3.5(5)	0.6(8)	5.2(9)	4.3 (7)	2.0(7)	6.1(12)	5.2(12)	3.3(10)	5.0(12)	3.1(6)		4.6(13)	3.2(7)
BBOA	3.0(5)	4.5(5)	2.6(4)	0.5(7)	6.1(11)	5.8 (9)+			4.3(10)		3.8(9)	2.5(5)	2.7(8)		1.2(3)≠
Sulfate	11.7(20)	15.5(17)	14.6(20)	2.1(28)	8.2(14)	16.8(27)	9.7(33)	19.0(37)	10.9(25)	8.3(25)	7.1(17)	10.0(21)	11.2(34)	12.5(35)	8.3(19)
Nitrate	9.4(16)	17.5(19)	12.1(17)	0.5(6)	6.1(11)	10.0(16)	4.8(16)	3.0(6)	4.5(10)	5.9(18)	7.5(18)	6.2(13)	3.5(11)	1.3(4)	12.2(28)
Ammonium	8.3(14)	12.7(14)	9.8(14)	1.0(14)	6.6(12)	10.0(16)	3.9(13)	6.1(12)	4.5(10)	4.1(13)	4.9(12)	4.6(10)	4.6(14)	4.1(12)	6.5(15)
Chloride	2.3(4)	2.8(3)	2.2(3)	0.3(3)	4.0(7)	0.5(1)	0.5(2)	0.3(1)	0.7(2)	1.0(3)	2.7(7)	1.5(3)	0.4(1)	0.5(2)	1.3(3)
BC	6.5(11)	11.3(12)	7.6(11)	0.8(11)	8.2(14)	1.8(3)	2.0(7)	3.4(7)	6.2(14)	3.0(9)	7.1(17)	8.2(17)	2.2(7)	3.5(10)	2.5(6)
OOA/OA (%)	71	66	78	61	52	58	76	68	48	69	30	67	74	66	67
OM/OC	2.02	2.03	2.08	1.76	1.85		1.55[a]		1.71	1.67	1.75	1.87	1.94		1.91[a]
O/C	0.65	0.65	0.69	0.46	0.52	0.41	0.40		0.39	0.36	0.43	0.50	0.60		0.59[a]
H/C	1.56	1.58	1.55	1.50	1.60	1.63	1.92		1.83	1.94	1.73	1.63	1.64		1.33[a]
$\overline{OS_C}$	-0.26	-0.28	-0.17	-0.59	-0.57	-0.81	-1.12		-1.04	-1.22	-0.87	-0.63	-0.44		-0.15[a]

References: 1. Huang et al., 2010; 2. Huang et al., 2012; 3. Gong et al., 2013; 4. He et al., 2011; 5. Huang et al., 2013; 6. Gong et al., 2012; 7. Huang et al., 2011; 8. Xiao et al., 2011; 9. Hu et al., 2013.

Supporting information of "Characterization of submicron aerosols influenced by biomass burning at a site in the Sichuan Basin, southwestern China"

Wei Hu, Min Hu[*], Wei-Wei Hu[#], Hongya Niu, Jing Zheng, Yusheng Wu, Wentai Chen, Chen Chen, Lingyu Li, Min Shao, Shaodong Xie, Yuanhang Zhang

State Key Joint Laboratory of Environmental Simulation and Pollution Control, College of Environmental Sciences and Engineering, Peking University, Beijing 100871, China

[#]now at: Cooperative Institute for Research in Environmental Sciences, University of Colorado, Boulder, CO 80309, USA

[*]Correspondence to: M. Hu (minhu@pku.edu.cn)

S1 Location of the observation site

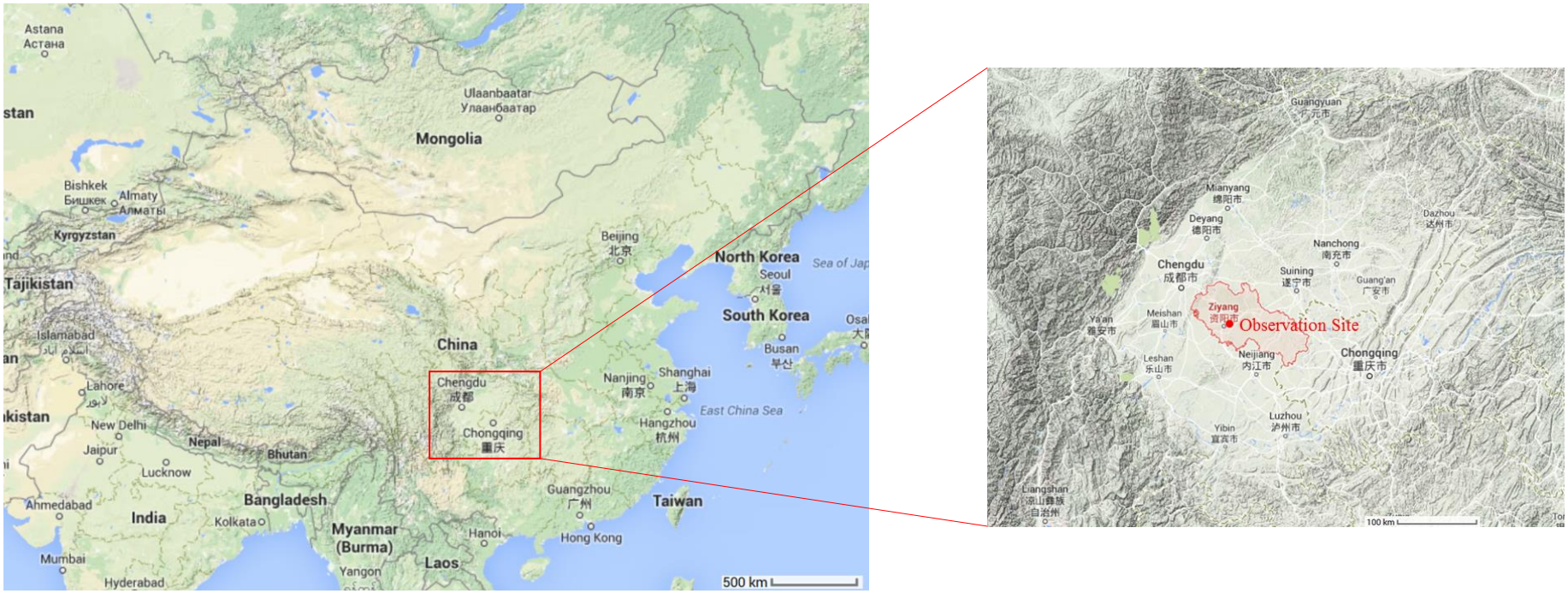

Figure S1. Location of the observation site in Ziyang in the Sichuan Basin. The topography of the Sichuan Basin is also shown (from Google Map).

S2 Backward trajectory of air parcels

The backward trajectories of air parcels during the campaign were calculated by NOAA's HYSPLIT4.9 model (www.arl.noaa.gov/hysplit.html). The total run time and height of start locations were set as 72 hours and 500 m, respectively. The result of backward trajectory clustering is shown in Fig. 1.

The climate and weather in the Sichuan Basin are relatively isolated. During the one-month long campaign, only in one day, 29 December, it was affected by the invasion of long-transported air mass from Northwest China accompanying with strong wind. In all the rest days, the air parcels were lingering in the basin due to the block of special basin terrain, and the atmospheric processes are dominated by the separate meteorology of the basin. Therefore, the pollutants in Sichuan Basin are difficult to diffuse in the static air. Local pollution is dominated in this region, while long-distance transportation has little impact.

S3 Determination of the PMF solution

Factor number from 1 to 10 and the different seeds (0-50) were selected to run in the model. A 4-factor solution was selected for the final results. Four PMF OA factors are semi-volatile oxygenated OA (SV-OOA; O/C=0.73), low-volatility oxygenated OA (LV-OOA; O/C=1.02), biomass burning OA (BBOA; O/C =0.32) and hydrocarbon-like OA (HOA, O/C =0.10). The performances of spectra and time series of the four factors at different f_{peak} were also investigated. The detailed information on how to select PMF factors can be found in Figure S2-S6 and Table S1-S3.

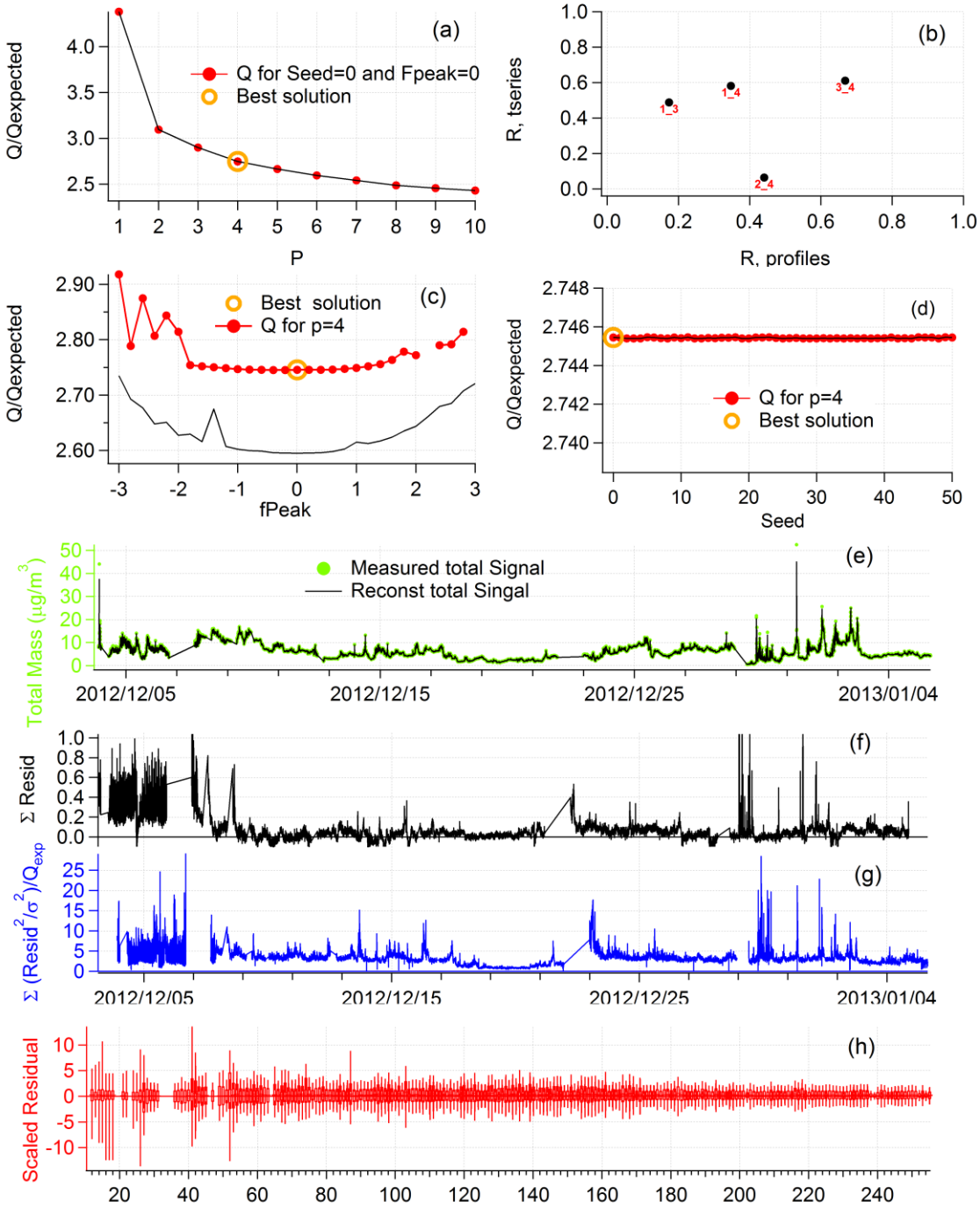

Figure S2 Diagnostics plots of PMF analysis on OA mass spectral matrix. Very stable PMF solution among different seed numbers (0-50) was also found, which suggests the PMF solution is robust here.

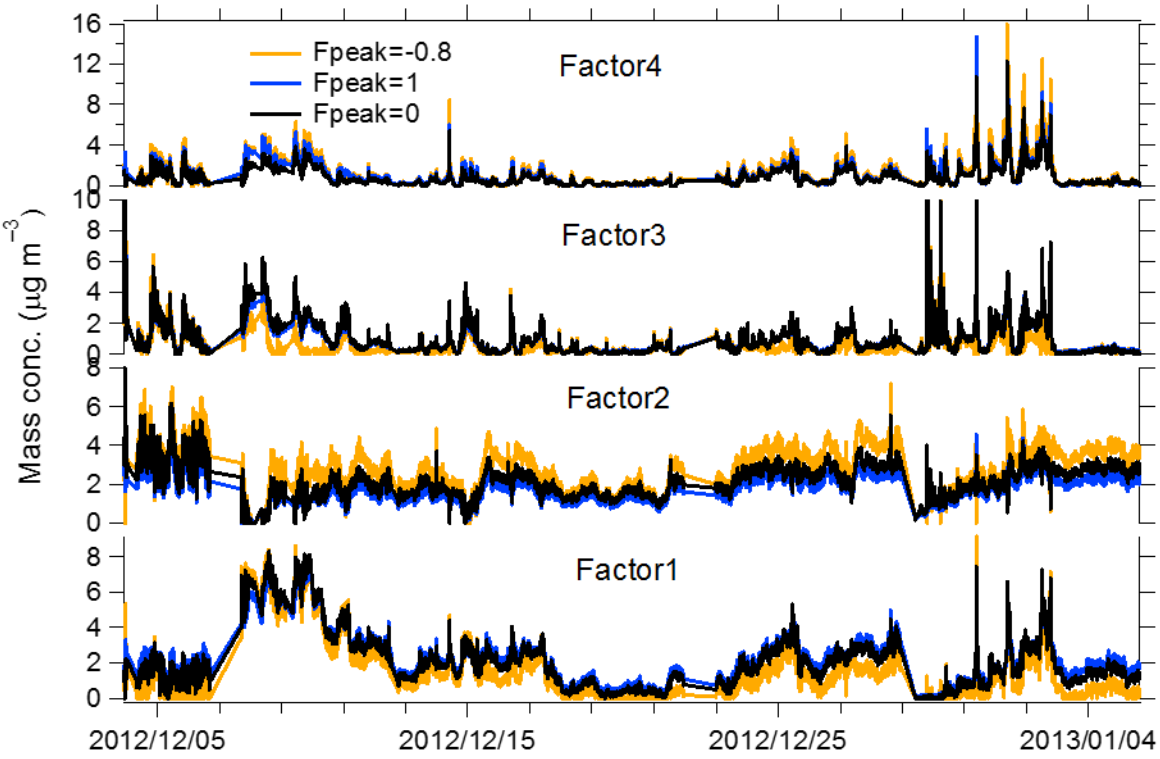

Figure S3. The spectra and time series of 4-factor solution at different f_{peak} values.

Table S1 Descriptions of PMF solutions obtained at Ziyang site.

Factor number	**Fpeak**	**Seed**	**Q/Q_{exp}**	**Solution Description**
1	0	0	4.38	Too few factors, large residuals at time periods and key m/z's
2	0	0	3.10	Too few factors, large residuals at time periods and key m/z's
3	0	0	2.90	Too few factors (OOA-, HOA- and BBOA-like). The Q/Q_{exp} at different seeds (0-50) are very unstable. Factors are mixed to some extend based on the time series and spectra.
4	**0**	**0**	**2.75**	**Optimum choices for PMF factors (LV-OOA, SV-OOA, HOA and BBOA). Time series and diurnal variations of PMF factors are consistent with the external tracers. The spectra of four factors are consistent with the source spectra in AMS spectra database.**
5-10	0	0	2.66-2.43	Factor split. Take 5 factor number solution as an example, SV-OOA and HOA were split into three factors with similar spectra (**Fig. S4-S6**), however, different time series. When factor num. = 6, there is extra split factor from BBOA.
4	-3 to 3	0	2.75-2.92	In FPEAK range from −0.8 to1.0, factor MS and time series are nearly identical.

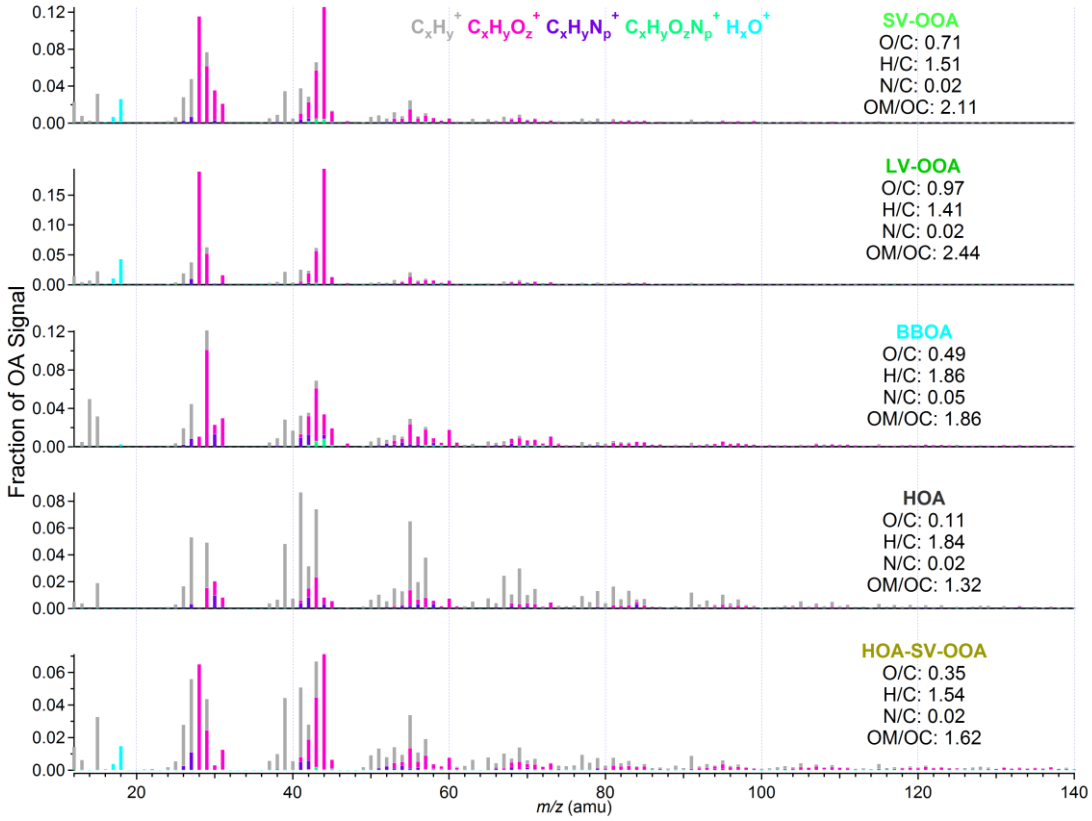

Figure S4. Unit mass spectra of OA factors for 5-factor solution. SV-OOA and HOA for four-factor solution were split into three factors with similar spectra (Fig. S6), marked as SV-OOA, HOA, and HOA-SV-OOA. The other two are marked as LV-OOA and BBOA. The elemental ratios and OA/OC ratios of each component are also added.

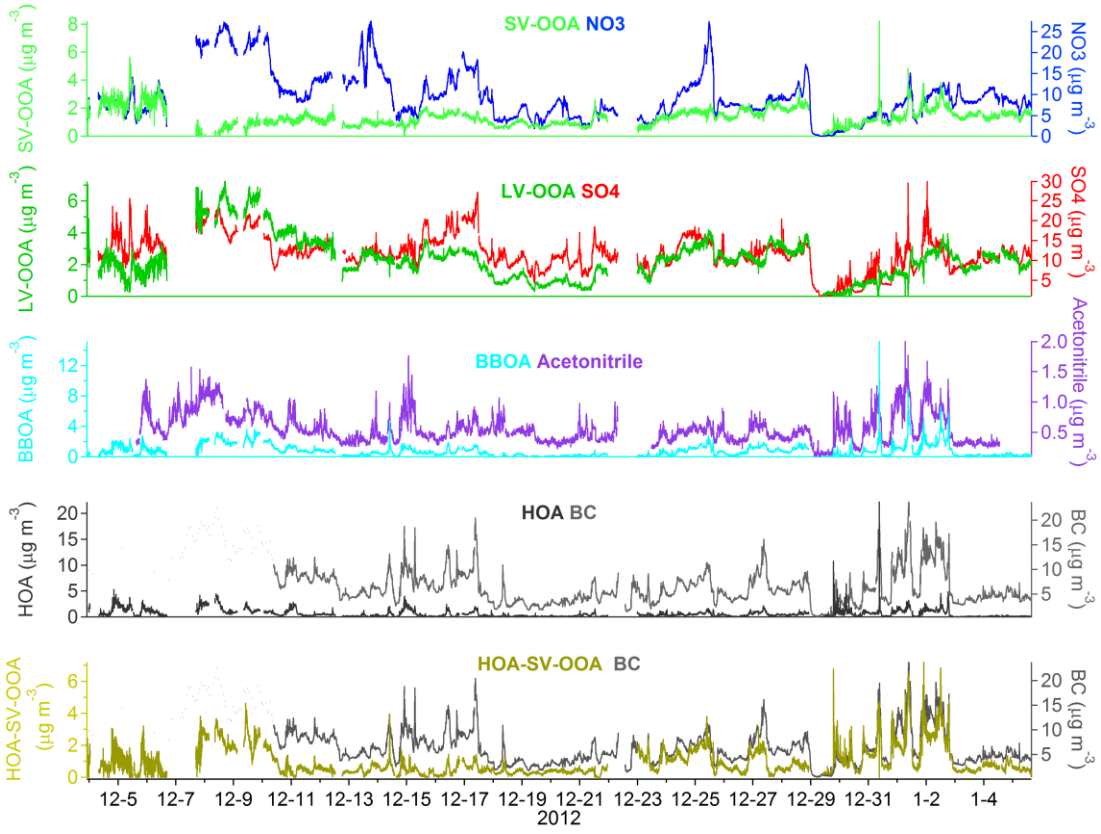

Figure S5. Time series of OA fractions for five-factor solution (marked as SV-OOA, HOA, HOA-SV-OOA, LV-OOA and BBOA) and external tracers (sulfate, nitrate, BC, and acetonitrile).

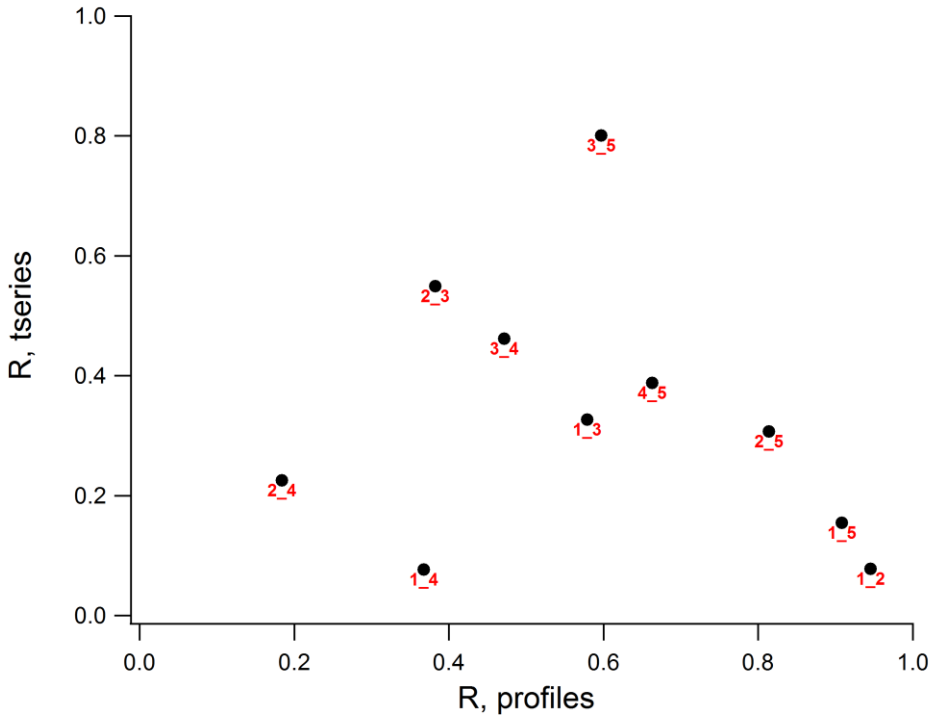

Figure S6. Correlation of time series and unit mass spectra of OA factors for 5-factor solution.

Table S2 The uncentered correlation coefficients between the MS of OA factors resolved in this study and the average MS of OA factors.

	Ziyang				**Average**						
	LV-OOA	SV-OOA	HOA	BBOA	LV-OOA	SV-OOA	HOA	BBOA	CCOA	COA	Vehicle-OA
LV-OOA	1.00				0.99	0.92					
SV-OOA	0.98	1.00			0.99	0.97					
HOA	0.38	0.52	1.00				0.96	0.89	0.65	0.96	0.88
BBOA	0.48	0.59	0.88	1.00			0.86	0.93	0.65	0.81	0.68

Note: The average MS of OA factors are summarized by Hu (2012). The MS of OA factors resolved in studies over China are from He et al. (2010, 2011), Hu et al. (2013, 2016) and Huang et al. (2010, 2011). Other MS of OA factors are from AMS Spectral Database (Unit Mass Resolution). Specifically, the published spectra used for the average MA of each OA factor are listed as follows. **LV- and SV-OOA:** He et al., 2011; Hu et al., 2016; Huang et al., 2011. **HOA:** Aiken et al., 2009; He et al., 2011; Hu et al., 2016. **BBOA:** Aiken et al., 2009; He et al., 2010, 2011; Huang et al., 2011; Lanz et al., 2008; Ng et al., 2010; Weimer et al., 2008; **COA:** He et al., 2010; Hu et al., 2016; Huang et al., 2010; Mohr et al., 2009; **CCOA:** Hu et al., 2013; Vehicle-OA: Canagaratna et al., 2004; Mohr et al., 2009.

Table S3 Correlation coefficients (Pearson's R) of OA factors with gaseous and aerosol species. Correlation coefficients higher than 0.60 are in bold.

	LV-OOA	SV-OOA	HOA	BBOA
SO_4^{2-}	**0.65**	0.36	0.26	0.30
NO_3^-	**0.66**	0.31	0.15	0.21
NH_4^+	**0.68**	0.28	0.36	0.34
Cl^-	0.22	-0.08	0.57	0.49
BC	**0.75**	0.18	**0.73**	**0.77**
$C_2H_4O_2^+$	**0.77**	0.28	**0.80**	**0.85**
SO_2	0.10	0.09	0.39	0.44
NO_x	0.31	-0.13	**0.62**	0.47
NO_y	0.39	-0.09	**0.64**	0.51
O_3	-0.31	0.08	-0.32	-0.21
CO	0.20	-0.09	0.49	0.42
Acetaldehyde	0.34	0.26	**0.65**	**0.77**
Acetonitrile	0.44	-0.02	**0.73**	**0.68**
Toluene	0.57	-0.39	**0.78**	0.52
Benzene	0.55	-0.28	**0.76**	0.58
Acetone	0.48	0.14	0.49	0.54
LV-OOA	**1.00**			
SV-OOA	0.37	**1.00**		
HOA	0.53	0.01	**1.00**	
BBOA	0.55	0.25	**0.78**	**1.00**

S4 Diurnal patterns of chemical species in PM_1 and gaseous pollutants

The diurnal patterns of main chemical components in submicron aerosols in Ziyang were shown in Fig. S4. The diurnal patterns of organics and BC were more obvious than those of other species. Both of them showed two peaks appearing in the morning (about 9:00-10:00 local time, LT) and evening (about 20:00 LT). The concentration of organics may be elevated with local primary sources, such as emissions from vehicle, biomass burning and coal combustion, as well as secondary formation. The diurnal variations of specific factors contributed to organic aerosols are as refer to Sect. 3.2. The concentration of BC was enhanced daily in the two time intervals, probably caused by the contributions of primary emissions related to local residence.

The diurnal variation of nitrate also showed a weak bimodal pattern. One peak in the morning was a little later than those of organics and BC, and the other was in the evening. The concentration of nitrate was significantly affected by gas-particle partitioning. The precursors of ammonium nitrate, e.g. gaseous nitric acid and ammonia, were in favor of converting from the gaseous phase to particulate nitrate in the morning and nighttime due to lower temperature and higher humidity. In the nocturnal atmosphere, NO_3 and N_2O_5 radicals, constitute an important chemical system (Brown, 2003). In the cases of Beijing and Shanghai, Pathak et al. (2011) postulated that nighttime enhancement of nitrate was related to the heterogeneous hydrolysis of N_2O_5. Furthermore, the concentration of nitrate was reduced in the afternoon, which may not only be associated with the volatilization of nitric acid and ammonia, but also be influenced by the dilution of pollutants due to the uplift of atmospheric boundary layer (Zhang et al., 2005).

Sulfate showed no evident diurnal pattern and much more steady in the whole day, indicating the regional formation and accumulation of sulfate. According to the effect of neutralization, the diurnal variation of ammonium should be of comprehensive characteristics of sulfate and nitrate. However, the pattern of ammonium was not so obvious and much more like that of sulfate. The diurnal variation of chloride was opposite to that of atmospheric temperature for its semi-volatility as ammonium chloride, with higher concentrations in the nighttime. In

addition, it was mostly emitted from combustion processes for the similar diurnal patterns with primary source tracers, such as SO_2 and CO (Zhang et al., 2005; Hu et al., 2012).

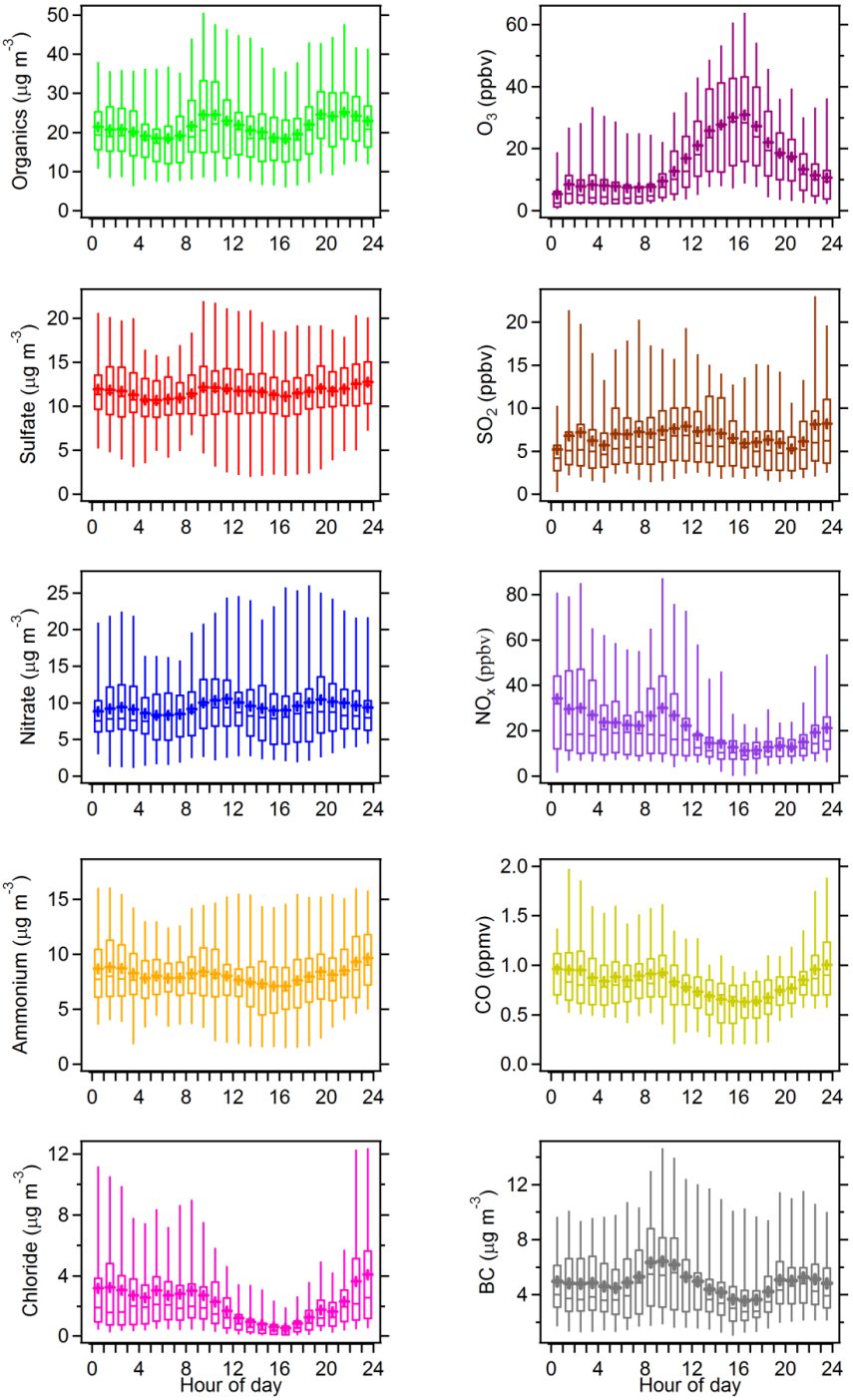

Figure S7. Diurnal patterns of chemical species of submicron particles and gaseous pollutants at Ziyang site.

S5 Morphology, mixing state and elemental compositions of particles

Atmospheric particles at Ziyang site were collected in several days. Here several groups of samples collected in foggy and hazy days, 21-22 December 2012, were chosen for preliminary illustration the properties of single particles by using TEM-EDX. The RH began to decrease from saturated (100%) to unsaturated (66%) in the afternoon of 21 December (Fig. 1a). The samples of the first group were collected in this process and the rest samples were collected in unsaturated humidity conditions, and the sampling time for each sample was 30 seconds. The analysis in detail will be shown in another paper. The morphology and the mixing state are shown in TEM photographs of single particles as Fig. 4a-d, and the elemental compositions for typical particles are shown in Fig. 4e.

As Fig. 3a-d shown, single particles collected in hazy days were mostly spherical and in internal mixing state, and dominated by particles marked as Type A and Type B. Both types of particles were consisted of volatile substances for their color was lightened and bubbles formed under the direct TEM detector light, i.e. electron beam damage. Therefore, they were considered to be secondary transformed in the atmosphere. The elemental compositions of 15 single particles were detected by EDX randomly (Fig. 3e). The percentages of sulfur-, chlorine- and potassium- containing particles were 93%, 40%, and 33%, indicating they may contain sulfate (Li and Shao, 2010; Ueda et al., 2011), and mixed with particles from primary sources such as coal combustion and biomass burning. In addition, some freshly emitted and aged soot aggregates (Type C) were also observed and only accounted for a small part in each sample. To our knowledge, particles of Type B were hygroscopic. After the decrease of RH, the concentration of submicron particles reduced from 69 μg m^{-3} to 39 μg m^{-3} due to the evaporation of water in hygroscopic particles such as particles of Type B (Lee et al., 2007). The particles collected at 19:30 LT shrank to smaller sizes than those collected at 14:51 LT. In general, the morphology and mixing state of particles varied not significantly during the hazy days.

S6 Secondary formation and aging process of OA

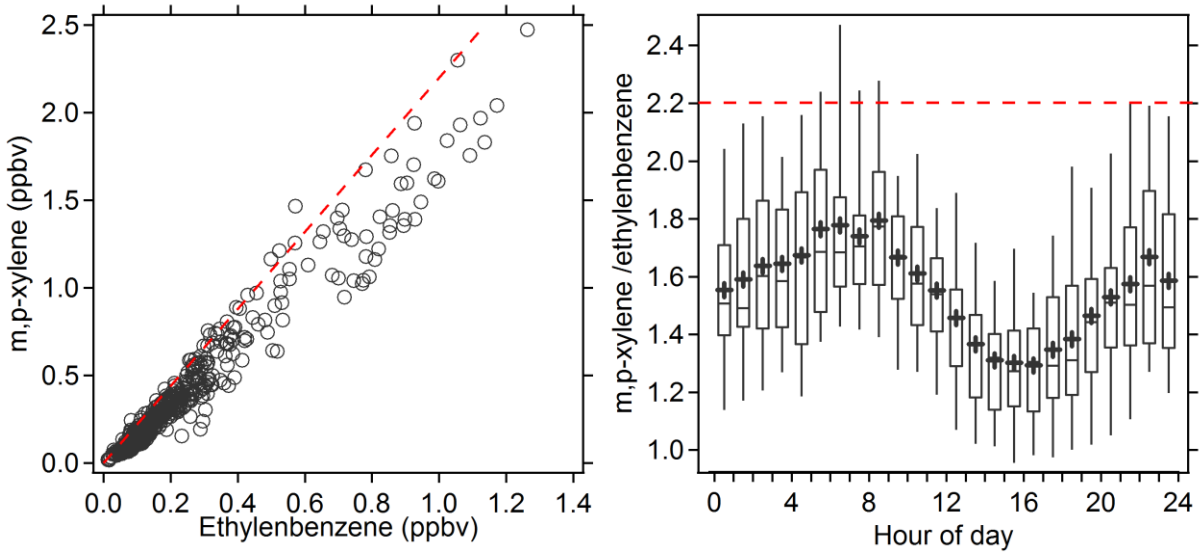

Figure S8. Correlation between m, p-xylene and ethylbenzene during the observation period at Ziyang site (left) and diurnal variation of the ratio of m, p- xylene to ethylbenzene (right). The highest ratio of m, p-xylene to benzene was about 2.2 (dash lines), which was used as the initial emission ratio of them for the calculation of photochemical age. For several data point of the ratio greater than 2.2, the calculated photochemical age less than zero were unified to zero.

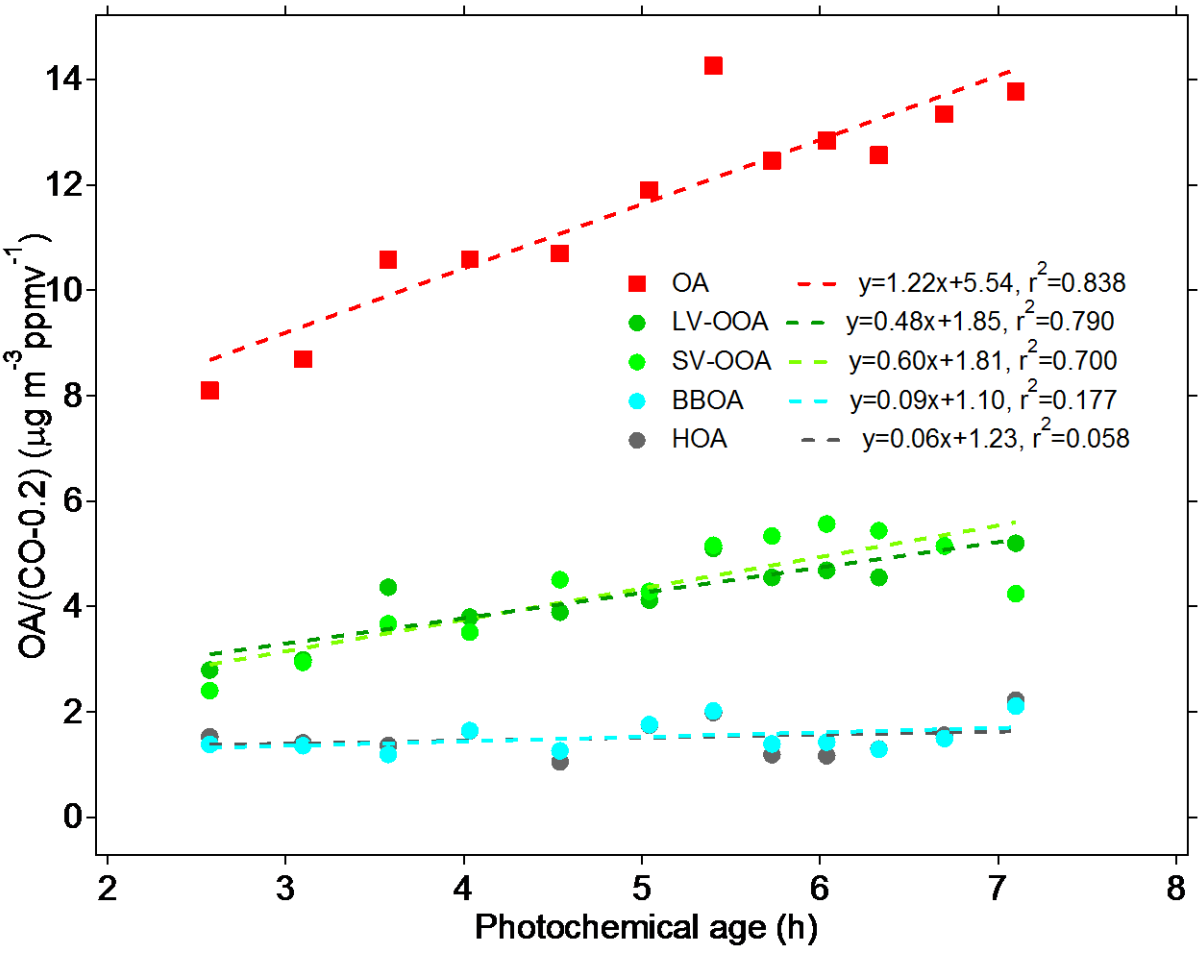

Figure S9. Variations of OA/ΔCO and PMF resolved OA factors to ΔCO with the increase of photochemical age (in the range of 2.6~7.1 hours).

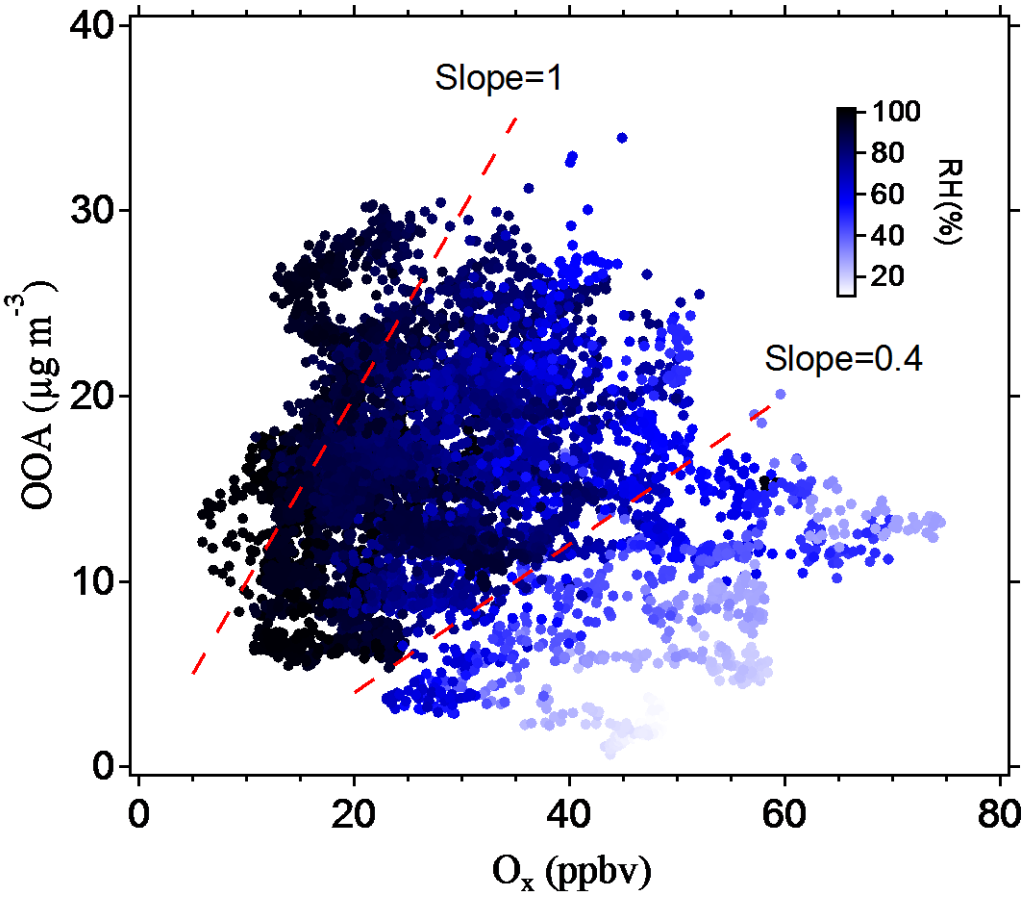

Figure S10. Scattering plot of OOA mass concentrations against O_x concentrations. Data points are color coded by RH.

References

Aiken, A. C., Salcedo, D., Cubison, M. J., Huffman, J. A., DeCarlo, P. F., Ulbrich, I. M., Docherty, K. S., Sueper, D., Kimmel, J. R., Worsnop, D. R., Trimborn, A., Northway, M., Stone, E. A., Schauer, J. J., Volkamer, R. M., Fortner, E., de Foy, B., Wang, J., Laskin, A., Shutthanandan, V., Zheng, J., Zhang, R., Gaffney, J., Marley, N. A., Paredes-Miranda, G., Arnott, W. P., Molina, L. T., Sosa, G., and Jimenez, J. L.: Mexico City aerosol analysis during MILAGRO using high resolution aerosol mass spectrometry at the urban supersite (T0) - Part 1: Fine particle composition and organic source apportionment, Atmos. Chem. Phys., 9, 6633-6653, 2009.

Brown, S. S.: Nitrogen oxides in the nocturnal boundary layer: Simultaneous in situ measurements of NO_3, N_2O_5, NO_2, NO, and O_3, J. Geophys. Res. Atmos., 108, doi: 10.1029/2002JD002917, 2003.

Canagaratna, M. R., Jayne, J. T., Ghertner, D. A., Herndon, S., Shi, Q., Jimenez, J. L., Silva, P. J., Williams, P., Lanni, T., Drewnick, F., Demerjian, K. L., Kolb, C. E., and Worsnop, D. R.: Chase Studies of Particulate Emissions from in-use New York City Vehicles, Aerosol Sci. Tech., 38, 555-573, 10.1080/02786820490465504, 2004.

Gong, Z., Lan, Z., Xue, L., Zeng, L., He, L., and Huang, X.: Characterization of submicron aerosols in the urban outflow of the central Pearl River Delta region of China, Front. Environ. Sci. Eng., 725-733, 2012.

Gong, Z., Xue, L., Sun, T., Deng, Y., He, L., and Huang, X.: On-line measurement of PM_1 chemical composition and size distribution using a high-resolution aerosol mass spectrometer during 2011 Shenzhen Universiade, Scientia Sinica Chimica, 43, 363-372, 2013.

He, L. Y., Huang, X. F., Xue, L., Hu, M., Lin, Y., Zheng, J., Zhang, R., and Zhang, Y. H.: Submicron aerosol analysis and organic source apportionment in an urban atmosphere in Pearl River Delta of China using high-resolution aerosol mass spectrometry, J. Geophys. Res. Atmos., 116, 2011.

He, L. Y., Lin, Y., Huang, X. F., Guo, S., Xue, L., Su, Q., Hu, M., Luan, S. J., and Zhang, Y. H.: Characterization of high-resolution aerosol mass spectra of primary organic aerosol emissions from Chinese cooking and biomass burning, Atmos. Chem. Phys., 10, 11535-11543, 10.5194/acp-10-11535-2010, 2010.

Hu, W. W.: The sources and secondary formations of sub-micron organic aerosol in the typical atmospheric environments of China, Doctor of Philosophy, Peking University, Beijing, China, 2012.

Hu, W. W., Hu, M., Deng, Z. Q., Xiao, R., Kondo, Y., Takegawa, N., Zhao, Y. J., Guo, S., and Zhang, Y. H.: The characteristics and origins of carbonaceous aerosol at a rural site of PRD in summer of 2006, Atmos. Chem. Phys., 12, 1811-1822, 2012.

Hu, W. W., Hu, M., Yuan, B., Jimenez, J. L., Tang, Q., Peng, J. F., Hu, W., Shao, M., Wang, M., Zeng, L. M., Wu, Y. S., Gong, Z. H., Huang, X. F., and He, L. Y.: Insights on organic aerosol aging and the influence of coal combustion at a regional receptor site of central eastern China, Atmos. Chem. Phys., 13, 10095-10112, 2013.

Hu, W. W., Hu, M., Hu, W., Jimenez, J. L., Yuan, B., Chen, W., Wang, M., Wu, Y., Chen, C., Wang, Z., Peng, J., Yang, K., Zeng, L., and Shao, M.: Chemical composition, sources and aging process of sub-micron aerosols in Beijing: contrast between summer and winter. J. Geophys. Res. Atmos., doi: 10.1002/2015JD024020, 2016.

Huang, X. F., He, L. Y., Hu, M., Canagaratna, M. R., Kroll, J. H., Ng, N. L., Zhang, Y. H., Lin, Y., Xue, L., Sun, T. L., Liu, X. G., Shao, M., Jayne, J. T., and Worsnop, D. R.: Characterization of submicron aerosols at a rural site in Pearl River Delta of China using an Aerodyne High-Resolution Aerosol Mass Spectrometer, Atmos. Chem. Phys., 11, 1865-1877, 2011.

Huang, X. F., He, L. Y., Hu, M., Canagaratna, M. R., Sun, Y., Zhang, Q., Zhu, T., Xue, L., Zeng, L. W., Liu, X. G., Zhang, Y. H., Jayne, J. T., Ng, N. L., and Worsnop, D. R.: Highly time-resolved chemical characterization of atmospheric submicron particles during 2008 Beijing Olympic Games using an Aerodyne High-Resolution Aerosol Mass Spectrometer, Atmos. Chem. Phys., 10, 8933-8945, 2010.

Huang, X. F., He, L. Y., Xue, L., Sun, T. L., Zeng, L. W., Gong, Z. H., Hu, M., and Zhu, T.: Highly time-resolved chemical characterization of atmospheric fine particles during 2010 Shanghai World Expo, Atmos. Chem. Phys., 12, 4897-4907, 2012.

Huang, X. F., Xue, L., Tian, X. D., Shao, W. W., Sun, T. L., Gong, Z. H., Ju, W. W., Jiang, B., Hu, M., and He, L. Y.: Highly time-resolved carbonaceous aerosol characterization in

Yangtze River Delta of China: Composition, mixing state and secondary formation, Atmos. Environ., 64, 200-207, 2013.

Lanz, V. A., Alfarra, M. R., Baltensperger, U., Buchmann, B., Hueglin, C., Szidat, S., Wehrli, M. N., Wacker, L., Weimer, S., Caseiro, A., Puxbaum, H., and Prevot, A. S. H.: Source attribution of submicron organic aerosols during wintertime inversions by advanced factor analysis of aerosol mass spectra, Environ. Sci. Tech., 42, 214-220, 2008.

Li, W., and Shao, L.: Mixing and water-soluble characteristics of particulate organic compounds in individual urban aerosol particles, J. Geophys. Res. Atmos., 115, 2010.

Mohr, C., Huffman, J. A., Cubison, M. J., Aiken, A. C., Docherty, K. S., Kimmel, J. R., Ulbrich, I. M., Hannigan, M., and Jimenez, J. L.: Characterization of primary organic aerosol emissions from meat cooking, trash burning, and motor vehicles with high-resolution aerosol mass spectrometry and comparison with ambient and chamber observations, Environ. Sci. Tech., 43, 2443-2449, 2009.

Ng, N. L., Canagaratna, M. R., Zhang, Q., Jimenez, J. L., Tian, J., Ulbrich, I. M., Kroll, J. H., Docherty, K. S., Chhabra, P. S., Bahreini, R., Murphy, S. M., Seinfeld, J. H., Hildebrandt, L., Donahue, N. M., DeCarlo, P. F., Lanz, V. A., Prévôt, A. S. H., Dinar, E., Rudich, Y., and Worsnop, D. R.: Organic aerosol components observed in Northern Hemispheric datasets from Aerosol Mass Spectrometry, Atmos. Chem. Phys., 10, 4625-4641, 10.5194/acp-10-4625-2010, 2010.

Pathak, R. K., Wang, T., and Wu, W. S.: Nighttime enhancement of $PM_{2.5}$ nitrate in ammonia-poor atmospheric conditions in Beijing and Shanghai Plausible contributions of heterogeneous hydrolysis of N_2O_5 and HNO_3 partitioning, Atmos. Environ., 45, 1183-1191, 2011.

Xiao, R., Takegawa, N., Zheng, M., Kondo, Y., Miyazaki, Y., Miyakawa, T., Hu, M., Shao, M., Zeng, L., Gong, Y., Lu, K., Deng, Z., Zhao, Y., Zhang, Y. H.: Characterization and source apportionment of submicron aerosol with aerosol mass spectrometer during the PRIDE-PRD 2006 campaign. Atmos. Chem. Phys. 11, 6911-6929, 2011.

Ueda, S., Osada, K., and Takami, A.: Morphological features of soot-containing particles internally mixed with water-soluble materials in continental outflow observed at Cape Hedo, Okinawa, Japan, J. Geophys. Res. Atmos., 116, 2011.

Weimer, S., Alfarra, M. R., Schreiber, D., Mohr, M., Prévôt, A. S. H., and Baltensperger, U.: Organic aerosol mass spectral signatures from wood-burning emissions: Influence of burning conditions and wood type, J. Geophys. Res. Atmos., 113, 10.1029/2007jd009309, 2008.

Zhang, Q., Alfarra, M. R., Worsnop, D. R., Allan, J. D., Coe, H., Canagaratna, M. R., and Jimenez, J. L.: Deconvolution and quantification of hydrocarbon-like and oxygenated organic aerosols based on aerosol mass spectrometry, Environ. Sci. Tech., 39, 4938-4952, 2005.